

PhD degree in Medical Nanotechnology  
European School of Molecular Medicine (SEMM),  
University of Milan and University of Naples “Federico II”  
Settore disciplinare: FIS/03

**SURFACE FUNCTIONALIZED GOLD  
NANOPARTICLES AS ATTACHMENT INHIBITORS  
FOR HEPARAN SULFATE-BINDING VIRUSES**

*Marco D’Alicarnasso*

IFOM, CEN

Matricola n. 823513

*Supervisor:* Prof. Francesco Stellacci

Institute of Materials, EPFL, Lausanne, Switzerland

Istituto Neurologico “Carlo Besta”, Milan

*Added supervisor:* Dr. Silke Krol

Istituto Neurologico “Carlo Besta”, Milan

Anno Accademico 2014-2015

*“Equipped with this modern knowledge, I have, returning through the little death from my earlier lives, been able to compare the heavens then and now. And the stars do change. I have seen pole stars and pole stars and dynasties of pole stars. The pole star to-day is in Ursa Minor. Yet, in those far days I have seen the pole star in Draco, in Hercules, in Vega, in Cygnus, and in Cepheus. No; not even the stars abide, and yet the memory and the knowledge of them abides in me, in the spirit of me that is memory and that is eternal. Only spirit abides. All else, being mere matter, passes, and must pass.”*

Jack London

A mio padre

# TABLE OF CONTENTS

<b>LIST OF ABBREVIATIONS</b> .....	7
<b>FIGURE INDEX</b> .....	9
<b>ABSTRACT</b> .....	10
<b>I. INTRODUCTION</b> .....	11
<b>Chapter 1</b> .....	11
1.1 Viruses: structure and life cycle.....	11
1.2 Virus attachment and recognition of target cells .....	13
1.2.1 Role of Heparan sulfate proteoglycans (HSPGs) in the attachment process ..	14
1.3 Virus entry into the cell.....	17
1.4 Post-entry events .....	20
<b>Chapter 2</b> .....	22
2.1 Current strategies to fight viruses .....	22
2.1.1 Vaccines .....	22
2.1.2 Antiviral drugs .....	23
2.1.3 Virucidal molecules .....	26
<b>Chapter 3</b> .....	28
3.1 Nanotechnology and its healthcare applications.....	28
3.2 Nanomaterials used as antivirals.....	30
3.3 Nanomaterials used as virucidal agents .....	35
<b>Chapter 4</b> .....	37
4.1 Sulfonated NPs as broad spectrum agents for HS-binding viruses.....	37
4.2 Viruses used for the experiments .....	38
<b>II. AIM OF THE STUDY</b> .....	43
<b>III. MATERIALS AND METHODS</b> .....	44
<b>Materials</b> .....	44
3.1 Synthesis of functionalized Au-NPs .....	44
3.2 Cell Culture .....	45
3.3 Viruses .....	46
3.3.1 Lentivirus: production and purification .....	46
3.3.2 Adenovirus (Ad) .....	48
3.3.3 Adeno-associated virus (AAV).....	48
3.3.4 Herpes simplex virus type 1 and type 2 (HSV-1 and HSV-2).....	49
3.3.5 Human Papilloma pseudovirus (HPV-16 PsV) production .....	49

3.4 Antiviral drug 3'-azido-3'-deoxythymidine (AZT).....	49
<b>Methods</b> .....	50
3.5 <i>In vitro</i> cell-toxicity assay.....	50
3.6 Cell-surface staining .....	51
3.7 Au-NPs preparation for antiviral assay studies.....	51
3.8 Antiviral Assays.....	51
3.8.1 Pseudotyped Lentiviruses (LV-VSV-G, LV-gp160), Adenovirus and AAVs inhibition assay. ....	51
3.8.2 HSV-1, HSV-2 antiviral assay.....	52
3.8.3 HPV-16 PsV antiviral assay.....	52
3.9 Time of addition (TOA) experiments .....	53
3.10 Virucidal assay.....	53
3.11 Attachment assay .....	54
3.12 Entry assay .....	54
3.13 Quantification of transduced cells (GFP+) .....	54
3.13.1 FACS analysis.....	54
3.13.2 Confocal Laser Scanning Microscopy (CLSM) .....	55
3.14 Western Blot analysis .....	55
3.15 Dynamic Light Scattering (DLS) and $\zeta$ -potential .....	56
3.16 Cryo-Electron Microscopy (cryo-EM) .....	56
<b>IV. RESULTS</b> .....	57
4.1 Characterization of Au-NPs.....	57
4.2 Cytotoxicity Assay.....	58
4.3 Antiviral assays on HSPG-dependent viruses.....	59
4.3.1 LV-VSV-G.....	60
4.3.2 HSV-1/2 and HPV-16 PsV .....	64
4.3.3 LV-gp160.....	65
4.3.4 AAV2 and AAV5 .....	68
4.4 Time of addition experiments .....	70
4.5 Entry and Attachment Assays.....	75
4.6 Virucidal Assay.....	77
4.7 Cryo-Electron Microscopy (cryo-EM) of HSV-2 and MUS:OT.....	82
<b>V. DISCUSSION</b> .....	85
5.1 Inhibition of viruses by sulfonate-presenting NPs (MUS, MUS:OT) .....	85
5.2 Antiviral mechanism of action of MUS:OT NPs.....	90

5.2.1 Time of addition.....	90
5.2.2 Entry vs attachment assay.....	92
5.3 Virus inactivation by MUS:OT NPs.....	93
5.4 Cryo-EM study of the NP/virus interaction.....	95
<b>VI. CONCLUSIONS AND FUTURE OUTLOOK.....</b>	<b>97</b>
<b>VII. REFERENCES.....</b>	<b>99</b>

# LIST OF ABBREVIATIONS

AAV = Adeno-Associated Virus

Ab = Antibody

Ad = Adenovirus

Ag-NPs = Silver nanoparticles

AIDS = Acquired Immunodeficiency Syndrome

ATCC = American Type Culture Collection

Au-NPs = Gold nanoparticles

AZT = 3'-azido-3'-deoxythymidine

CAR = Coxsackie and Adenovirus Receptor

CHIKV = Chikungunya Virus

CHO = Chinese Hamster Ovary

Cryo-EM = Cryo-Electron Microscope

CLSM = Confocal Laser Scanning Microscopy

DENV = Dengue Virus

DLS = Dynamic Light Scattering

EBV = Epstein-Barr virus

FACS = Fluorescence Activated Cell Sorting

FBS = Foetal Bovine Serum

GAG = Glycosaminoglycan

GFP = Green Fluorescent Protein

HAADF = High Angle Annular dark field

HEK293 = Human Embryonic Kidney

HeLa = Human cervical carcinoma

HeLa T4+ = HeLa cells expressing human CD4 protein

HS = Heparan Sulfate

HSV-1 = Herpes Simplex Virus type 1

HSV-2 = Herpes Simplex Virus type 2

HPV-16 = Human Papilloma Virus 16

HIV = Human Immunodeficiency Virus

HSPG = Heparan Sulphate Proteoglycan

LV = Lentivirus

LV-gp160 = Lentivirus pseudotyped with gp160  
LV-VSV-G = Lentivirus pseudotyped with VSV-G  
M = Molarity  
MEM = Minimum Essential Media  
MES = mercaptoethane sulfonate  
MRI = Magnetic Resonance Imaging  
MUS = 11-mercapto-1-undecanesulphonate  
MW = Molecular weight  
NPC = Nuclear Pore Complex  
NPs = Nanoparticles  
NNRTI = Non-Nucleoside Reverse Transcriptase Inhibitor  
NRTI = Nucleoside Reverse Transcriptase Inhibitor  
PBS = Phosphate-Buffered Saline  
PEG= Polyethylene Glycol  
PFA = Paraformaldehyde  
PFU = Plaque Forming Units  
PsV = Pseudovirus  
RT = Retrotranscriptase  
RSV = Respiratory Syncytial Virus  
SEAP = Secreted Alkaline Phosphatase  
SDS = Sodium Dodecyl Sulfate  
SPIONs = Superparamagnetic Iron Oxide Nanoparticles  
STEM = Scanning Transmission Electron Microscopy  
TEM = Transmission Electron Microscopy  
VLP = Virus Like Particles  
VSV = Vesicular Stomatitis virus  
VSV-G = Vesicular Stomatitis G protein  
w/v = weight / volume  
WHO = World Health Organization  
 $\zeta$ -potential = zeta potential



# FIGURE INDEX

Figure 1. The replicative cycle of retroviruses .....	12
Figure 2. Structure of heparan-sulfate proteoglycans (HSPGs).....	14
Figure 3. Virus entry into cells. ....	17
Figure 4. HIV life cycle and targets for anti-HIV agents. ....	26
Figure 5. Nanomaterials used for biomedical application and list of nanomaterials in clinical use. ....	28
Figure 6. Cytotoxicity of NPs evaluated with PI. ....	58
Figure 7. Schematic representation of the LV-VSV-G inhibition assay. ....	59
Figure 8. LV-VSV-G inhibition assay with sulfonated NPs (MUS:OT, MUS).....	60
Figure 9. LV-VSV-G inhibition assay with MUS:OT NPs in different cell lines.....	61
Figure 10. Experiments to validate antiviral activity of MUS:OT NPs.....	63
Figure 11. Antiviral assay of HSPG-binding viruses with MUS:OT NPs.....	64
Figure 12. Characterization of LV-gp160 and HeLa T4+ cells. ....	66
Figure 13. Confocal Laser Scanning Microscopy (CLSM) images of LV-gp160 incubated with NPs.....	67
Figure 14. Confocal Laser Scanning Microscopy (CLSM) images AAVs (AAV2; AAV5) with MUS:OT NPs.....	69
Figure 15. Schematic representation of the time of addition (TOA) experiments.....	70
Figure 16. TOA experiments with MUS:OT. ....	72
Figure 17. Comparison of MUS:OT and AZT antiviral mechanism of action.....	74
Figure 18. Schematic representation of entry and attachment of LV-VSV-G in presence of MUS:OT NPs.....	76
Figure 19. Entry and attachment assays with LV-VSV-G in presence of MUS:OT. ....	77
Figure 20. Virucidal assays of LV-VSV-G and Ad5.....	79
Figure 21. Virucidal assays of HSV-2 with MUS:OT NPs. ....	80
Figure 22. Virucidal assays of LV-VSV-G with MUS:OT NPs versus time. ....	81
Figure 23. Cryo-EM images of HSV-2.....	84
Figure 24. Virucidal assay with MUS:OT NPs and possible mechanisms of virus inactivation.....	94

# ABSTRACT

Infectious diseases account for one fifth of global mortality. Although many efforts have been made to prevent and treat specific viral diseases (e.g. hepatitis B, AIDS) with vaccines and drugs, we still lack effective and biocompatible broad-spectrum antiviral agents, especially against re-emerging (e.g. Dengue virus) and newly emerging viruses (e.g. Ebola virus). Current advances in nanotechnology opened new frontiers in developing novel antivirals that can interact and inactivate a large number of viral pathogens. Nanoparticles (NPs) – particles in the size range 1-100 nm – can be finely engineered on their surface to interfere with key events of infections shared by many viruses, above all the attachment to the host cell. The aim of the present work is to assess the role of gold nanoparticles (Au-NPs) capped with sulfonate molecules as potential inhibitors toward human viruses binding sulfated polysaccharides on the cell membrane. Results showed that sulfonated NPs have powerful antiviral as well as virucidal activity. Their applications may lead to substantial improvements in virus-spread control not only as novel wide-spectrum therapeutic agents but most importantly as novel active materials to be employed in emergency situations, for example in personal protective equipment, waste management, virus containment.

# I. INTRODUCTION

## Chapter 1

### 1.1 Viruses: structure and life cycle

Viruses are obligatory intracellular parasites that critically rely on the presence of a host to replicate and generate new virus progeny. They can be considered as nanoscopic (20-200nm) Trojan horses evolved to hijack cell synthetic machinery and transfer their genome into the cytosol or the nucleus of the cell (Smith & Helenius 2004; Marsh & Helenius 2006). In fact, they are able to activate endogenous cellular responses that allow their entry and the subsequent integration of their genes for initiating productive infection. Viruses are made of nucleic acids (RNA or DNA) enclosed in a shell of tightly packed proteins, called capsid (Marsh & Helenius 2006). They can be divided in two groups, based on whether they are surrounded by a lipid bilayer membrane originating from the cell membrane of the host cell (enveloped viruses), or non-enveloped viruses, that only have a protein exterior (Jolly & Sattentau 2013). Other structural components of viruses can be matrix proteins, membrane glycoproteins or enzymes (i.e. reverse transcriptase) (Marsh & Helenius 2006). Given the differences in morphology, structural composition and tropism the process of viral infection is extremely dynamic and consists of multiple steps: 1) the attachment of the virion to the cell surface followed by specific binding to receptors, 2) the penetration into the cell, 3) the uncoating, 4) the biosynthesis which comprises replication of the genome, transcription and translation, 5) the assembly of viral particles in infected cells, and 6) the extracellular release of newly formed viruses (Smith & Helenius 2004). The main phases of virus infective cycle are depicted in Figure 1.

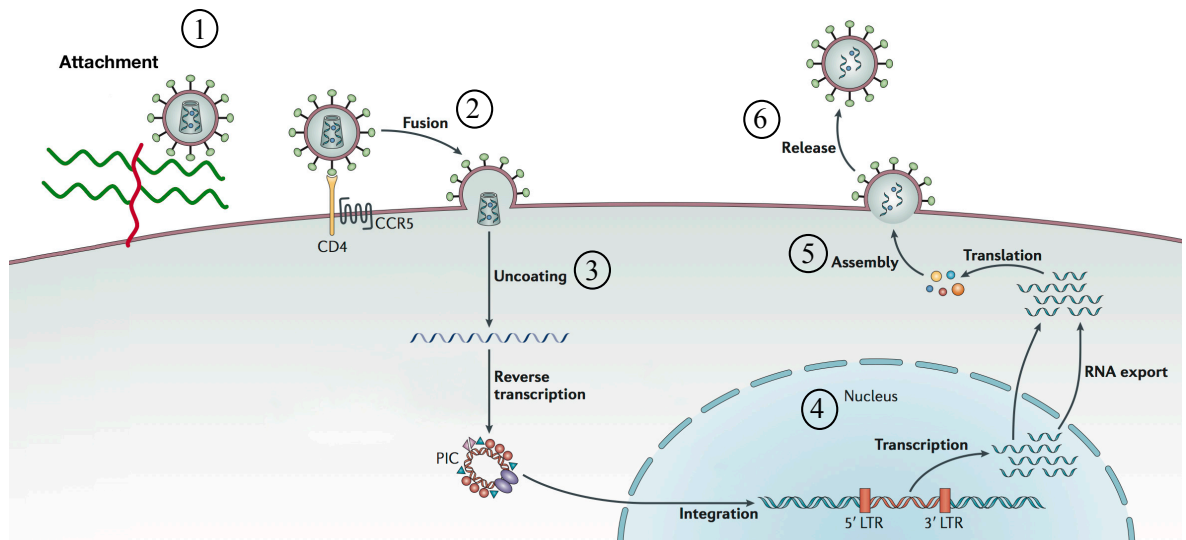


**Figure 1. The replicative cycle of retroviruses**

The figure illustrates the main steps of retrovirus (e.g. Human immunodeficiency virus-(HIV) replication, numbered from 1 to 6. (1) Virus binds to the attachment factor (heparan sulfate proteoglycans (HSPGs)) via its surface glycoprotein, gp120; HIV interacts with specific entry receptors (CD4) and co-receptors (CCR5) and fuses (2) with the host cell membrane; (3) Uncoating of the viral capsid and release of viral genome (RNA) and proteins into the cytoplasm; (4) Biosynthesis, retrotranscription of the viral RNA, integration of the pre-integration complex (PIC) into the nucleus, transcription and translation of the HIV RNA and proteins. (5) Assembly of new viruses and (6) release and maturation of new infectious virions. Image modified from (Barré-Sinoussi et al. 2013) *Nature Review Microbiology*. (2013) © Macmillan Publishers Limited.

## **1.2 Virus attachment and recognition of target cells**

In order to initiate a productive infection, viruses must first attach themselves to the surface of a host cell (Smith & Helenius 2004). Despite the differences among the wide range of viruses identified to date, all of them carry external structures, usually proteins, on their outer surface that enable the attachment and consequent recognition of target cells. Interactions between viruses and cell are mediated by two different kinds of molecules: 1) attachment factors, such as heparan sulfates or other carbohydrate structures on the cell surface and 2) entry receptors. The former merely serves to immobilize the particles on the cell surface in close proximity to the receptor, whereas the latter promotes viral entry into a cell by inducing conformational changes and activating signalling pathways. Recently, numerous viral attachment factors and entry receptors have been identified (Jolly & Sattentau 2013) and the crystal structures of several viruses and viral proteins have been solved (Kwong et al. 1998; Rossmann et al. 2002; Skehel & Wiley 2000). The association between viral proteins and attachment factors is reversible and thus make the attachment a relatively nonspecific process. Since viruses may encounter unfavourable conditions for cellular attachment (e.g. presence of competitive ligand) they have evolved to limit random three-dimensional propagation to quickly bind to the cell glycocalyx, the first physical structure encountered once cell surface is approached (Jolly & Sattentau 2013). The glycocalyx is a ubiquitous coating of carbohydrates conjugated to proteins (glycoproteins) and lipids (glycolipids), expressed on cell plasma membranes. The glycocalyx contains negatively charged moieties given by a group of glycoproteins called proteoglycans. Hence, the two major targets for viral attachment are glycoproteins and glycolipids (Jolly & Sattentau 2013).

### 1.2.1 Role of Heparan sulfate proteoglycans (HSPGs) in the attachment process

Amongst the attachment factors, heparan sulfate proteoglycans (HSPGs) are frequently involved during the initial virus/cell interactions. They are ubiquitously expressed as part of the glycocalyx on cell surfaces and in the extracellular matrix. HSPGs are composed of a core protein and several heparan sulfate (HS) glycosaminoglycan (GAG) chains which are linear carbohydrate polymers of repeating disaccharides of glucosamine units (N-acetylglucosamine or N-sulfated glucosamine) and -uronic acids (glucuronic or iduronic acids) (Bishop et al. 2007) (Figure 2).

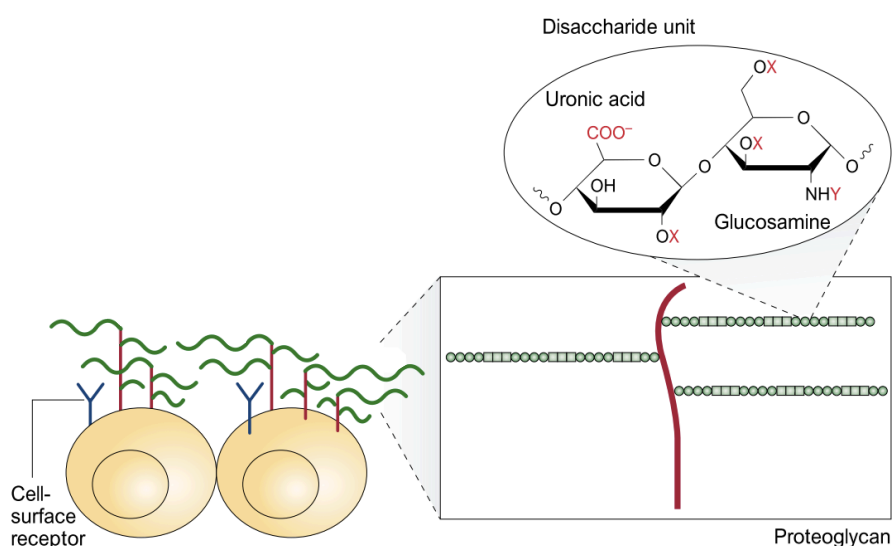


**Figure 2. Structure of heparan-sulfate proteoglycans (HSPGs).**

HSPGs consist of a core protein (red lines) and one or more covalently linked heparan sulfate (HS) glycosaminoglycans (GAG) chains. Zooming in further, HSGAG are composed of disaccharide units of uronic acid linked to glucosamine. Each disaccharide unit can be sulfated at different positions of the uronic acid and/or the glucosamine (designed with red X or Y). Green squares represent the highly sulfated region within the polysaccharide chain, whereas green circles are those undersulfation. Image modified from (Sasisekharan et al. 2002) © *Nature Rev. Cancer* (2002) Nature Publishing Group

HSPGs comprise a highly diverse group of molecules that can be divided in three main subfamilies: 1) the membrane-spanning proteoglycans (syndecans, betaglycans and CD44v3), 2) the glycosphosphatidylinositol (GPI)-linked proteoglycans (glypicans) and 3)

the secreted extracellular matrix (ECM) proteoglycans (agrin, collagen XVIII and perlecan) (WuYang et al. 2011; Bishop et al. 2007). Cell surface HSPGs function as co-receptors for HS-binding ligands, serving as a scaffold that localizes the ligands to the cell surface, enabling their interaction with their respective signalling receptors (Bartlett & Park 2011). Indeed, HS normally binds to a wide variety of growth factors, chemokines, enzymes and matrix components and regulates numerous cell physiological processes such as metabolism, transport, information transfer, support and regulation at the systemic level as well as at the cellular level (WuYang et al. 2011; Bishop et al. 2007). It has been demonstrated that HSPGs can also function as primary receptors mediating the endocytosis of polycationic macromolecules and cationic peptides via macropinocytosis, clathrin-dependent or -independent endocytosis (Poon & Gari 2007) (Christianson & Belting 2014). Despite the physiological roles of HSPGs, they can also contribute, under certain conditions, to the development of pathological status, as in the case of cancer, facilitating primary tumour growth and modulating the process of angiogenesis (Sasisekharan et al. 2002). Moreover, HSPGs can serve as attachment factors for a wide number of pathogens including bacteria, protozoa as well as several viruses belonging to different families (Bernfield et al. 1999). As it is shown in Table 1, cellular HS is known to be used as attachment receptor for DNA as well as RNA virus families (WuYang et al. 2011). In viral pathogenesis, HSPGs are commonly exploited by multiple viruses (HS-binding viruses) as low affinity co-receptors that entrap and concentrate particles on host cell surfaces facilitating the following binding to receptors with a higher affinity. Such attachment strategy allows the pathogen to reach the cognate secondary receptor, even if it is expressed at low numbers on the cell surface (Spillmann 2001).

**Table 1. List of viruses that use heparan sulfates as attachment factor.** Adapted from

(WuYang et al. 2011)

Virus Genome	Virus Family	Virus Genus	Virus Specie	Receptor Type	
DNA	Herpesviridae	Simpexvirus	Herpes simplex virus <sup>[4]</sup>	Specific receptor	
		Varicellovirus	Varicella-zoster virus <sup>[5]</sup>	Unknown	
		Cytomegalovirus	Human herpesvirus 5 <sup>[6]</sup>	Unknown	
	Poxviridae	Orthopoxvirinae		Pseudorabies virus <sup>[7]</sup>	Unknown
				Bovine herpesvirus 1 <sup>[8]</sup>	Unknown
			Vaccinia virus <sup>[9]</sup>	Unknown	
		Papovaviridae	Papillomavirus	Human papillomavirus <sup>[10]</sup>	Initial receptor
		Hepadnaviridae	Orthohepadnavirus	Hepatitis B virus <sup>[11]</sup>	Unknown
		Parvoviridae	Dependovirus	Adeno-associated virus type 2 <sup>[12]</sup>	Initial receptor
		RNA	Paramyxoviridae	Paramyxovirus	Human parainfluenza virus type 3 <sup>[13]</sup>
Pneumovirus	Human respiratory syncytial virus <sup>[14]</sup>			Initial receptor	
Picornaviridae	Cardiovirus		Theiler's virus <sup>[15]</sup>	Unknown	
	Aphthovirus		Foot-and-mouth disease virus <sup>[16]</sup>	Initial receptor	
	Enterovirus		Swine vesicular disease virus <sup>[17]</sup>	Initial receptor	
Flaviviridae	Flavivirus		Dengue virus <sup>[18]</sup>	Initial receptor	
			Tick borne encephalitis virus <sup>[19]</sup>	Initial receptor	
Togoviridae	Hepatitis C virus		Hepatitis C virus <sup>[20]</sup>	Unknown	
	Pestivirus		Swine fever virus <sup>[21]</sup>	Unknown	
	Alphavirus		Sindbis virus <sup>[22]</sup>	Initial receptor	
			Ross River virus <sup>[23]</sup>	Unknown	
			Venezuelan equine encephalitis virus <sup>[24]</sup>	Unknown	
Retroviridae	Lentivirus		Human immunodeficiency virus type 1 <sup>[26]</sup>	Initial receptor	
	BLV-HTLV retroviruses		Human T-cell leukemia virus <sup>[27]</sup>	Unknown	
Coronaviridae	Coronavirus		A vian coronavirus infectious bronchitis virus <sup>[28]</sup>	Unknown	

Many human pathogenic viruses have been identified as HS-binding (Liu & Thorp 2002), for example Herpes simplex virus type 1 and 2 (HSV-1 and 2) (Cheshenko et al. 2007), Human papillomavirus (HPV) (Shafti-keramat et al. 2003), Human immunodeficiency virus type 1 (HIV-1) (Connell & Lortat-Jacob 2013), Dengue virus (DENV) (Hilgard & Stockert 2000). Historically, HSV-1 was the first viral pathogen that has been reported to use HS as attachment receptor. The interaction with HS carrying a specific sulfonation pattern allows both HSV-1 attachment and penetration through specific binding sites of HSV glycoproteins. Interestingly, it has been found that the addition of HS or its drug mimetic heparin inhibits viral attachment and entry into cultured cells after treatment. This mechanism can be due to direct competition with cellular HS and/or other GAG receptors (Guibinga et al. 2002).



### 1.3 Virus entry into the cell

The transfer of the viral genetic content and accessory proteins into the host cells involves two distinct processes: fusion with host membrane, in case of enveloped viruses, or endocytosis for non-enveloped viruses (Figure 3).

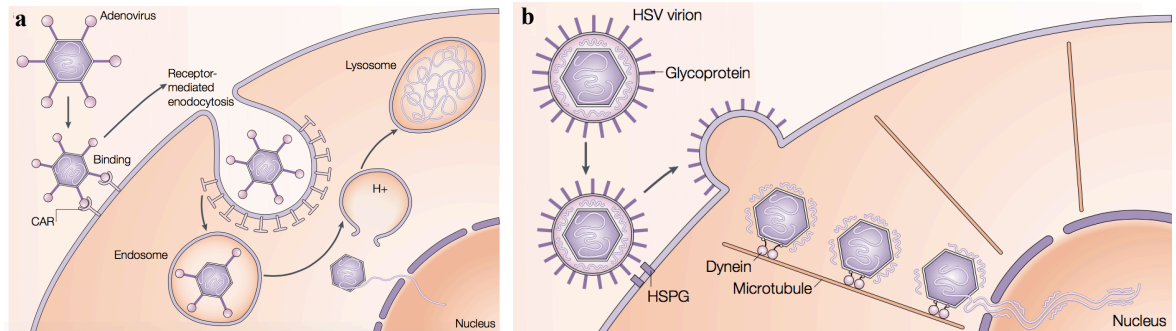


**Figure 3. Virus entry into cells.**

(a) Adenovirus virions bind to a primary receptor, the Coxsackie and Adenovirus receptor (CAR) and to co-receptors (integrins) on the host cell membrane. This complex triggers various cell responses, including clathrin-mediated viral endocytosis. Adenovirus is then delivered to intracellular endosomes which acidification ( $H^+$ ) allows the virus to escape in the cytosol. Intracellular signalling leads to Adenovirus transport towards the nucleus where it docks to nuclear pore complex receptors, disassembles and releases its double stranded DNA (Davidson & Breakefield 2003; Meier & Greber 2004). (b) Herpes simplex virus (HSV) virions infect host cells through initial attachment between viral envelope glycoproteins and heparan sulphate proteoglycan (HSPGs) on the plasma membrane. Virion envelope then fuses with the membrane of the host cell and the capsid is released in the cytoplasm and moves by dynein-mediated transport to the nucleus. HSV double-stranded DNA can then be transferred into the nucleus through the nuclear pore (Choudhary et al. 2011). Image modified from (Davidson & Breakefield 2003) *Nat. Rev. Neuroscience* © Wiley-Liss Inc (1998).

The majority of viruses need internalization via endocytosis in order to infect target cells (Marsh & Helenius 2006). This entry strategy is exploited by viruses because it offers several advantages. Viruses are driven into the cytoplasm by endocytic vesicles that can traverse the barriers consisting of the membrane cortex and the highly structured cytoplasm. A further advantage is represented by the fact that incoming viruses are exposed to a mildly acidic pH

in endosomes which in turn triggers the virus uncoating (Smith & Helenius 2004; Marsh & Helenius 2006). Two main endocytic pathways are frequently used by viruses:

1. **Clathrin-Mediated Endocytosis.** It is a process that enables the uptake of viruses into the cytosol from the surface using clathrin-coated vesicles (McMahon & Boucrot 2011). Such endocytic route is commonly used by viruses and it is usually rapid and efficient. The incoming viruses are transported into endosomes which acidic milieu triggers changes in viral conformation leading to endosome escape. Considering the wide range of viruses that are known to use clathrin-mediated endocytosis, only those with a diameter of approximately 30 nm (e.g. rhinovirus) can fit into clathrin-coated vesicles without altering their formation. Viruses having a larger diameter size from 80 to 150 nm (e.g. reovirus and influenza A) require clathrin-coated vesicles to increase their size in order to accommodate the viral particle (McMahon & Boucrot 2011). It has been demonstrated that a lot of different cofactors, adaptors, and kinases belonging to many different classes are involved in the formation of clathrin-coated pits and vesicles (Robinson 2004), thus highlighting the complexity of this endocytic pathway.
2. **Clathrin-Independent Endocytosis.** Some viruses exploit clathrin-independent endocytosis mechanisms for cell entry. An example is SV40 virus that uses the caveolar/rafts pathways, specialized in the internalization of lipids including cholesterol, GPI-anchored proteins, and components of cholesterol rich microdomains (lipid rafts) (Anderson et al. 1996). The capsids of SV40 and the related polyomavirus are composed of 72 homopentameric VP1 protein units that resemble cholera toxin B chain pentamers (Stehle et al. 1996). These viruses bind to the sugar moiety of gangliosides and enter cells via caveolar/raft pathways that are dependent on cholesterol and the activation of tyrosine- kinase signalling cascades (Tsai et al. 2003; Pelkmans et al. 2001; Smith et al. 2003). Two steps are involved in the caveolar/raft pathway: initially, viruses are delivered to pH-neutral caveosomes and then they are transported via microtubules, to the endoplasmic reticulum (ER) where penetration occurs (Pelkmans et al. 2001). Other

viruses that use caveolar/raft endocytosis include Echovirus 1 (EV1), a picornavirus that binds to integrins, and Coxsackie virus B (CVB) that infects human Caco-2 epithelial cells (Pietiäinen et al. 2005).

Moreover, although the majority of viruses can infect cells exploiting the endocytic mechanisms, some viruses belonging to different families (such as vaccinia, adeno, picorna) can take advantage of an alternative internalization mechanism known as macropinocytosis (Mercer & Helenius 2009). Macropinocytosis is a transient actin-dependent endocytic process that leads to internalization of fluids and membranes into large vacuoles. Indeed, virus particles can activate signalling pathways that trigger cytoskeletal rearrangements in the form of membrane ruffling or blebbing, with the subsequent formation of large vacuoles (macropinosomes) that allows the internalization and penetration of viruses into the cytosol of the cell (Mercer & Helenius 2009). Several recent studies have reported that this kind of endocytic route is used by many viruses such as Vaccinia virus, Adenovirus type 3 (Ad3) , EV1, CVB and Ebola virus (Mercer & Helenius 2008; Meier et al. 2002; Liberali et al. 2008; Coyne et al. 2007; Saeed et al. 2010). Indeed, mature vaccinia virions are able to enter the cell through macropinocytic mechanisms mimicking the uptake of apoptotic bodies. As demonstrated by Mercer et al., addition of mature vaccinia virions to cells leads to an increased uptake of fluids and the internalized particles co-localize with fluid phase markers (Mercer & Helenius 2008; Huang et al. 2008). The association of mature virions with cells induces the formation of plasma membrane blebs, which are apoptotic bodies rapidly filled up with actin and actin-associated proteins. The consequent retraction of blebs allows the internalization of adjacent virions along with fluids. Similarly, Ad3, a non-enveloped double stranded DNA virus, can activate Rac1-mediated macropinocytosis after binding to its cellular receptor (CD46). Adenovirus is found in large, uncoated vacuoles and its internalization coincides with enhanced fluid uptake as observed by electron microscopy study (Amstutz et al. 2008; Sirena et al. 2004). Moreover, viruses belonging to the picornaviridae family like EV1 and CVB make use of macropinocytosis to infect cells. The

evidence is given by the fact that virions co-localize with fluid phase markers and both require  $\text{Na}^+/\text{H}^+$  exchangers and kinases (i.e. PKC, PLC) for a productive entry and thus infection (Mercer & Helenius 2008). Virus entry by macropinocytosis is a process still incompletely characterized and its relevance remains restricted only to a limited number of viruses. It is still unclear how many types of macropinocytosis exist and how many viruses can trigger such internalization pathways. Viruses, especially those particles too large for clathrin-mediated endocytosis, might have evolved this alternative entry strategy, preferable over phagocytosis, to broaden their tropism. Another plausible reason can be the evasion from the immune system. In fact, virions internalized within macropinosomes are probably not exposed to receptors and other factors that trigger innate immune responses (Mercer & Helenius 2008; (Kerr & Teasdale 2009).

#### **1.4 Post-entry events**

Once viruses have been internalized inside the cell, their capsids are disassembled and viral genome as well as viral accessory proteins are released. Many viruses with DNA genome release their genetic content into the nucleus in order to start replication and transcription whereas RNA viruses, with a few exceptions, start the replication in the cytosol. The mechanisms of capsids' disassembly (uncoating) are multiple and in some cases viruses exploit host cell factors, ribosomes, proteasomes and cytoskeleton motor proteins. For example, Adenoviruses exploit dynein, kinesin and nucleoporins in order to open up viral capsids that are attached to the Nuclear Pore Complex (NPC) (Pérez-Berná et al. 2012). After virus replication and biosynthesis, newly synthesized viral parts are reassembled to make infectious virions. The assembly of viral components is a very complex process divided in three main phases, that must be tightly regulated: 1) the formation of provirions or procapsids, 2) the packaging of viral genome and 3) the maturation of provirions into infectious virions (Steven et al. 2005). Usually, infectious progeny of enveloped virus

particles leave the cells by budding and secretion, while non-enveloped viruses undergo release by cell lysis, even though some may escape by secretory mechanisms after budding into membrane bound compartments. In conclusion, post-entry events lead first to the disintegration of viruses, with a loss in their bodily integrity, and then to the reconstruction of infectious progeny from newly synthesized viral parts. Taken together these processes (disintegration and reconstruction) represent the most fundamental aspects in viruses' life cycle and represent a distinctive feature of viruses (Wolkowicz & Schaechter 2008).

# Chapter 2

## 2.1 Current strategies to fight viruses

In the era of globalization, characterized by widespread and rapid human movements, viral infections are becoming a global health emergency both for developed and poor countries. Infectious diseases account for ~20% of global mortality, with viral diseases responsible for about one third of these deaths (Lozano et al. 2012). Despite advanced diagnostic tools (e.g. genomic sequencing, proteomics, epigenomics) that facilitate detection, identification, and control of infections, the ongoing outbreak of Ebola as well as Chikungunya (CHIKV) and Dengue virus (DENV) underlines human vulnerability to viral pathogens. Nowadays three main strategies are available to fight viral infections: vaccines that prevent infections, antiviral drugs that can treat infectious diseases and virucidal substances that render pathogens non-infective before they interact with the host.

### 2.1.1 Vaccines

Conventionally, the most widely used approach for long-term prevention is vaccination that has led to the effective eradication and confinement of important viral pathogens. Indeed, vaccines are the most powerful tool to prevent viral infections and have accomplished remarkable decreases of virus-related diseases wherever applied (Plotkin 2005). Vaccines are currently made of suspensions of killed microbes or purified and concentrated proteins/polysaccharides from pathogens which stimulate body's immune system (Plotkin 2009). Initially, starting from Pasteur's observations, viruses were attenuated by exposure to high temperatures, oxygen and chemicals. In the twentieth century methodological breakthrough, such as the attenuation of viruses by their growth in cell culture and complete virus inactivation, have led to the development of vaccines against important human viral pathogens like poliovirus, measles virus, mumps virus, rubella virus, varicella zoster virus (Plotkin & Plotkin 2011) (Plotkin 2005). Deep understanding of the mechanisms of virus-

host interaction as well as viral structure have improved the rational design of vaccines. Furthermore, new strategies exploiting virus-like particles have broadened the field of effective vaccination. Moreover, with the advances in molecular biology and genetic engineering, it became possible to create inactivated antigens and attenuated pathogens through directed mutations in their nucleic acids. Thus live recombinant viruses and bacteria, if themselves are not causing illness (apathogenic), may be used as live vaccines (Plotkin 2005). Indeed, in recent years such viral vectors expressing genes encoding for relevant viral proteins as well as virus-like particles and multiprotein structures that mimic native viruses but lack viral genes have been tested in preclinical and clinical studies for improved vaccines against a plethora of viruses (Roldão et al. 2015). Although passive immunotherapy and preventive vaccines are widely diffused, there is an increasing need to develop effective viral inhibitors that can interfere with enzymes involved in the late steps of viral replication, hence blocking further virus propagation.

### **2.1.2 Antiviral drugs**

Despite the success of vaccination programs against human pathogens, such as smallpox, polio, measles, mumps and rubella, the vaccine approach have so far proved to be ineffective with other life-threatening viruses, particularly HIV and Hepatitis C Virus (HCV) (Littler & Oberg 2005). Over the last 30 years, research has thus focused on the development of antiviral drugs effective in the treatment of infections or debilitating diseases caused by three main types of viral pathogens (Littler & Oberg 2005), Table 2. The basic strategies used to design antiviral drugs can target either viral proteins or cellular proteins (De Clercq 2002). Compounds designed to hit viral proteins are more specific, less toxic and with a narrow spectrum of antiviral activity but they are prone to virus-drug resistance development. On the other hand, antivirals targeting cellular proteins have a broader activity spectrum and less chance of resistance development, but higher likelihood of toxicity. The

development of antiviral drugs is strictly dependent on the nature of the virus as well as on the target type of host cell (De Clercq 2002).

**Table 2. Approved antiviral drugs for human deficiency virus (HIV), hepatitis C virus (HCV), herpes simplex virus (HSV) type 1 and type 2.** Table adapted from (Szunerits et al. 2015)

Virus	Antiviral Agent	Administration	Viral Target
HIV	Efavirenz, Nevirapine, Rilpivirine		Non-nucleoside reverse transcriptase inhibitor
	Indinavir		Recombinant protease inhibition
	Raltegravir		Integrase strand transfer inhibitor
	Maraviroc		Antagonists of CCR5 receptor
	Tenofovir	Oral	Nucleotide reverse transcriptase inhibitor
	Atazanavir, Ritonavir, Lopinavirb,		
	Ritonavir, Saquinavir, Tipranavir,		Protease inhibitors
	Darunavir, Indinavir		
	Abacavir, Didanosine,		Nucleoside reverse transcriptase inhibitors
	Emtricitabine, Lamivudine		
Dapivirine	Intravaginal rings	Non-nucleoside reverse transcriptase inhibitor	
Enfuvirtide	Subcutaneous injection	Inhibitor of gp 41	
Zidovudine	Oral + intravenous	Reverse transcriptase inhibitor and stop DNA elongation	
HCV	Ribavirin	Oral	Nucleoside analogue
	Pegylated interferon- $\alpha$	Subcutaneous	Major histocompatibility complex stimulator
HSV	Acyclovir	Oral, topical, intravenous	Inhibitor DNA syntheses
	Penciclovir	Topical	DNA elongation inhibitor
	Famciclovir, Brivudin, Valaciclovir	Oral	DNA elongation inhibitor
	Idoxuridine	Intravenous	DNA elongation inhibitor
	Trifluridine	Eye drops	DNA elongation inhibitor

Being viruses obligate intracellular parasites that depend on the host cell for their replication, only a limited number of virus-specific enzymes can be targeted by antiviral drugs without harming the host. Moreover, each virus has specific metabolic functions, making the development of broad spectrum antiviral drugs difficult (Lembo & Cavalli 2010; Szunerits et al. 2015). Antiviral molecules can target viral processes both extracellularly and intracellularly and thus block the spread of viral infection. The current antiviral repertoire includes two main types of molecules:

- 1) Inhibitors of early events of the infection, like viral adsorption and virus-cell fusion.** Negatively charged polymers, for example polysulfates, polysulfonates, polycarboxylates, polynucleotides, polyoxometalates and negatively charged albumin have been shown to inhibit, in *in vitro* studies, HIV as well as HSV replication, by preventing virus attachment to the membrane of target cells.



Polyanions exhibit two main important properties: broad spectrum activity and low induction of viral resistance in cell culture. However, the activity of polymeric anions *in vivo* is hampered by several drawbacks like short plasma half-life (1-2 hours), rapid degradation in the gut and in plasma and poor ability to penetrate and target infected tissues and cells. The therapeutic usefulness of polyanions *in vivo* will be far from satisfactory and therefore it has been suggested to be used in combination with efficient drug delivery systems in order to exploit their antiviral activity (Lüscher-Mattli 2000). Antiviral drugs can act as antagonist of viruses' co-receptors and thus used to block the fusion between the viral envelope and the cellular plasma membrane. Several compounds (bicyclam AMD3100 and TAK779) have been shown to block HIV entry into the cells as antagonists of the co-receptors CXCR4 and CCR5 (De Clercq 2015; Dragic et al. 2000).

2) **Inhibitors of viral intracellular replicative processes.** Antiviral molecules can act intracellularly, targeting viral enzymes essential in the replicative cycle of viruses, such as the viral DNA polymerase, the reverse transcriptase (RT) and viral integrase and protease. Nucleoside analogues, like acyclic guanosine analogues (acyclovir, penciclovir) or thymidine analogues (brivudin), are used for the treatment of herpesvirus infections and target viral DNA polymerase (De Clercq 2002; Szunerits et al. 2015). The RT is a key enzyme in the replicative cycle of retroviruses, such as HIV, as it synthesizes the proviral DNA, which will then be integrated into the host cell genome and passed on to all progeny cells. RT was identified as a suitable target for antiviral drugs and several nucleoside and nucleotide analogues acting as competitive substrates terminating DNA synthesis have been developed (Littler & Oberg 2005). The process of reverse transcription (from RNA to DNA) is inhibited by the use of nucleoside reverse transcriptase (NRTIs) and non-nucleoside reverse transcriptase inhibitors (NNRTIs) acting as competitive substrates/inhibitors of the respective natural substrates (dNTPs) at the catalytic site of RT. The mechanism of

action of NRTIs, such as zidovudine (azidothymidine, AZT) is depicted in Figure 4.

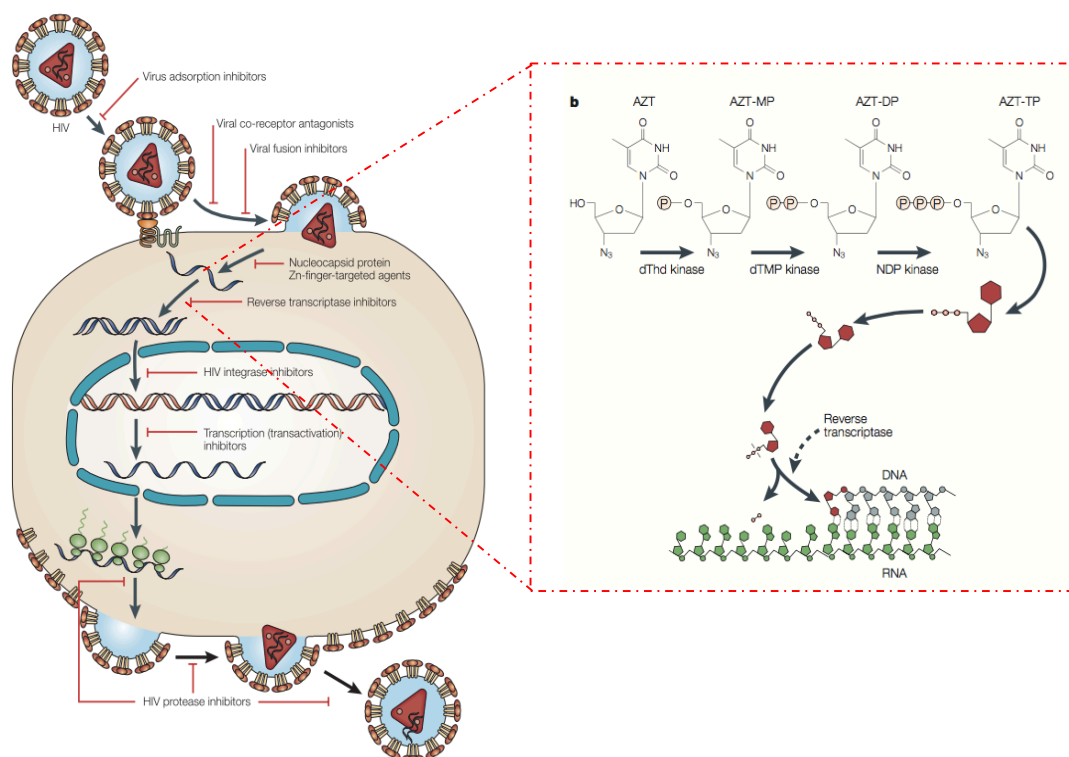


**Figure 4. HIV life cycle and targets for anti-HIV agents.**

The five major families of antiretroviral drugs are: 1) adsorption and fusion inhibitors that block attachment and entry of HIV virions into the host cell, 2) nucleoside or nucleotide reverse transcriptase inhibitors (NRTIs) and 3) non-nucleoside reverse transcriptase inhibitors (NNRTIs) that block the activity of the reverse transcriptase (RT), 4) integrase inhibitors that block the integration of proviral DNA into the host cell DNA, 5) protease inhibitors that interfere with assembly of new infectious virions (Mallipeddi & Rohan 2010). Enlarged the antiviral mechanism of action of 3'-azido-2,3-dideoxythymidine (AZT). AZT is dideoxynucleoside analogue able to stop the replicative cycle of retrovirus, such as HIV, by acting as a chain terminator for the reverse transcription (RNA→DNA) reaction. It can interact with the RT once it has been phosphorylated consecutively inside the host cell by cellular kinases in the form of 5'-triphosphate derivative. Images modified from (De Clercq, 2002) © *Nature Rev. Drug Discov.* (2002) and (De Clercq, 2004) © *Nature Review Microbiology* (2002) Nature Publishing Group.

### 2.1.3 Virucidal molecules

Although immunization, through vaccines, still represents the most effective way to prevent viral infections, other preventive measures against pathogens are also available. Approaches

that limit the spread of viruses are normally accomplished by the application of disinfectant, or virucidal agents, which inactivate viruses on contaminated surfaces or on human hands (Ohtake et al. 2010). Indeed, virucides can attack and inactivate the extracellular viral particles (virions) by physical contact. Oppositely, to virustatic drugs, virucidal molecules act directly and rapidly by either damaging the virion capsid or penetrating into the virion and destroying its genome. As a result, the viral particle integrity could be affected and thus will be no longer able to infect (Galabrov 2007; Al-jabri et al. 2000). Four main application fields of the virucidal agents could be distinguished: 1) disinfectant of the environment, 2) sterilization of biological products, 3) antiviral chemotherapy and 4) elimination of viruses from food, sanitary products and cosmetics. The recent failures of phase III experimental vaccines against HIV highlighted the need of new strategies (e.g. topical formulations of virucidal agents) to limit the infections of HIV through sexual contact (Tripathi et al. 2007). Consequently, the attention of the researchers have focused on seeking several molecules with virucidal activity against HIV-1. Al-Jabri et al. (Al-jabri et al. 2000) observed virucidal activity of four synthesized tyrosine-conjugate bile salt derivatives (di-iodo-deoxycholytyrosine (DIDCT), di-iodo-chenodeoxycholytyrosine (DICDCT), di-iodo-cholyglycyltyrosine (DICGT) and deoxycholytyrosine (DCT)) against three different laboratory-adapted strains of HIV-1 (RF, IIIB and MN) at nanomolar concentrations. Furthermore, other substances like monopercitric acid (MPCA) or chlorcyclizine and ciprofloxacin HCl were found to have virucidal activity against vaccinia virus and HIV respectively (Wutzler & Sauerbrei 2004; Chakrabarty et al. 2000). The main issue regarding the clinical application of virucidal agents is toxicity to human tissues. Virucides can be severely toxic to cells and tissue and hence cannot be used. Thus, the development of non-toxic and effective virucidal agents are needed to prevent the spread of infectious diseases through human contact with contaminated surfaces.

# Chapter 3

## 3.1 Nanotechnology and its healthcare applications

Nanotechnology by definition is the “*intentional design, characterization, production and application of materials, structures, devices, and systems by controlling their size and shape in the nanoscale range (1-100 nm)*” (Kim et al. 2010). Given the nanoscopic dimension of nanomaterials, they can interact with biological molecules and systems with a resultant usefulness for medical applications. The most commonly nanostructured materials employed in medicine and approved by the Food and Drug Administration (FDA) or in clinical trials, are depicted in Figure 5.

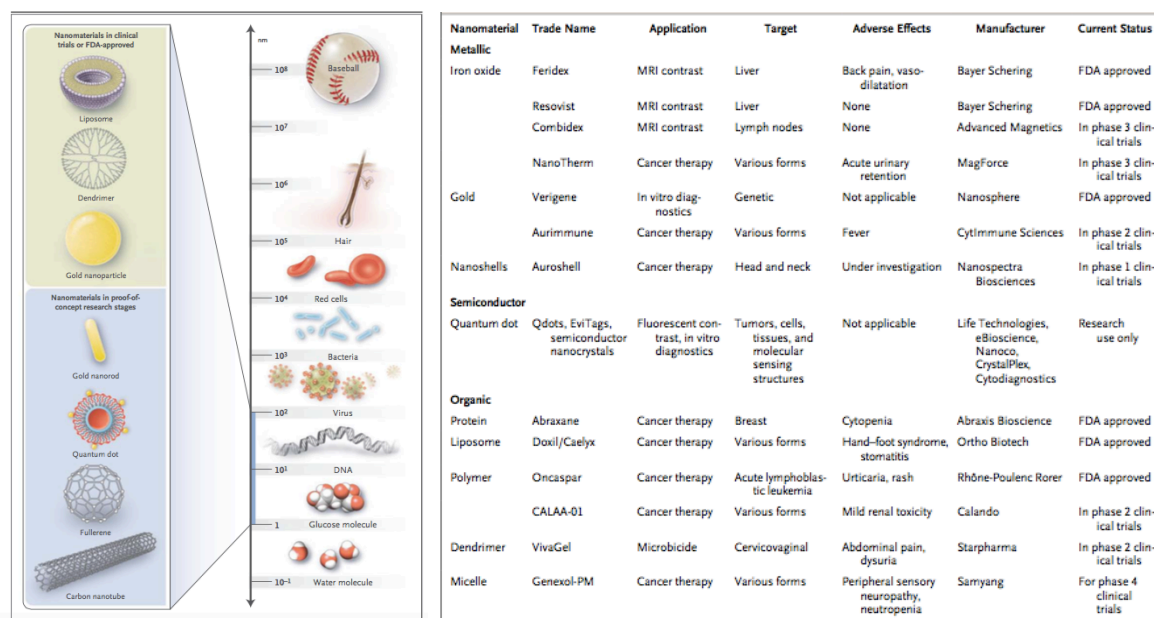


**Figure 5. Nanomaterials used for biomedical application and list of nanomaterials in clinical use.**

Materials in the nanometer range (1-100 nm) are extensively studied for their application in clinics. Some have already been approved by Food and Drug Administration (FDA) while some others are in the proof-of-concept stage in research laboratories. Image modified from (Kim et al. 2010) © *N. Engl. J. Med.* (2010) Massachusetts Medical Society

The main advantages of nanomaterials, compared to atoms or macroscopic materials, is given by their high ratio of surface area to volume as well as their ability to be engineered and have different sizes, shapes and chemical compositions. These properties allowed

nanoscale materials to be used for different application within the field of healthcare (Wagner et al. 2006) (Kim et al. 2010). Nanostructured materials are used as drug delivery vehicles and can improve the bioavailability and pharmacokinetics of approved drug molecule. In case of organic nanomaterials, their hollow or porous core allows the loading of numerous therapeutic agents within a single carrier particle. The use of such nano-carriers enable to finely control their rate of degradation and the consequent release of the therapeutic agents (e.g. antineoplastic drugs). Moreover, nanomaterials can extravasate from blood and accumulate into tumours tissues when tumour vasculature has pores smaller than 200 nm (Hobbs et al. 1998). Nano-carriers can be coated with several polymers, such as polyethylene glycol, which improve their half-life in the blood circulation, prevent the recognition to the immune system and reduce their rapid metabolism and clearance. The controlled release of drugs with nano-carriers ensure their therapeutic action in localized sites thus minimizing adverse effects in healthy tissues (Prencipe et al. 2009; Alexis et al. 2008). Another important application of nanomaterials is for *in vivo* imaging. Indeed, NPs are used as sensitive contrast agents, particularly for magnetic resonance imaging (MRI) and ultrasound, for cancer imaging. The use of superparamagnetic iron oxide nanoparticles (SPIONs) in MRI allows to easily discriminate between tissue with NPs and those without, exploiting their difference in the precession frequency of the proton. SPIONs, used in association with dextran, can detect possible lymph node metastases in prostate cancer owing to their ability to cross the lymphatic vessels and be taken up by macrophages within lymph nodes. Compared to a conventional MRI, the injection of SPIONs increases the diagnostic sensitivity (90.5% vs 35.4%) and specificity (97.9% vs 90.4%) in the detection of tumors far from its primary site (Harisinghani et al. 2007). A key application of nanomaterials (nanotubes, nanowires) is their use as novel sensors for diagnostics. Such enhanced sensors can improve the sensitivity, simplify the readout or amplify the detection threshold of diagnostic devices (Kim et al. 2010). Gold nanoparticles (Au-NPs) bound to the antibody that recognizes the human chorionic gonadotropin (anti-hCG) are used in lateral-flow *in*

*vitro* diagnostic assay (LFA) as a sensitive detection tool in the urine pregnancy test (Posthuma-Trumpie et al. 2009). Moreover, Au-NPs are also used to detect genetic mutations in high-throughput genomic detection devices without the need for polymerase-chain-reaction (PCR) amplification. This approach circumvents the problems associated with conventional fluorescent probes for microarray (photobleaching) and enable the detection of multiple markers with 95% sensitivity having a detection threshold of  $10^{-18}$  M (Nam et al. 2003) (Kim et al. 2010).

Furthermore, mechanical properties and biocompatibility of medical implants can be improved by the use of nanomaterials. Examples include nano-hydroxyapatite (HA) that is used for hard tissue regeneration, especially for orthopaedic and dental application. Nanosized hydroxyapatite particles (< 100 nm), compared to the synthetic HA, are more similar to the natural crystalline structure of HA found in bones. This key feature allows improved cell proliferation due to better cellular adherence with the host cells (Zakaria et al. 2013).

Within this context, among all the nanomaterials designed for clinical applications (liposomes, dendrimers, quantum dots, carbon nanotubes) NPs have gained a lot of attention in pharmaceutical research and development (R&D) for their wide range of applications ranging from drug delivery systems to imaging agents (De Jong & Borm 2008).

### **3.2 Nanomaterials used as antivirals**

Nanomaterials have shown to be a powerful tool for the development of potential and effective pharmaceuticals. The possibility to modify objects at the nanoscale level with enhanced physicochemical properties allow the application of nanomaterials in the field of virology as promising tools for the treatment of viral infections. In particular, nanomaterials can be used in two different ways to fight viral infections:

1. **Nanomaterials as drug nanocarriers**, able to deliver antiviral drugs/molecules

currently on the market improving their physicochemical parameters (bioavailability, drug solubility and pharmacokinetics) (Lembo & Cavalli 2010). Considering nano-delivery systems used in antiviral therapies, they can be divided into six main groups, according to their size and structural composition:

*1.1 Liposomes.* Liposomes are lipidic vesicles that contain an aqueous volume. Their size ranges from a minimum of 20 nm up to microns. Liposomes are used to deliver either hydrophilic drugs, entrapped within their inner aqueous space, or hydrophobic drugs, within the lipid membranes (Lembo & Cavalli 2010). Liposomes preparations, made of various phospholipid compositions, have been characterized as delivery systems of acyclovir drug against genital herpes. They have been incorporated in hydrogels prepared from Carbopol resins that conferred excellent bioadhesive properties and represented a vehicle suitable for vaginal self-administration. *In vitro* release studies revealed that, in this formulation, liposomes incorporated in the hydrogel are applicable as delivery system with a resulting localized and sustained release of encapsulated acyclovir (Filipovic et al. 2005).

*1.2 Micelles.* Colloidal structures such as polymeric micelles have been used to enhance the effective delivery of antiretroviral drugs for HIV. Polymeric micelles prepared with block copolymers of poly(ethylene)oxide-polypropylene oxide (PEO/PPO), also known as Pluronic (such as P85), can inhibit the efflux transporters which are responsible for the low bioavailability on CNS permeability of several antiretroviral drugs. Permeability of zidovudine, nelfinavir and lamivudine is enhanced when co-administered with P85 in bovine brain microvessel endothelial cells and macrophages in *in vitro* models (Mallipeddi & Rohan 2010; Hädicke & Blume 2013).

*1.3 Microspheres.* Microspheres, small spherical particles with diameters in the micrometer range, have been used as drug delivery systems for antiviral drugs. Those manufactured from synthetic materials, like polymeric nanospheres, have been used

as gastroretentive delivery system to improve the oral bioavailability of acyclovir or as a topical formulations to increase the local concentration of acyclovir in the HSV site of infection (Dhaliwal et al. 2008; de Jalón et al. 2001).

*1.4 Dendrimers.* Dendrimers are a class of well-defined hyperbranched polymers with unique properties, such as nanoscale globular shape, well-defined functional groups at the periphery, hydrophobic and hydrophilic cavities. These properties, in particular the highly regular branching pattern and the well defined numbers of exposed functional groups, make them attractive for the binding of drugs, including antivirals, and thus as effective nanocarriers. Acyclovir-thiophosphate dendrimer conjugates have been produced and could be used as water-soluble macromolecular prodrugs (Salamon 2003).

*1.5 Hydrogels.* Antiviral drugs can be incorporated into copolymers hydrogels. Efavirens, a non-nucleoside reverse transcriptase inhibitor (NNRTI) with low aqueous solubility, has been incorporated into polyethylene oxide/polypropylene oxide block copolymer hydrogels for the treatment of HIV in children (Malmsten 2011).

*1.6 Nanoparticles.* Polymeric nanoparticles, such as polyhexacyanacrylate nanoparticles, have been proposed as carriers of antiviral agents for HIV infections *in vitro*. Particles loaded with either the protease inhibitor saquinavir (Ro 31-8959) or the nucleoside analogue zalcitabine (2',3' -dideoxycytidine) have been tested for their antiviral activity in primary human monocytes/macrophages. Saquinavir loaded NPs have been found to be ten times more effective than the drug itself in aqueous solution (1 nM vs 10 nM) (Bender et al. 1996). Similarly, metal NPs like Au-NPs have been tested as an efficient delivery system for small interfering RNAs (siRNAs) against Dengue virus (DENV) infections (Paul et al. 2014). *In vitro* studies showed that anti-DENV siRNAs complexed with cationic Au-NPs enter Vero cells and reduce the replication and the release of infectious virions of DENV serotype 2



(DENV-2). The antiviral ability AuNP-siRNA complexes was exerted both in pre- and post-infection conditions. Moreover, siRNAs complexed with NPs could still inhibit DENV-2 when incubated with RNase, demonstrating that in such formulation siRNAs were less vulnerable to degradation. These findings along with the lack of anti-DENV drugs or vaccines highlight the importance of this nanoparticles delivery system as potential novel anti-DENV strategy cooley (Paul et al. 2014).

- 2. Nanomaterials as active antiviral compounds.** Nanomaterials can themselves interact with viral particles and block the infectious cycle at its very early stages (Lembo & Cavalli 2010). Additionally to their ability to deliver antiviral drugs, nanomaterials can be exploited as antiviral molecules due to their unique features, such as size as well their versatile functionalization properties. In particular, metal nanoparticles, such as gold nanoparticles (Au-NPs) or silver nanoparticles (Ag-NPs) are emerging as promising nanopharmaceutical drugs respect to conventional antiviral molecules. Indeed, considering their small size and, consequently, their high surface area, NPs can engage multivalent interactions with infectious virions and thus interfere with early events of the infection. Regarding Ag-NPs, several recent studies have reported their potential application as antivirals. Elechiguerra et al. (Elechiguerra et al. 2005) described the use of Ag-NPs with three different capping agent molecules (foamy carbon, poly N-vinyl-2-pyrrolidone (PVP) and bovine serum albumin (BSA)) as anti-HIV agents. Ag-NPs were found to inhibit HIV-1 at non-toxic concentrations by *in vitro* assays in a dose-dependent manner. Moreover, through the aid of high angle annular dark field (HAADF) scanning transmission electron microscopy (STEM), they determined that Ag-NPs, within the range of 1-10 nm, were not randomly attached to the virus but they established spatial relationship with the HIV-1 envelope. The Ag-NPs were found to interact with gp120 glycoprotein knobs which are responsible for the attachment and subsequent infection of host cells (Elechiguerra et al. 2005). The mode of action of PVP functionalized Ag-NPs against HIV-1 was further elucidated by Lara et al. (Lara et al. 2010). The antiviral

activity of Ag-NPs was exerted both extracellularly, by blocking the initial HIV-1 absorption, particularly the gp120-CD4 interaction, and intracellularly, showing antiviral activity at post-entry stages, after the cell had been infected. Silver ions could bind RNA or DNA molecules and thus reduce the reverse or proviral transcription rates. In another study, the inhibitory ability of coated Ag-NPs was evaluated with Respiratory Syncytial Virus (RSV) (Sun et al. 2008). Nanoparticles, capped with various proteins (PVP, BSA or recombinant F protein from RSV (RF 412)), were analysed by different techniques for their ability to bind to RSV virions. Transmission electron microscopy (TEM) studies revealed that only PVP-coated Ag-NPs could bind to the viral surface with a regular arrangement, whereas BSA or RF 412-conjugated NPs seemed to interact with RSV, but without a specific association or spatial arrangement. The small size (4-8 nm) and uniformity of PVP-coated NPs, compared to the other two functionalized NPs, lead to hypothesize that they could interact with the RSV envelope glycoproteins (G proteins) which serve as receptor binding protein. These findings along with infectivity assays, which showed that only PVP-coated NPs could inhibit RSV infection, allowed to conclude that Ag-NPs conjugated with PVP protein could bind to RSV glycoproteins involved in the binding to the receptor, thus interfering with viral attachment to the host cell (HepG2) and resulting in the inhibition of viral infection. Other similar studies pointed out the role of NPs coated with different molecules as potential inhibitors of diverse pathogenic viruses. Baram-Pinto et al. described the use of both silver and gold functionalized NPs as useful tools against HPV and HSV-1 (Baram-Pinto et al. 2010; Baram-Pinto et al. 2009). The capping molecule chosen for both the metal particles was mercaptoethane sulfonate (MES) which was intended to mimic HS, the virus binding sites on the cells. Their results indicated that both Ag-MES and Au-MES nanoparticles, but not the soluble MES molecule, could inhibit HSV-1 infection by blocking the attachment and thereby the entrance of the virus into the cell and/or by preventing the cell-to-cell spread of the virus. The use of Au-NPs as antivirals has also been explored

by Papp et al. (Papp et al. 2010). They demonstrated that Au-NPs capped with sialic acid (SA)-terminated glycerol dendron could successfully inhibit the binding of the influenza virus to the plasma membrane. In their study they found that only 14 nm, and not 2 nm, NPs were able to effectively inhibit viral infection in both hemagglutination and inhibition assays. Differently from the aforementioned studies, nanoparticles can exert their antiviral ability by enhancing the immunogenicity against the pathogen without interacting with virions. One interesting application of these new technologies has been used in the treatment of influenza. Scientists created nanoparticles fully covered with hemagglutinin, the attachment protein exploited by H1N1 virus, in order to induce elevated immune responses and counteract its high mutation rate and its ability to efficiently evade host immune system (Kanekiyo et al. 2013).

### **3.3 Nanomaterials used as virucidal agents**

Among the wide range of nanotechnological applications in the field of virology, like drug carrier or antivirals, an emerging field of research explores the use of nanomaterials as virucidal agents. In particular, the use of nanosystems to inactivate infectious particles may be advantageous compared to physical and chemical inactivation approaches, and may significantly contribute to the prevention of viral infection. Lara et al. have suggested that Ag-NPs exert anti-HIV activity binding to viral gp120 glycoprotein and thus acting as virucidal agent, inactivating the HIV-1 after a short exposure of infectious viruses to Ag-NPs, or as inhibitors of viral entry (Lara et al. 2010). Virucidal activity against cell-free HIV-1 was also observed by Bastian A. R. with the use of modified peptide triazole inhibitor (KR13) alone or conjugated to Au-NPs (Bastian et al. 2011). Another potential nanoparticulate system with virucidal action was the gold/copper sulfide (Au/CuS) NPs. Broglie et al. showed that using norovirus GI.1(Norwalk) virus like particles (VLP) as model for human norovirus, they could inactivate viruses by degradation and damage of capsid

proteins (Broglie et al. 2015). Other nanomaterials such as dendrimers or polymeric nanomicelles were also tested for their virucidal activity. The former, SPL7013 dendrimer, formulated in a mucoadhesive carbopol gel (VivaGel) was tested as topical microbicides. Telwette and co-workers found that SPL7013 dendrimer had potent virucidal activity against certain strains of HIV-1 (X4 and R5X4) .

## Chapter 4

### 4.1 Sulfonated NPs as broad spectrum agents for HS-binding viruses

Current advances in nanotechnology opened new frontiers in developing novel antivirals that can interact and inactivate a large number of viral pathogens. Indeed, as demonstrated by several recent studies (Papp et al. 2010; Baram-Pinto et al. 2010), functionalized NPs can be coated on their surface with ligands (molecules) that hinder initial virus-cell interactions, in particular the binding to permissive cells. Molecules bound to the surface of NPs can expose their functional groups mimicking the natural virus receptor and competing for its binding to the cell. Within this context, an attractive strategy to block the adsorption of viruses on cells is using sulfonates as NPs' capping ligands, owing to their potential antiviral activity against the whole subset of viruses specifically binding sulfates on cells (HS-binding viruses). To address this issue, in the present study we investigated the ability of Au-NPs exposing different amounts of sulfonated molecules as antiviral agents. Two types of sulfonated NPs have been selected on the basis of the different ligands arrangements on their surfaces: nanoparticles homogeneously coated by a homoligand shell of 11-mercapto- 1-undecanesulphonates (MUS), called MUS NPs, and nanoparticles that are instead composed by a striated shell of a longer hydrophilic (MUS) and a shorter hydrophobic (1- octanethiol, OT) ligand regularly arranged in ribbon-like domains on the surface, called MUS:OT NPs (Jackson et al. 2004; Uzun et al. 2008). These sulfonated NPs were used in previous experiments for their ability to penetrate cell membrane and were further characterized for their low toxicity in *in vitro* studies. Verma et al. found that NPs coated with amphipathic ligands (MUS:OT) organized in striped domains on their surfaces were able to cross the cell membrane spontaneously, via energy-independent mechanisms, without creating pores and causing damage. In the same study, they demonstrate that NPs functionalized with similar molecules randomly arranged on the surface, unlike MUS:OT, were up taken by conventional endocytic energy-dependent pathways (Verma et al. 2008). Given the low

toxicity profile of MUS:OT NPs as well as their unique biological properties, these NPs were selected as potential antivirals. The use of sulfonate engineered NPs, able to interact with viruses dependent on HSPGs binding, would be a promising strategy compared to the common antiviral strategies for three main reasons. First, the site of action will be extracellular and so more accessible than usual intracellular targets. Second, this approach is not virus specific and therefore could be able to prevent the infection of a wide spectrum of viruses. Third, its efficacy will not be challenged by virus mutations that are the main reason for the development of antiviral drug resistances. Previous attempts proposed sulfated polysaccharides and other negatively charged molecules as competitive antagonists of virus attachment to cells (Lembo et al. 2008; Rupp et al. 2007; Ghosh et al. 2008). However, despite the large number of studies demonstrating their efficacy in preclinical models, sulfated polysaccharides failed in clinical trials (Pirrone et al. 2011). Compared to the aforementioned molecules, sulfonate engineered nanoparticles offer additional advantages, above all a high local concentration of spatially oriented sulfonate residues, chemically bound to NPs and mimicking HSPG host cell surface.

## 4.2 Viruses used for the experiments

In this study, we assessed the role of sulfate presenting NPs with several viruses:

1. **Herpes simplex virus type 1 and 2 (HSV-1, HSV-2).** HSV-1 and HSV-2 belong to the family of Herpesviridae, enveloped DNA viruses. HSV-1 is a common human viral pathogen infecting 70-90% of the world population. Viruses of this subfamily establish lifelong infections by entering a non-replicating latent state, thus avoiding host immune response (Nicoll et al. 2012). Primary infection with HSV, as well as reactivation, are associated with oral (HSV-1) and genital (HSV-2) lesions, ocular diseases, and in rare cases encephalitis (Hadigal & Shukla 2013). The HSV complex structure is composed of a highly ordered protein-shell capsid which encloses the

double-stranded linear DNA (McGeoch et al. 2006). The capsid is surrounded by a layer containing more than twenty different viral and host proteins. A host-derived membrane envelope, with about a dozen viral glycoproteins embedded in the lipid bilayer, forms the outer boundary of the viral particle. Five of these glycoproteins (gB, gC, gD, and the complex of gH and gL) mediate the entry of HSV-1 into the host cells (Subramanian & Geraghty 2007). HSV-1 primary attachment proteins (gB or gC) interact with the host cell by binding to HSPGs (Choudhary et al. 2011). The subsequent step is entry into the cell, which involves binding to a specific entry receptor and is cell-type dependent. Neurons and Vero cells are infected by direct fusion at the plasma membrane and release of the capsid into the cytosol, while in keratinocytes and HeLa cells entry involves different forms of endocytosis (Karasneh & Shukla 2011). A broad spectrum of entry receptors, along with a variety of entry mechanisms, enable HSV-1 to infect almost all cell types (including lymphocytes, epithelial cells, fibroblasts, and neurons).

2. **Human papilloma virus (HPV).** HPV is one of the most common causes of sexually transmitted diseases in both men and women around the world, with prevalence rates varying with the studied population and geographical localization (de Sanjosé et al. 2007). Most HPV infections are transient, and some studies show that the majority of sexually active individuals are exposed to and acquire infection from this virus at some phase in their life (Baseman & Koutsky 2005). HPVs can generally be divided into two tropism groups: those that infect the keratinized surface of the skin, causing common warts, and those that infect the mucosa of the mouth, throat, respiratory tract, and especially the anogenital tract (Burd 2003; Mistry et al. 2008). Today, more than 120 different HPV types have been catalogued, and about 40 can infect the epithelial cells of the anogenital tract and other mucosal areas of the human body (Bernard et al. 2010). Those viruses are classified according to their involvement in the genesis of benign or malignant lesions: 1) low-risk oncogenic HPV (LR-HPV)

are those associated with anogenital warts, which are benign, hyperproliferative lesions with a very limited tendency for malignant progression, mostly caused by HPV 6 and 11, 2) high-risk oncogenic HPV (HR-HPV) that are strongly associated with premalignant and malignant cervical lesions, especially caused by HPV 16 and 18 (Bosch et al. 2008; de Villiers et al. 2004). Persistent infection with HR-HPV is unequivocally established as necessary for the onset of cervical cancer (Bosch et al. 2002). HPV is a non-enveloped virus that contains a double-stranded, closed circular DNA genome, associated with histone-like proteins and protected by a capsid with icosahedron symmetry, formed by two protein types. Each capsid is composed of 72 capsomeres, each of which is composed of five monomeric units that join to form a pentamer corresponding to the major protein capsid (L1). The L1 pentamers are distributed forming a network of intra- and interpentameric disulfide interactions, which stabilize the capsid (Sapp et al. 1995). L2 protein is the secondary component of viral capsid and is located within the virion.

3. **Lentiviral vectors (LV).** Lentiviral vectors, derived from HIV, were created as efficient vehicles for gene transfer owing to their ability to infect dividing and non-dividing cells. The first lentiviral gene delivery system was described by Naldini et al. (Naldini L. et al. 1996) in 1996 consisting in the use of a replication-incompetent HIV vector capable of transducing non-dividing neurons when injected into rat brains. Lentiviral vector production requires the co-transfection of several plasmids expressing lentiviral structural and enzymatic proteins along with “a vector plasmid” carrying the genetic cargo of interest into Human Embryonic Kidney (HEK) 293T cells (Peltier & Schaffer 2010). First and second-generation of lentiviral vectors were constituted by three different plasmids while third-generation vectors are based on four plasmids. Use of lentiviral vectors systems is particularly desirable given their extraordinary ability to accommodate heterologous envelope proteins and thus acquire novel cellular tropism and intracellular behaviour (Durand & Cimarelli



2011). Incorporation of different proteins, called pseudotyping, is a process common to all retroviruses and allows to engineer viral particles with envelope proteins, such as the vesicular stomatitis G protein (VSV-G), that mediate viral entry into a wide variety of cells. Similarly, lentiviral vectors can be pseudotyped with envelope proteins (gp160) that specifically target cellular receptors (CD4) expressed on the selected cell type (e.g. lymphocytes). These features allowed lentiviral vectors to become an important laboratory tool for the transduction of cell types resistant to gene transfer (e.g. dendritic cells and neurons) as well as for their use as safe and non-pathogenic replicas of HIV for the study of HIV biology, (tropism, penetration, genome integration) (Anon 2006).

4. **Adeno associated viruses (AAVs).** AAVs, non-enveloped DNA viruses (25 nm), belong to the family of *Parvoviridae* and are able to infect and replicate into a wide range of human and nonhuman cells, in presence of a helper virus (Adenovirus or herpesvirus). To date twelve human serotypes of AAVs (AAV1 to AAV12) and hundreds from nonhuman primates have been discovered (Daya & Berns 2008). AAVs possess key features such as, lack of pathogenicity, wide range of infectivity, ability to establish long-term transgene expression and site-specific integration/episomal maintenance (Wu et al. 2006), features that make them suitable for gene therapy applications. Indeed, recombinant AAVs (rAAVs) are frequently used as delivery vehicles for gene transfer and are already being used in more than 20 human clinical trials, as in the case of AAV microdystrophin gene vectors for Duchenne muscular dystrophy (DMD) (Athanasopoulos et al. 2004). The presence of several human AAV serotypes, with distinct tropism, allow their selective use toward specific types of cells. Serotype two (AAV2) is the most characterized AAV. It initially binds to HSPG which act as cell attachment factor and subsequently engage interactions with two coreceptors,  $\alpha_v\beta_5$  integrin and fibroblast growth factor

receptor 1 (FGFR-1) that trigger its endocytic uptake of AAV2 (Büning et al. 2003). On the other hand, serotype 5 (AAV5) has a different cell surface attachment mechanism and binds alpha 2-3 sialic acid (Kaludov et al. 2001).

5. **Adenovirus (Ad).** Adenoviruses are non-enveloped, double stranded DNA viruses of approximately 90 nm in diameter. Viral DNA and core proteins are enclosed in an icosahedral capsid composed of hexon and penton proteins along with elongated fiber proteins. Adenoviruses belonging to the species C (Ad2 and Ad5) are widely used as genetic transfer vehicles. Adenovirus-based vectors are attractive candidates for gene therapy because their genome is well characterized and easy to manipulate and they have a broad tropism which allows to infect a wide variety of dividing and non dividing cells (Tatsis & Ertl 2004; Zhang & Bergelson 2005; Meier & Greber 2004).

## II. AIM OF THE STUDY

Considering the rapid diffusion of viruses and the limits in contrasting their spread, in the present work we have investigated the use of nanoparticles as wide-spectrum antiviral agent. To achieve this purpose, we used Au-NPs coated with sulfonate molecules. Our hypothesis was that the NPs interfere, through competition mechanism, with the attachment step and hence blocking the infectious cycle of whole subset of viruses that attach and recognize target cells by binding heparan sulfates as part of the glycocalyx exposed on cell membrane. We studied in detail the mechanism of action using as a model virus a replication defective virus (LV) as well as wild-type pathogenic viruses, such as HSV-1 and HSV-2.

# III. MATERIALS AND METHODS

## Materials

### 3.1 Synthesis of functionalized Au-NPs

NPs were synthesized in-house and consist of an inorganic gold core coated with a self-assembled monolayer (SAM) of thiolated organic molecules. Two types of monolayer-protected Au-NPs were investigated for their potential antiviral activity:

- 1) NPs coated with negatively charged sulfonated alkanethiols, 11-mercapto-1-undecanesulphonate (MUS) alone, referred as MUS NPs
- 2) NPs capped with 2:1 molar mixture of MUS and 1-octanethiol (OT) ligand, referred as MUS:OT (66:34)

In addition, in order to assess the ability of sulfonated NPs to inhibit HSPG-dependent viruses, we included in the study gold NPs functionalized with oligo ethylene glycols (EG<sub>2</sub>-OH) NPs used as control for non-sulfonated NPs.

Briefly, for MUS and MUS:OT NPs synthesis, 1.2 mmol of gold salt (HAuCl<sub>4</sub>) were dissolved in 200mL of ethanol and 1.2 mmol of the desired thiol ligand mixture was added while stirring the reaction solution. Subsequently, a saturated ethanol solution of sodium borohydride (NaBH<sub>4</sub>) was added dropwise for 2 h. The solution was stirred for 3 h and the reaction flask was then placed in a refrigerator overnight. The product was washed several times (3 to 5) by suspending and centrifuging (5500 rpm) in methanol, ethanol and then acetone. NPs were washed 5 times with deionized water using Amicon Ultra-15 centrifugal filter devices (10k NMWL) in order to remove unbound ligands and side products (as determined by <sup>1</sup>H NMR). Non-sulfonated Au-NPs (EG<sub>2</sub>-OH NPs) were synthesized in-house according to a modified Stucky procedure (Zheng & Stucky 2006). The reaction was performed in a 100 ml 3-neck round bottom flask in a total volume of 20 ml of a mixture of dimethylformamide and 20% Methanol (Sigma Aldrich, Italy), at 100 °C on an oil bath under

reflux. Briefly, 0.25 mmol of Chloro(triphenylphosphine)gold(I) (Sigma Aldrich, Italy) and 0.125 mmol of HS-(CH<sub>2</sub>)<sub>6</sub>-(OCH<sub>2</sub>CH<sub>2</sub>)<sub>2</sub>-OH (ProChimia Surfaces, Poland) were dissolved in 15 ml of solvent and then stirred in a 100 ml 3-neck round bottom flask for at least 20 min. When the reaction temperature is reached, 2.5 mmol of Borane tert-butylamine complex previously dissolved in 5ml of solvent were added in one portion to the reaction mixture. The solution color turns from transparent to light brown and then slowly to deep red. The reaction is left stirring at 100°C for 1h 30'. Afterward, the heating is turned off and the solution is left stirring for additional 3h. To recover the nanoparticles, 80 ml of acetone (Sigma Aldrich, Milan, Italy) were added to the solution that was placed at 4°C overnight. A black precipitate of Au-NPs was suspending and centrifuging at 3220g for 20' in washed acetone. The black precipitate was left to dry under vacuum. Subsequently the black precipitate was dissolved in ultrapure deionized water (18.2 MΩ cm at 25°C, Millipore, Italy) and dialysed extensively against ultrapure deionized water in a 2L beaker for 72h. Removal of residual salts from the synthesis was checked by measuring the conductivity of a 0.5 mg/ml solution of nanoparticles, which had to be below 5 μS/cm. The solution obtained after the dialysis was then concentrated through diafiltration with Vivaspin 6 ml (Sartorius, SIGMA Aldrich, Italy) to a final volume between 1-2 ml. This volume was then lyophilised (freeze dried) and the powder recovered (the process decreases the yield to circa 30-35 mg). All the NPs were characterized by TEM and zeta potential. All chemicals were purchased from Sigma Aldrich except for the MUS ligand, which was synthesized in-house according to the previously published method (Verma et al. 2008). All solvents purchased were reagent grade and purged with nitrogen gas for more than 30 minutes prior to the reaction.

### **3.2 Cell Culture**

HeLa (human cervical carcinoma cell line), HEK293T (human embryonic kidney), Jurkat (human T lymphocyte cell line), CHO-K1 (Chinese hamster ovary cell line), Vero (African

green monkey fibroblastoid kidney cells) and HT-1080 (human fibrosarcoma cell line) were purchased from ATCC (American Type Culture Collection, Rockville, MD). HEK293T and HT-1080 cells were cultured in Dulbecco's modified Eagle's medium (DMEM; Euroclone) containing 10% foetal bovine serum (FBS), 1% L-glutamine and 1% penicillin/streptomycin. HeLa cells were cultured in Eagle's minimal essential medium (MEM - Invitrogen, Carlsbad, CA) supplemented with 10% FBS SA, 1% L-glutamine and 1% penicillin/streptomycin (Euroclone). Jurkat cells were maintained in RPMI 1640 (Euroclone, Carlsbad, CA) supplemented with 10% FBS and 1% L-glutamine and 1% of penicillin and streptomycin. CHO-K1 were cultured in Ham's F12-K medium (Invitrogen) supplemented with 10% FBS SA, 1% L-glutamine and 1% penicillin/streptomycin. Vero cells, were grown in MEM medium (Gibco/BRL, Gaithersburg, MD) supplemented with 10% heat inactivated foetal calf serum (FCS; Gibco- BRL), and 1% antibiotic-antimycotic solution (Zell Shield, Minerva Biolabs GmbH, Berlin, Germany). 293TT cell line, derived from human embryonic kidney cells transformed with the simian virus 40 (SV40) large T antigen (Buck et al. 2006), was cultured in DMEM (Gibco-BRL, Gaithersburg, MD) supplemented with heat-inactivated 10% foetal calf serum (FCS; Gibco- BRL), Glutamax-1 1% (Invitrogen, Carlsbad, CA) and nonessential amino acids 1% (Sigma Aldrich, Steinheim, Germany). All cells lines were grown in humidified atmosphere with CO<sub>2</sub> (5%) at 37°C. HeLa cells expressing human CD4 protein on the cell surface (HeLa T4+) were purchased from NIH AIDS reagent program. HeLa T4+ were cultured in DMEM (Euroclone) containing 10% foetal bovine serum, 2mM L-glutamine and 1% penicillin/streptomycin at 37°C in humidified atmosphere with 5% CO<sub>2</sub>.

### **3.3. Viruses**

#### **3.3.1 Lentivirus: production and purification**

Lentiviruses (LV), that are engineered viral vectors obtained from the human

immunodeficiency virus (HIV), are the most widely used viral tool for gene delivery due to their ability to mediate potent transduction and stable expression into dividing and non-dividing cells. Lentiviral particles can be manipulated to carry different glycoproteins (GPs) derived from other enveloped viruses (pseudotyping) allowing to an extension of the tropism. In this study, two pseudotyped lentiviral vectors were produced differing only for the expression of their enveloped proteins: LV carrying the G protein of the vesicular stomatitis virus (VSV-G) and LV exposing the glycoprotein of HIV (gp160). Production of such phenotypically mixed virus particles was accomplished in three steps: 1) calcium phosphate transient co-transfection of HEK293T cells with all necessary plasmids, 2) concentration of viral vectors using PEG 6000 and 3) purification by ultracentrifugation on a sucrose cushion (Tiscornia et al. 2006). Generation of infectious lentiviral particles required the expression of essential genes in HEK293T cells through several plasmids: 1) lentiviral expression plasmid (pRRLSIN.cPTT.PGK-GFP.WPRE), carrying the transgene sequence encoding GFP, 2) plasmids encoding packaging proteins (pMDLg/pRRE, pRSV-Rev), with gag, pol, rev and tat genes and finally 3) pseudotyping plasmid (pMD2.G) encoding the envelope glycoprotein of VSV (VSV-G) or plasmid encoding the envelope protein of HIV (gp160). The Env plasmid encoding for gp160 of HxB2 strain of HIV was kindly donated by Prof. Didier Trono (Laboratory of virology and genetics at École polytechnique fédérale de Lausanne - EPFL). The HIV-Env plasmid was previously amplified through transformation of chemically competent *E.coli* (One Shot<sup>®</sup>, Invitrogen) and then purified using QIAGEN Plasmid Maxi Kit. Lentiviral particles were collected 48 hours after transfection. LV particles were then concentrated by precipitation using PEG-it<sup>™</sup> (System Biosciences, SBI) and resuspended in PBS. Concentrated virus was transferred in cryo-tubes and stored at -80°C. Subsequently, the titer was calculated as the number of functional particles able to deliver their genetic materials in cells (transducing units/ml - TU/ml) and determined in HeLa cells using serial dilutions of lentiviral preparation,

evaluating the percentage of GFP positive cells by flow cytometry. Lentiviral stocks, produced in-house, had titers ranging from  $\approx 5 \times 10^6$  TU/ml to  $\approx 5 \times 10^8$  TU/ml and were used at  $10^5$ - $10^6$  TU/ml in cell experiments.

In order to obtain lentiviral stocks with higher degree of purity for Western blot and DLS experiments, lentiviral particles stored at  $-80^\circ\text{C}$  were rapidly thawed and further purified through ultracentrifugation on 20% (w/v) sucrose cushion. Viral preparations (200  $\mu\text{l}$ ) were layered on 1.5 ml of 20% sucrose in PBS into ultracentrifuge tubes (Beckman Coulter Inc). Subsequently, samples were ultracentrifuged at 19000 rpm for 2h at  $20^\circ\text{C}$  using a Beckman SW41 (Beckman Coulter Inc) swinging bucket rotor. Finally, the supernatant was discarded and the virus pellet was resuspended in 50  $\mu\text{l}$  of PBS.

### **3.3.2 Adenovirus (Ad)**

Purified human recombinant Adenovirus (Ad) type 5 encoding for green fluorescent protein (GFP) was purchased from vector Biolabs (Philadelphia, PA, USA). According to manufacturer's data, Adenovirus was centrifuged using two sequential caesium chloride (CsCl) gradients, resuspended in PBS with 5% (w/v) glycerol and stored at  $-80^\circ\text{C}$ . Furthermore, the product was tested for sterility and titrated with UV spectrophotometric measurement at 260 nm calculating the number of viral particles (vp/ml) that resulted to be  $5 \times 10^{10}$  vp/ml.

### **3.3.3 Adeno-associated virus (AAV)**

Different serotypes of recombinant Adeno-associated viruses (AAVs) encoding GFP (AAV2-GFP, AAV5-GFP) were purchased from Vector Biolabs (Philadelphia, PA, USA). According to manufacturer's data, AAVs were purified through serial gradients of caesium chloride (CsCl) and titrated measuring genome particles (GC/ml). AAVs had a titre of roughly  $1 \times 10^{13}$  GC/ml and were stored at  $-80^\circ\text{C}$  in PBS with 5% glycerol.



### **3.3.4 Herpes simplex virus type 1 and type 2 (HSV-1 and HSV-2)**

Clinical isolates of HSV-1 and HSV-2 were kindly provided by Prof. M. Pistello, (University of Pisa, Italy). HSV-1 and HSV-2 strains were propagated and titrated by plaque assay on Vero cells. Virus stocks were maintained frozen at -80 °C.

### **3.3.5 Human Papilloma pseudovirus (HPV-16 PsV) production**

Plasmids and 293TT cells used for pseudovirus (PsV) production were kindly provided by John Schiller (National Cancer Institute, Bethesda, MD). HPV-16 PsVs were produced according to previously described methods (Buck et al. 2005). Briefly, 293TT cells were transfected with plasmid expressing the papillomavirus major and minor capsid proteins (L1 and L2, respectively), together with a reporter plasmid expressing the secreted alkaline phosphatase (SEAP), named pYSEAP. Capsids were allowed to mature overnight in cell lysate; the clarified supernatant was then loaded on top of a density gradient from 27% to 33% to 39 % Optiprep (Sigma-Aldrich, St. Louis, MO) at room temperature for 3 h. The material was centrifuged at 28000 rpm for 16 h at 4°C in an SW41.1 rotor (Beckman Coulter, Inc., Fullerton, CA) and then collected by bottom puncture of the tubes. Fractions were inspected for purity in 10% sodium dodecyl sulfate (SDS)–Tris–glycine gels, titrated on 293TT cells to test for infectivity by SEAP detection, and then pooled and frozen at -80°C until needed. The L1 protein content of PsV stocks was determined by comparison with bovine serum albumin standards in Coomassie-stained SDS-polyacrylamide gels.  $\mu$

### **3.4 Antiviral drug 3'-azido-3'-deoxythymidine (AZT)**

The antiretroviral drug AZT was purchased from Sigma-Aldrich and stored at –20°C. It was dissolved in water and aliquots were prepared before *in vitro* experiments.

## Methods

### 3.5 *In vitro* cell-toxicity assay

The toxicity of Au-NPs was examined using propidium iodide (PI, Sigma) flow cytometric assay or MTS [3-(4,5-dimethylthiazol-2-yl)-5-(3-carboxymethoxyphenyl)-2-(4-sulfophenyl)-2H-tetrazolium] assay. Propidium iodide, a fluorescent stain for nucleic acid, allows to calculate the amount of dead cells due to its inability to penetrate into live cells. Indeed, PI could only penetrate into cells that exhibit compromised plasma membrane and intercalates into double stranded DNA. Once the dye is bound to DNA it is excited at 488 nm and emits at a maximum wavelength of 617 nm. The percentage of viable cells was measured following the same experimental conditions as for the NPs/virus interaction study. Cells were incubated with different concentrations of NPs (from 0.1 µg/ml to 100 µg/ml – 0.1 nM to 100 nM) for 48 h at 37°C. After incubation with nanomaterials, cells were harvested by trypsin, washed with 1ml PBS supplemented with 1% BSA and the pellet was resuspended in 500 µl of PBS. Finally, 2 µl of PI, at the concentration of 50 µg/ml in PBS, were added to the samples and incubated for 5 min at RT in the dark. PI fluorescence was immediately determined on a FACS CANTOII flow cytometer (Beckton Dickinson, San Jose, CA). Unstained cells were used as negative control samples. The results were analysed using BD FACSDiva software. For the MTS assay, cell cultures seeded in 96-well plates were incubated with different concentrations of NPs or ligand under the same experimental conditions as described for the antiviral assays. Cell viability was determined by the CellTiter 96 Proliferation Assay Kit (Promega, Madison, WI, USA) according to the manufacturer's instructions. Absorbance was measured using a Microplate Reader (Model 680, BIORAD) at 490 nm. The effect on cell viability at different concentrations of nanoparticles was expressed as percentage of live cells, by comparing the absorbance of treated cells with the one of cells incubated with culture medium.

### **3.6 Cell-surface staining**

The expression of CD4 proteins on the surface of HeLa T4<sup>+</sup> cells was determined by antibody staining of cell markers and quantified by FACS analysis. Briefly, cells were harvested, centrifuged at 3000 rpm for 5 min and washed once with PBS 1% BSA. Pellet was incubated for 30 min with PBS 5% BSA, washed with PBS 1% BSA and incubated for 1 h at RT with mouse APC anti-human CD4 primary antibody (TONBO Biosciences). The antibody was kindly donated by Dr. Maria Rescigno (Immunobiology of Dendritic Cells and Immunotherapy Laboratory – European Institute of Oncology (IEO), Milan – Italy). The APC anti-human CD4 antibody was diluted 1:1000 in PBS 1% BSA. After three washing steps with PBS 1% BSA cells were fixed with formaldehyde 2% and incubated for 20 min on ice. Finally, cells were washed with PBS 1% BSA, resuspended in PBS and analysed measuring the percentage of stained cells (APC<sup>+</sup> cells) by flow cytometry.

### **3.7 Au-NPs preparation for antiviral assay studies**

NPs were dissolved in Milli-Q grade water, sonicated for 20 min at room temperature and then filtered with a 0.22 µm filter in order to sterilize and remove precipitates. Before the use with cells, an appropriate amount of 10x PBS was added to the NPs solutions in order to obtain the final concentration ready to use in 1x PBS.

### **3.8 Antiviral Assays**

#### **3.8.1 Pseudotyped Lentiviruses (LV-VSV-G, LV-gp160), Adenovirus and AAVs inhibition assay.**

Pseudotyped Lentiviruses or Adenovirus or AAV2/5, carrying GFP as reporter gene, were resuspended in PBS and incubated with increasing concentrations of sulfonated or non-sulfonated NPs, at concentrations from 0.01 µg/ml (0.01 nM,  $\approx 10^9$  NPs) to 100 µg/ml (100 nM,  $\approx 10^{13}$  NPs), in PBS for 1h at 37°C prior to cell infection. The mixture of

virus/nanoparticles was subsequently added to permissive cells and transduction was stopped after 48h. Cells were fixed with 1% p-formaldehyde (PFA), resuspended in PBS and analysed. Transduction efficiency, calculated as the % GFP+ cells, of LV-VSV-G and Adenovirus was measured by flow cytometry whereas confocal laser scanning microscopy was used to for LV-gp160 and AAVs.

For LV-VSV-G and Adenovirus, inhibition assay was carried out in 12-well plates with  $10^5$  cells. HeLa, Jurkat and HT-1080 cells were used for LV-VSV-G while HeLa cells for Adenovirus, using roughly  $10^5$  TU/ml of LV-VSV-G or Adenovirus.

Inhibition assays for LV-gp160 and both serotypes of AAVs (AAV2 and AAV5) were performed on  $\mu$ -Slide 8 well Glass Bottom plates (Ibidi®) with  $\approx 2 \times 10^4$  cells (HeLa T4+ cells for LV-gp160 and CHO-K1 cells for AAVs) with an equal amount of viruses. The same experimental procedure was followed for the inhibition assay of antiretroviral drug (AZT) with LV-VSV-G in HeLa cells.

### **3.8.2 HSV-1, HSV-2 antiviral assay.**

The antiviral effect of MUS:OT NPs on HSV- 1 and HSV-2 infection was evaluated by a plaque reduction assay. Each virus was incubated with increasing concentrations of NPs (0.01  $\mu$ g/ml to 100  $\mu$ g/ml), for 1h at 37°C and then added to the permissive cell line. Following virus adsorption (2h at 37°C), the virus inoculum was removed; cells were washed and then overlaid with a medium containing 1.2 % methylcellulose (Sigma). After 24 h (HSV-2) or 48 h (HSV-1) post incubation at 37°C, cells were fixed and stained with 0.1 % crystal violet in 20 % ethanol and viral plaques were counted.

### **3.8.3 HPV-16 PsV antiviral assay.**

HPV-16 PsV was incubated with increasing amount of MUS:OT NPs (0.01  $\mu$ g/ml to 100  $\mu$ g/ml) for 1h at 37°C. PsV-NPs mixture was added to 293TT cells and incubated for 72h.

The SEAP content in the supernatant was determined using a Great Escape SEAP Chemiluminescence Kit (BD Clontech, Mountain View, CA) as directed by the manufacturer. Thirty minutes after the addition of the substrate, samples were read using a Wallac 1420 Victor luminometer (PerkinElmer Life and Analytical Sciences, Inc., Wellesley, MA).

### **3.9 Time of addition (TOA) experiments**

In order to determine whether the MUS:OT NPs could exert their antiviral activity before or after virus infection, acting as antiviral molecules (such as AZT), a time-of-addition experiment was performed on 12-well plates with LV-VSV-G ( $10^5$  TU/ml) in a final volume of 1 ml. Indeed, MUS:OT NPs, from 0.1  $\mu\text{g/ml}$  (0.1 nM,  $\approx 10^{10}$  NPs) to 100  $\mu\text{g/ml}$  (100 nM,  $\approx 10^{13}$  NPs), or AZT (used as a control for its mechanism of action as antiviral drug) were incubated with HeLa and HT-1080 cells ( $10^5$  cells/well) at 37°C for long (3h, 2h) or for short (30 min, 10 min) times before infection. Cells were then washed with PBS and LV was added for 1h at 37°C. After another washing step with PBS to eliminate unpenetrated virus, cells were kept at 37°C for 48h and analysed. In parallel, in order to evaluate how long the addition of a compound (NPs or AZT) can be postponed before the loss of its antiviral activity, NPs or AZT were incubated with cells at different times post infection (0, 10min, 30min, 1h, 3h). Then, cells were harvested and analysed after 48h at 37°C. NPs or AZT were also co-added with LV during the infection in order to evaluate their antiviral role when they get in contact with the virus without any previous incubation step. LV untreated, without NPs or AZT, was used as a control.

### **3.10 Virucidal assay**

The effect of sulfonated MUS:OT NPs upon infection of HSV-2, LV-VSV-G and Adenovirus was evaluated by incubating an effective inhibitory concentration of MUS:OT

NPs, > 100 µg/ml ( >100 nM, >10<sup>13</sup> NPs), with viruses for 2h at 37°C as previously described (Cavalli et al. 2012). After incubation, the residual virus infectivity was determined by titration at high dilutions.

### **3.11 Attachment assay**

Attachment assay was performed on 12-well plates with LV-VSV-G (10<sup>5</sup> TU/ml) in HT-1080 permissive cells (10<sup>5</sup> cells/well). Briefly, pre-chilled HT-1080 cells were transfected with Lentivirus and MUS:OT NPs at 100 µg/ml (100 nM, ≈10<sup>13</sup> NPs) for 1h at 4°C. Cells were washed with cold PBS for three times in order to eliminate unbound viruses and then the temperature was shifted to 37°C for 1h, to allow the bound viruses to get internalized in the cells. After three washes in PBS cells were incubated for 48h at 37°C and then analysed by flow cytometry for GFP expression.

### **3.12 Entry assay**

The role of MUS:OT NPs during the entry phase was evaluated on 12-well plates with LV-VSV-G (10<sup>5</sup> TU/ml). Permissive HT-1080 cells (10<sup>5</sup> cells/well) were pre-chilled and incubated with LV particles alone for 1h at 4°C. After three washes with cold PBS, cells were shifted at 37°C and treated with MUS:OT NPs at 100 µg/ml (100 nM, ≈10<sup>13</sup> NPs) for 1h. Finally, cells were washed with PBS and incubated at for 48h at 37°C analysed by flow cytometry for GFP expression.

### **3.13 Quantification of transduced cells (GFP+)**

#### **3.13.1 FACS analysis**

Cells were harvested by trypsin digestion, washed with PBS and fixed in 1% PFA (paraformaldehyde) in PBS for 10 min at room temperature. Approximately 20000 events (cells) were analysed per sample and cells with no virus were used as negative control in

order to determine the autofluorescence background. Transduced cells were calculated as the percentage of GFP<sup>+</sup> cells over the total population of cells analysed. The expression of the GFP protein on cells transduced with LV-VSV-G or Adenovirus was assessed through the BD FACSCalibur™ flow cytometer (BD Biosciences) and data were analysed with BD CELLQuest™ software (BD Biosciences).

### **3.13.2 Confocal Laser Scanning Microscopy (CLSM)**

Transduction efficiency (GFP<sup>+</sup> cells) of LV-gp160 and AAVs (AAV2, AAV5), in presence or absence of MUS:OT NPs, was visualized by using an inverted confocal laser scanning microscope (Leica TCS SP5) equipped with blue (488 nm) excitation laser line. Cells were previously fixed in 2% PFA (paraformaldehyde) in PBS for 10 min.

### **3.14 Western Blot analysis**

Western blot (WB) analysis was performed in order to confirm the expression of the proteins exposed on LV particles (VSV-G or gp160). Pseudotyped lentiviral vectors, LV-VSV-G and LV-gp160, were boiled for 30 min at 95°C, loaded and run on 4-20% precast polyacrylamide gel (Mini-PROTEAN® TGX™, BioRad). Proteins were then transferred onto a nitrocellulose membrane (0.45µm pore; Whatman Group). After blocking with 5% skimmed Milk in PBS for 2h at room temperature, proteins of interest were detected with specific primary antibodies: mouse monoclonal antibodies anti-HIV p24 (abcam®) diluted 1:2000, mouse monoclonal antibody anti-VSV-G tag (abcam®) diluted 1:2000 and goat polyclonal antibody anti-gp120 (abcam®) diluted 1:500. Primary antibodies were diluted in 5% skimmed Milk in PBS and incubated overnight, at 4°C. After three washes in PBST, appropriate HRP conjugated secondary antibodies, anti-mouse 1:10000 and anti-goat diluted 1:100000 in PBST were added for 40 min at room temperature. Finally, membranes were washed three times in PBST and peroxidase activity was detected with a light sensitive film using an ECL

Plus kit (Pierce) by mixing equal amounts of reagent 1 with reagent 2.

### **3.15 Dynamic Light Scattering (DLS) and $\zeta$ -potential**

A Zeta Nanosizer unit (Malvern) was used to perform dynamic light scattering and  $\zeta$ -potential measurements, equipped with a laser at 633 nm wavelength. The instrument was operating in back scattering mode (BSM) at an angle of 173°. Measurements were run at least 5 min (5 measurements for each sample, 25 runs, 5 seconds each). The measurements were performed at 25°C. NPs solution in water and PBS were sonicated 15 minutes at room temperature and filtered 3 times with filter having 0.22  $\mu\text{m}$  pore size before measurements. High concentration zeta cell kit was used to perform  $\zeta$ -potential measurements. The same conditions were applied to calculate the particle size distribution of purified lentiviral vectors (LV-VSV-G).

### **3.16 Cryo-Electron Microscopy (cryo-EM)**

Cryo-EM images were acquired at the SUNMIL group at École Polytechnique Fédérale de Lausanne (EPFL), Switzerland. Briefly, for cryo-EM imaging samples (3-4  $\mu\text{l}$ ) were deposited onto Quantifoil grids, blotted and plunge frozen with a Vitrobot and then acquired in a Tecnai G2 Spirit BioTWIN microscope (FEI) in low dose mode at 30kx magnification. HSV-2 ( $10^7$  PFU/mL) were incubated for 1.5h at 37°C with MUS:OT NPs (200  $\mu\text{g}/\text{ml}$ ).

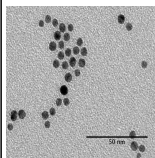
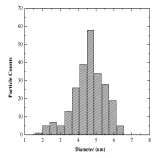
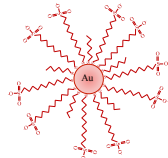
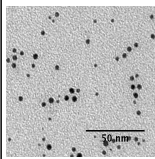
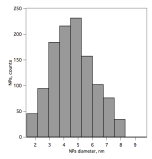
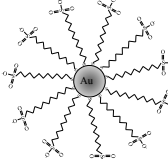
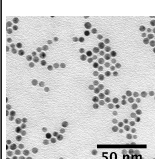
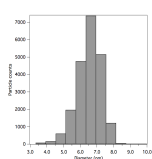
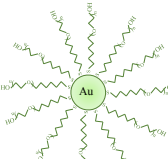


## IV. RESULTS

### 4.1 Characterization of Au-NPs

MUS:OT, MUS and EG<sub>2</sub>-OH NPs were synthesized in-house as described in materials and methods. In Table 3 is shown the physical-chemical characterization of Au-NPs having different surface functionalization. TEM measurements revealed that MUS:OT and MUS NPs had an average size of  $4.5 \pm 1.0$  nm and  $4.3 \pm 1.3$  nm respectively. The EG<sub>2</sub>-OH NPs size distribution by TEM shows an average core diameter of  $6.2 \pm 0.8$  nm. The hydrodynamic diameter of Au-NPs dispersed in water, was measured by DLS. As reported in Table 3 the size of NPs is around 8-10 nm. The MUS:OT and MUS NPs show a negative charge surface distribution around -30-40 mV, due to the sulfonated groups onto the NPs surface. Conversely, the EG<sub>2</sub>-OH NPs have a  $\zeta$ -potential close to zero, due to the lack of charged group onto the surface.

**Table 3. Morphological, physicochemical characterization and schematic representation of Au-NPs used in this study.**

	TEM Images	Size Distribution	Core Size* (nm)	Hydrodynamic diameter (nm)	$\zeta$ -Potential (mV)	Representation
MUS:OT			$4.5 \pm 1.0$	$9 \pm 1.2$	$-33.1 \pm 0.64$	
MUS			$4.3 \pm 1.3$	$8.5 \pm 1.5$	$-38.0 \pm 5.3$	
EG <sub>2</sub> -OH			$6.2 \pm 0.8$	$10 \pm 2.0$	$-8.5 \pm 1.2$	

\* determined from TEM images.

## 4.2 Cytotoxicity Assay

Since this study was aimed at assessing the inhibitory potential of sulfonated Au-NPs in presence of a large variety of viruses, it was essential to determine the cytotoxic effect of NPs on all the cell lines used. Cells were incubated for 48 hours with several concentrations of nanoparticles in parallel with untreated samples used as negative controls (Figure 6). Cell viability in HeLa, HT-1080, CHO-K1 and Jurkat cell lines was assessed by flow cytometry analysis (FACS) performing a PI staining. As it is shown in Figure 6, NPs did not exhibit any cytotoxic effect in the range of concentrations tested, from 1  $\mu\text{g/ml}$  up to 100  $\mu\text{g/ml}$ , with viability values maintained close to 100%. Regarding Vero cells and 293 TT cells the cytotoxic effect of NPs was evaluated by MTS and similar results were obtained (data not shown).

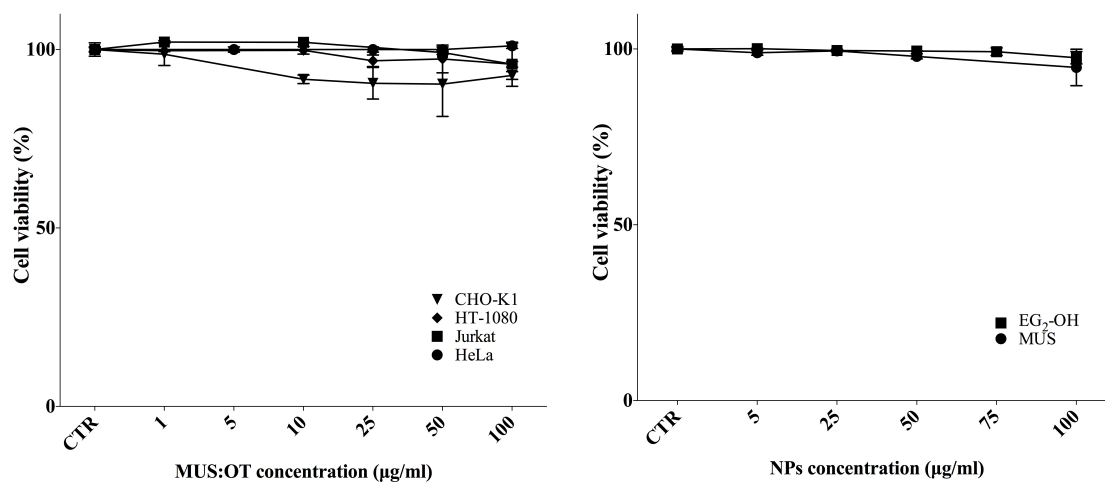


**Figure 6. Cytotoxicity of NPs evaluated with PI.**

Cell viability (%) in presence of MUS:OT NPs was tested on different cell lines after 48h incubation. (a) The dead cells were stained with PI and quantified by FACS: Jurkat (squares), HeLa (circles), HT-1080 (diamonds) and CHOK-1 (triangles). (b) Cell viability (%) after 48h incubation was evaluated in presence of EG<sub>2</sub>-OH (squares) and MUS (circles) NPs in HeLa cells.

### 4.3 Antiviral assays on HSPG-dependent viruses

The antiviral activity of sulfonate presenting NPs was tested on a subset of viruses that recognize cell surface HSPGs as first cell attachment receptors. This inhibition assay allowed understanding whether sulfonated NPs were able to diminish the level of transduced cells acting as antiviral agents, and also calculating their half maximal inhibitory concentration ( $IC_{50}$ ) in all viral systems tested.

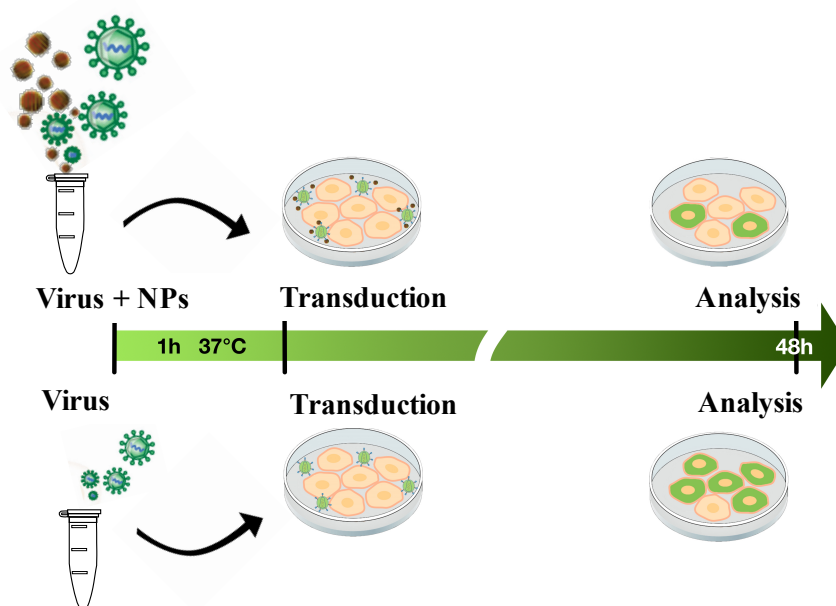


**Figure 7. Schematic representation of the LV-VSV-G inhibition assay.**

Pseudotyped lentivirus encoding for GFP (LV-VSV-G,  $10^6$  TU/ml) and sulfonated NPs, at different concentrations, were incubated in PBS for 1h at  $37^\circ\text{C}$ . Virus/NPs mixture was subsequently delivered to HeLa, Jurkat or HT-1080 permissive cells ( $10^5$  cells/well) for 48h at  $37^\circ\text{C}$  with growing medium enriched with 2% FBS. The final concentration of LV-VSV-G with cells was  $10^5$  TU/ml whereas NPs' concentration ranged from  $0.1 \mu\text{g/ml}$  ( $0.1 \text{ nM}$ ,  $\approx 10^{10}$  NPs) to  $100 \mu\text{g/ml}$  ( $100 \text{ nM}$ ,  $\approx 10^{13}$  NPs). Subsequently cells were harvested and fixed in 1% PFA and analysed by FACS for the expression of GFP. Transduction efficiency was calculated as the percentage of GFP+ cells over the total number of cells analysed. Cells with no virus were used as negative control whereas cells incubated with only virus, without NPs, was used as positive control.

### 4.3.1 LV-VSV-G

The first antiviral assay was carried out with pseudotyped lentivirus presenting the envelope glycoprotein of the Vesicular Stomatitis Virus (VSV-G). LV-VSV-G was chosen as viral model for this study for both its specificity toward sulfates as attachment receptors and for its broad tropism (Copreni et al. 2006; Durand & Cimarelli 2011). The assay was performed incubating LV-VSV-G for 1h at 37°C with increasing concentrations of the two kinds of sulfonate presenting NPs: MUS and MUS:OT. Subsequently, LV-VSV-G was delivered to permissive cell in the presence or absence of NPs (as a control) and GFP protein expression was evaluated. This first assay was conducted in HeLa cells as model of adherent cell line. As it can be observed from the dose-response plot (Figure 8a), both kinds of NPs revealed to be effective inhibitors of LV-VSV-G in HeLa cells. The most effective particles were MUS:OT NPs (Figure 8b), which displayed an  $IC_{50}$  of 1  $\mu\text{g/ml}$  (1 nM). MUS particles (Figure 8c) were also able to inhibit LV-VSV-G but less efficiently than MUS:OT particles. Indeed, the concentration of MUS NPs required to reach the half maximal inhibitory concentration resulted twice compared to MUS:OT NPs, 2.4  $\mu\text{g/ml}$  (2.4 nM).

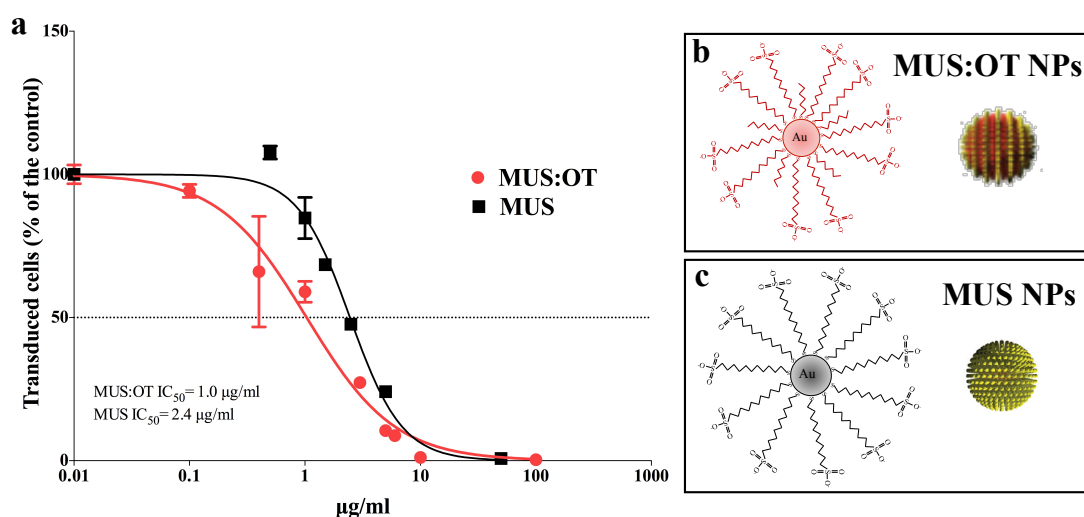


**Figure 8. LV-VSV-G inhibition assay with sulfonated NPs (MUS:OT, MUS).**

(a) LV-VSV-G expressing GFP was incubated for 1h at 37°C with increasing concentrations of MUS

(squares) or MUS:OT (circles) NPs prior to infection. Cells were analysed by FACS 48h post transduction. Transduction efficiency of lentiviral vector was affected by the presence of NPs. MUS:OT displayed an  $IC_{50}$  of 1  $\mu\text{g/ml}$  (95% CI 0.7- 1.3  $\mu\text{g/ml}$ ) whereas MUS had  $IC_{50}$  value equal to 2.4  $\mu\text{g/ml}$  (95% CI 1.9 - 3.3  $\mu\text{g/ml}$ ). Both  $IC_{50}$  values represent the final concentration in HeLa cells. Enlarged are depicted the schematic representation of (b) MUS:OT and (c) MUS NPs.

Despite the effectiveness of both structured (MUS:OT) and unstructured (MUS) NPs in inhibiting LV-VSV-G, the former was chosen for the successive inhibition studies, owing to their unique physicochemical properties as well as for their better inhibitory profile. Therefore, to prove that MUS:OT NPs could efficiently inhibit the transduction of LV-VSV-G on other cell types in a cell-independent way, similar inhibition experiments were performed in two different cell lines: HT-1080 and Jurkat cells. In particular, the use of Jurkat cells (immortalized T lymphocytes) were chosen as model of suspension growing cells. As it is shown in Figure 9, sulfonated NPs were found to inhibit the transduction of LV-VSV-G in both cell lines, with values of  $IC_{50}$  of 3  $\mu\text{g/ml}$  (3 nM) and 2  $\mu\text{g/ml}$  (2 nM) for Jurkat and HT-1080 cells respectively.

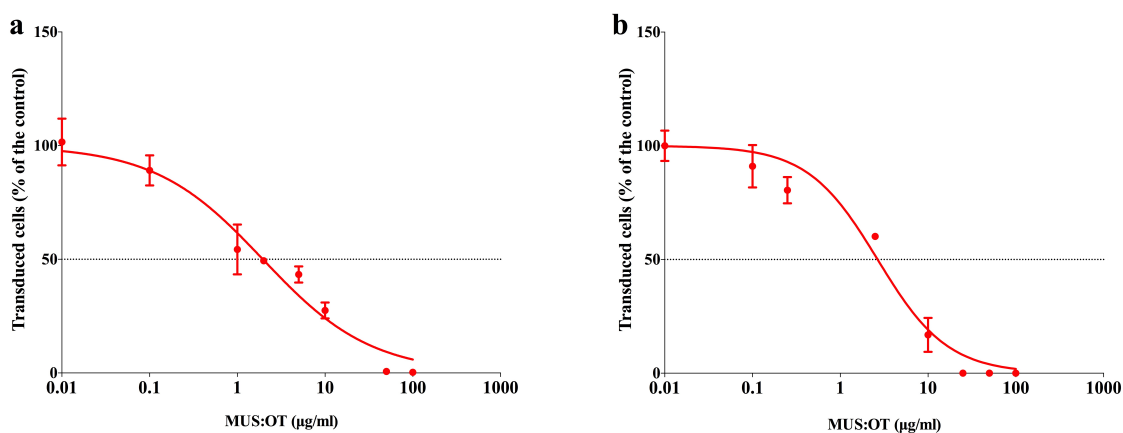


**Figure 9. LV-VSV-G inhibition assay with MUS:OT NPs in different cell lines.**

Transduction efficiency of LV-VSV-G was evaluated after incubation with increasing concentrations of MUS:OT NPs for 1h at 37°C. Virus/NPs mixture was then added to permissive cell lines. MUS:OT inhibited LV-VSV-G transduction in (a) Jurkat cells with  $IC_{50} = 2.6 \mu\text{g/ml}$  (95% CI 1.4 - 4.7  $\mu\text{g/ml}$ ) and in HT-1080 (b) with  $IC_{50} = 1.9 \mu\text{g/ml}$  (95% CI 1.1 - 3.2  $\mu\text{g/ml}$ ).

Having assessed the potent inhibitory activity of MUS:OT NPs in different cell lines with different growing conditions and with a different expression of cell membrane proteins, it was essential to exclude that the antiviral effect observed was not determined by the presence of the MUS itself. For comparison, an antiviral assay was run under similar experimental conditions using two concentrations of the soluble MUS ligand, at 0.1  $\mu\text{g/ml}$  (250 nM) and 1  $\mu\text{g/ml}$  (2.5  $\mu\text{M}$ ) in HeLa cells (Figure 10a). These amounts had been determined by thermogravimetric analysis (TGA) (Verma et al. 2008) as the same or ten times higher quantities of MUS that is present on MUS:OT NPs, at the  $\text{IC}_{50}$  concentration. As shown in Figure 10a, soluble MUS was found to be completely ineffective as antiviral at both concentrations tested. This control experiment suggested that only when the ligands were bound to the NPs they could efficiently act as antivirals. Furthermore, the inhibitory ability of MUS:OT NPs against LV-VSV-G was compared to an antiretroviral drug (AZT). Figure 10b shows that AZT could inhibit LV-VSV-G in a nanomolar range (80 nM), underlying the potential use of MUS:OT NPs as efficient antiviral. Similarly, to further confirm the antiviral activity of sulfonated MUS:OT NPs, other two control experiments were performed. Firstly, LV-VSV-G was incubated with Au-NPs, having roughly the same size of MUS:OT and their surface was functionalized with non-sulfonated ligands: EG<sub>2</sub>-OH coated NPs. This kind of NPs did not produce any inhibitory effect upon LV-VSV-G infection in HeLa cells (Figure 10c). The number of transduced cells remained approximately the same compared to the virus not incubated with NPs, even at 100  $\mu\text{g/ml}$  (100 nM), the highest concentration tested. In the second set of control experiments, MUS:OT NPs were assayed for their antiviral ability against Ad5, a virus that exploits other attachment receptors on their target cells (Figure 10d). In this case, sulfonated NPs failed to inhibit Ad5 at any of the concentrations tested. Taken together, these results suggested that only sulfonated NPs exerted an antiviral activity which is in turn restricted only to those viruses binding to HSPGs as attachment receptors (e.g. LV-VSV-G).

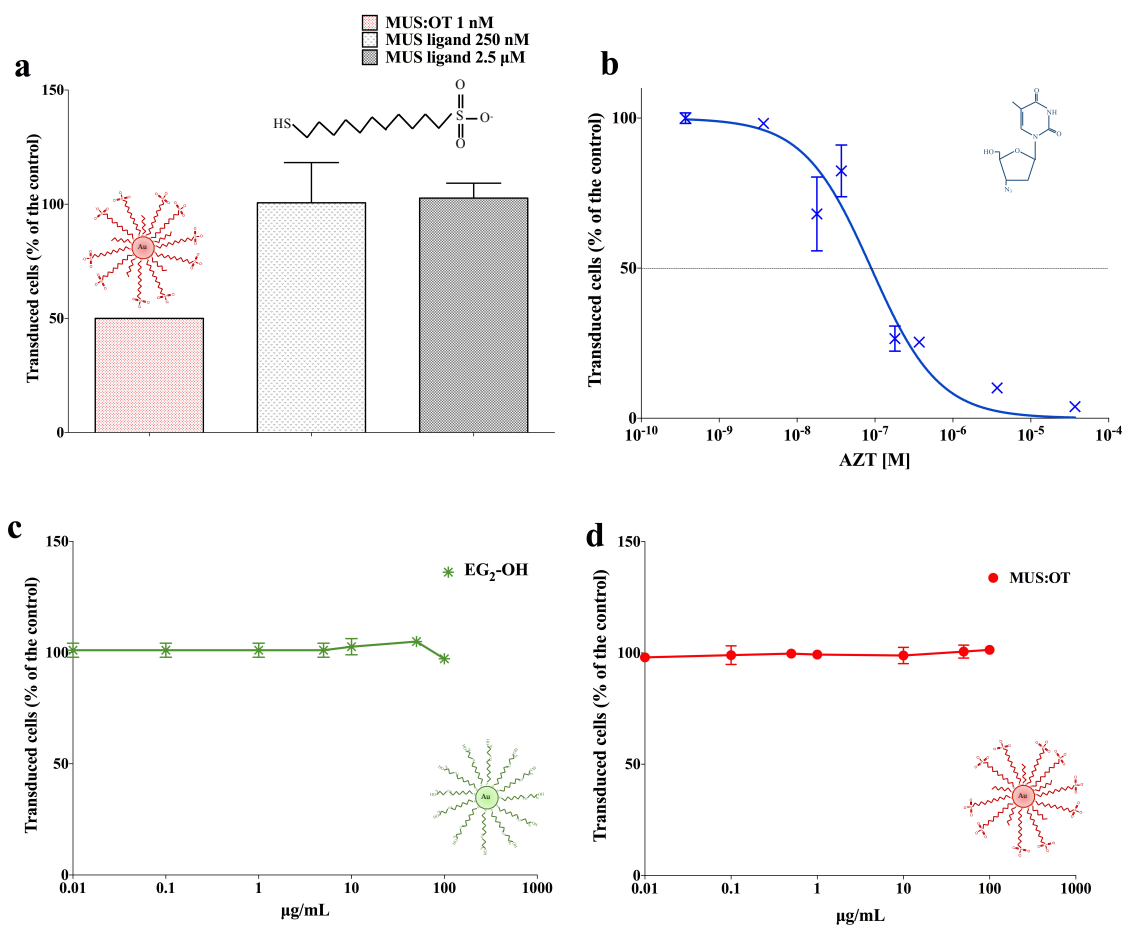


**Figure 10. Experiments to validate antiviral activity of MUS:OT NPs.**

Percentage of transduced cells was calculated by FACS after 48h. (a) The inhibition efficiency of MUS:OT NPs (red bar) for LV-VSV-G was compared to the use of the soluble MUS ligand (grey bars). LV-VSV-G was not inhibited by the ligand itself either using the same amount of MUS present in the MUS:OT NPs (light grey bar) nor with ten times higher concentration (dark grey bar). (b) Antiviral assay was performed incubating LV-VSV-G with antiviral drug (AZT). Calculated IC<sub>50</sub> of AZT (80 nM) was in the nanomolar range as for MUS:OT NPs (c) LV-VSV-G transduction efficiency evaluated after incubation with increasing amount of non sulfonated NPs (EG<sub>2</sub>-OH) and (d) Ad5 transduction efficiency evaluated after incubation with MUS:OT NPs.

### 4.3.2 HSV-1/2 and HPV-16 PsV

On the basis of these results, the antiviral activity of MUS:OT NPs was tested with other viral systems (not engineered viruses), that selectively recognize HSPGs as first cell attachment receptors. The antiviral assays were performed in the molecular virology laboratory in collaboration with Prof. Lembo at the University of Turin. Two human pathogenic viruses: wild-type HSV (type 1 and type 2) and HPV-16 PsV were selected for the inhibition study. The same experimental procedure of the inhibition assay used for LV-VSV-G (pre-infection incubation of NPs and viruses) was applied to HSV-1/2 and HPV-16 PsV. As it is shown in the dose-response curves (Figure 11), MUS:OT NPs were able to diminish the percentage of infected cells (Vero and 293TT cells) in a dose dependent manner. Regarding HSV viruses, type 2 was inhibited more efficiently than HSV-1 by MUS:OT NPs with an  $IC_{50}$  of 2  $\mu\text{g}/\text{ml}$  (2 nM) and 11  $\mu\text{g}/\text{ml}$  (11 nM), respectively (Figure 11a, b). Similarly, HPV-16 PsV was inhibited by MUS:OT NPs displaying an  $IC_{50}$  of 4  $\mu\text{g}/\text{ml}$  (4 nM) (Figure 11c).

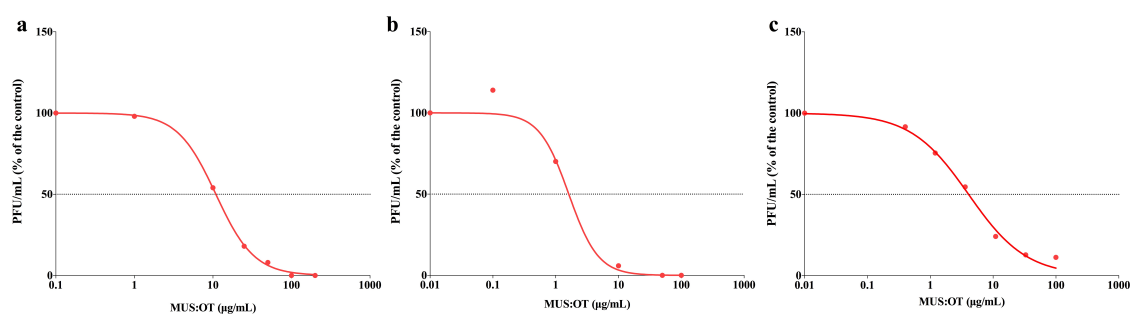


**Figure 11. Antiviral assay of HSPG-binding viruses with MUS:OT NPs.**

The antiviral assay with increasing amounts of MUS:OT NPs was performed on (a) HSV-1 (b) HSV-2 (c) HPV-16 PsV.



### 4.3.3 LV-gp160

Having assessed the ability of sulfonated NPs to drastically reduce the infection of wild-type human pathogenic viruses binding HSPGs (e.g. HSV-1 and HSV-2), MUS:OT NPs were assayed for their inhibition ability respect to pseudotyped lentivirus exposing the envelope protein of HIV (gp160) (Figure 12a). The gp160 glycoprotein, which is comprised of gp120 and gp41 subunits, is needed for the initial attachment of HIV on target cells through multivalent interactions with HSPGs. LV-gp160 particles were produced using a plasmid for the gp160 Env protein from the HXB2 strain of HIV. The gp160 Env plasmid was kindly donated by Prof. Didier Trono (Laboratory of virology and genetics at École Polytechnique Fédérale de Lausanne - EPFL). In order to demonstrate that the viral particles expressed the gp160 protein on their capsid, a SDS-PAGE gel was run in parallel with LV-gp160 and LV-VSV-G and western blot analysis was performed using antibodies directed against two key lentiviral proteins: p24, that is the inner capsid protein and gp120 or VSV-G, the glycoprotein exposed on the membrane of the viruses (Vandermeulen et al. 2012) (Figure 12b). As expected, both pseudotyped lentiviruses expressed the constitutive capsid protein (p24). On the other hand, the Env gp120 protein was detected only in LV-gp160 viruses while the VSV-G protein was present exclusively on LV-VSVG particles. After demonstrating the expression of gp160 on lentivirus envelope, we selected the appropriate cell line susceptible to HIV, and thus to LV-gp160, infection. HeLa T4+ cells were chosen for the antiviral assay because they express CD4, which is the primary binding receptor of HIV, responsible for its internalization during the process of infection. The expression of the CD4 on HeLa T4+, was confirmed by FACS analysis using a fluorescent anti-CD4 antibody. As expected, HeLa T4+ cells resulted positive for CD4 (99.60%) while HeLa cells, used as a negative control, were completely negative for its expression (Figure 12c). Moreover, to confirm that LV particles were correctly assembled, LV-VSV-G was further purified through sucrose cushion and analysed by DLS. Results showed that LV-VSV-G had a uniform distribution and average diameter of about 150 nm according to previously reported

papers (Vandermeulen et al. 2012) (Figure 12d).

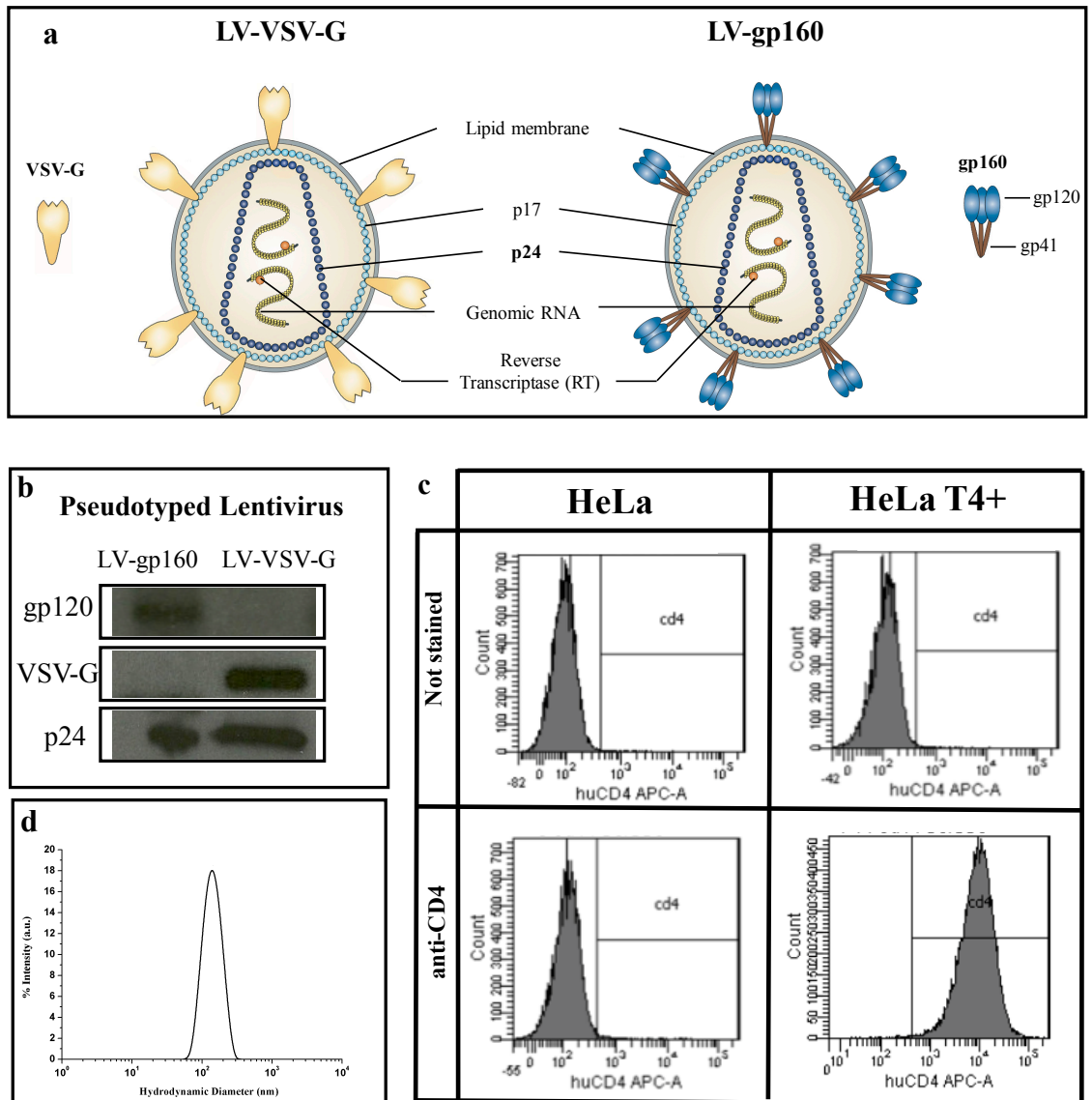


**Figure 12. Characterization of LV-gp160 and HeLa T4+ cells.**

(a) Comparison between LV-VSV-G and LV-gp160 with enlarged envelope glycoproteins (VSV-G and gp160). (b) Western blot analysis of envelope glycoproteins for both type of pseudotyped lentiviruses and (c) FACS analysis of HeLa T4+ for the expression of CD4. HeLa cells were used as negative control. (d) % Intensity (a.u.) vs hydrodynamic diameter (nm) by DLS of LV-VSV-G in PBS at room temperature.

Following the same experimental procedure as before, an inhibition assay of LV-gp160 incubated with or without MUS:OT NPs for 1 h 37°C and delivered to HeLa T4+ cells was performed. As it can be seen in Figure 13, sulfonated NPs were effective in inhibiting the LV-gp160 transduction at the concentration tested of 100 µg/mL (100 nM). In contrast, Au-NPs with non-sulfonated ligands (EG<sub>2</sub>-OH NPs), used at the same molar concentration, had no effect on LV-gp160 and the number of transduced cells resulted similar to the control virus without NPs.

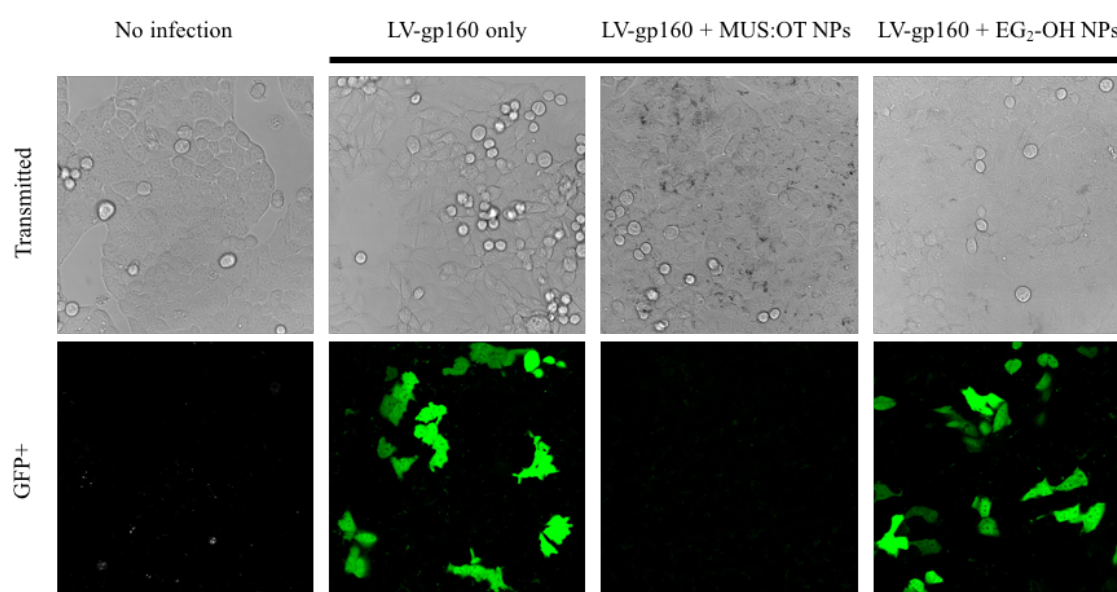


**Figure 13. Confocal Laser Scanning Microscopy (CLSM) images of LV-gp160 incubated with NPs.**

LV-gp160 was incubated with 100 µg/ml (100 nM) of MUS:OT or EG<sub>2</sub>-OH NPs for 1h 37°C before delivering the mixture to HeLa T4+ cells. Transduction efficiency, in terms of GFP+ cells (fluorescent cells), was evaluated by CLSM after 48h in cells fixed with 2% PFA. Transmitted light (upper panels) and green (GFP+, lower panels) channels are shown. Virus without NPs was used as a control.

#### **4.3.4 AAV2 and AAV5**

Finally, in order to strengthen the hypothesis of sulfonated NPs as antivirals within the class of HSPG-dependent viruses, a control experiment was carried out using one virus (AAV) in which two serotypes (AAV2 and AAV5) have different cell surface attachment receptors. AAV2 recognizes host cells through HSPGs while AAV5 binds to sialic acid as its primary cell attachment receptor. Results showed that the incubation of viruses with MUS:OT NPs influenced the capacity of AAVs to transduce CHO-K1 cells in a serotype-dependent manner. Serotype AAV2 was almost completely inhibited after pre-treatment with MUS:OT NPs, whereas in case of AAV5 no difference in infectivity was observed (Figure 14). These first results clearly highlighted the antiviral activity of sulfonated NPs against the subset of viruses binding HSPG. However, the antiviral assays could not discriminate whether the antiviral activity of the NPs was exclusively due to NPs-virus interactions and so impeding the attachment and the recognition of target cells, or whether the NPs were exerting their inhibitory ability at the intracellular level by interfering with key processes of the infection cycle. In order to further investigate the mechanism through which MUS:OT NPs could exert their antiviral effects at different phases of the infection cycle we designed a new set of experiments.

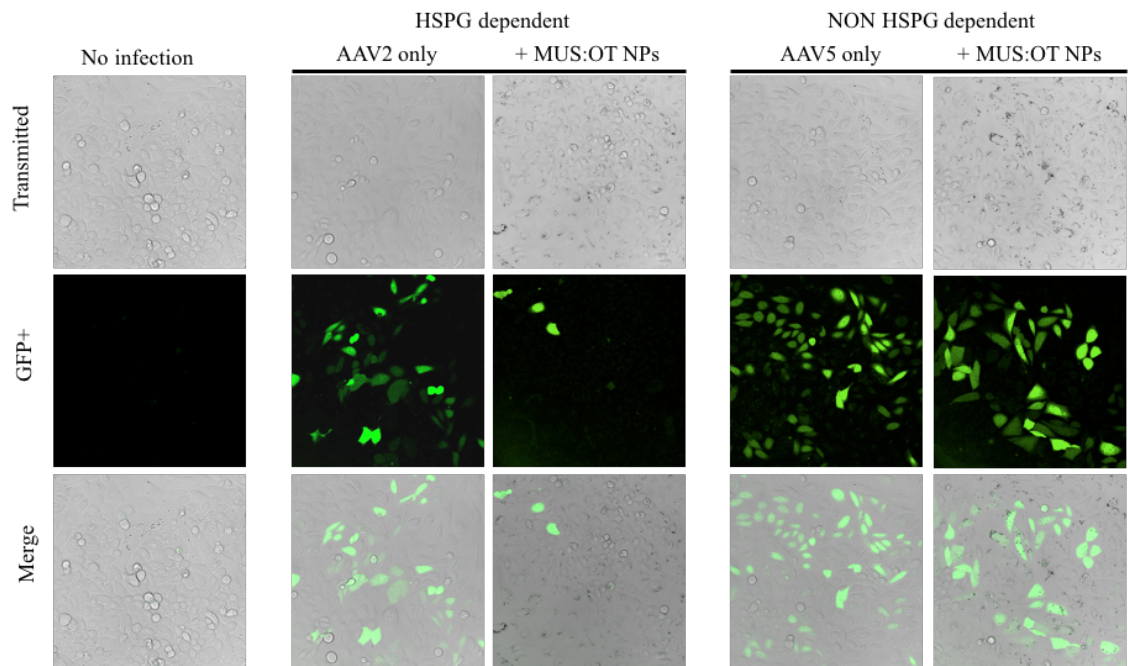


**Figure 14. Confocal Laser Scanning Microscopy (CLSM) images AAVs (AAV2; AAV5) with MUS:OT NPs.**

Sulfonated NPs, used at 100  $\mu\text{g/ml}$  (100 nM) and the virus was incubated for 1h at 37°C prior to addition to CHO-K1 cells. Transduction efficiency in terms of GFP+ cells was evaluated by CLSM. Transmitted light (upper panels) and green (GFP+, lower panels) channel are shown. Virus without NPs was used as a control.

#### 4.4 Time of addition experiments

A Time of addition (TOA) assay was performed in order to determine which stage(s) of the infectious cycle was affected by the MUS:OT NPs (Figure 15). The possible mechanisms of inhibition of sulfonated NPs were investigated using LV-VSV-G as model viral system. Therefore, for TOA experiments MUS:OT NPs, from 0.1  $\mu\text{g/ml}$  (0.1 nM) to 100  $\mu\text{g/ml}$  (100nM), were co-added with viruses ( $10^5$  TU/ml) during the transduction phase on permissive cells, or they were added before (before - b) or after (post - p) LV-VSV-G inoculum (Figure 16).

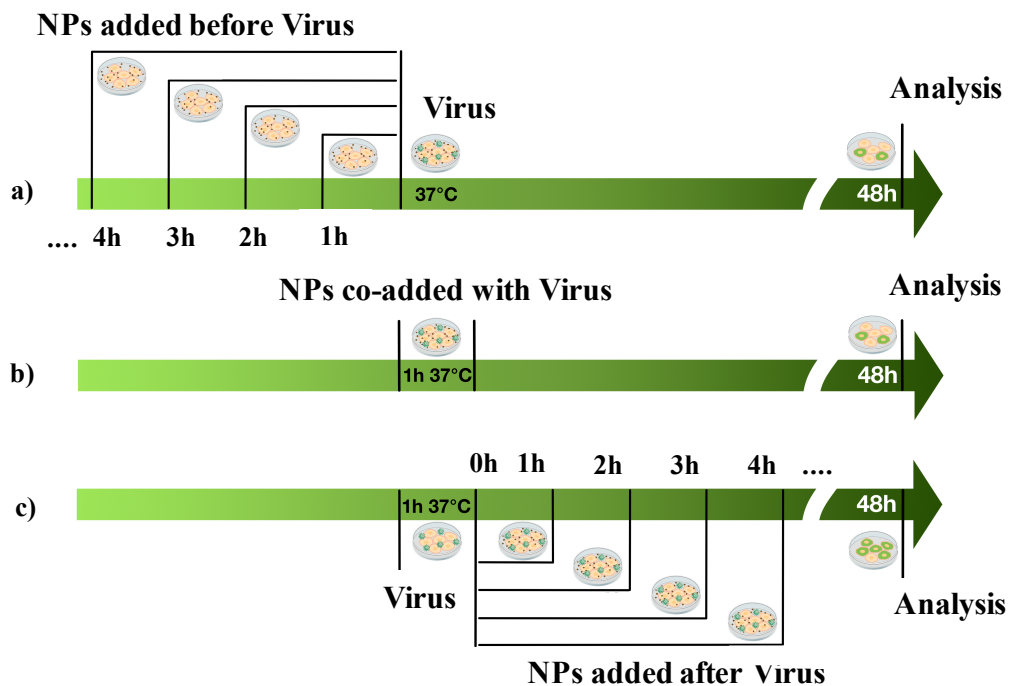


**Figure 15. Schematic representation of the time of addition (TOA) experiments.**

- (a) NPs are incubated with cells at different time points before virus inoculum
- (b) NPs are incubated along with viruses (co-addition)
- (c) NPs are added after virus inoculum

Initially, MUS:OT NPs were added to cells at 37°C for long (8h) or short (1h) times before LV-VSV-G inoculum (Figure 16a). The pre-incubation assay was carried out using MUS:OT NPs at 100 µg/ml (100 nM), a concentration that exhibited the best inhibitory effects in the antiviral assays. Transduction of LV-VSV-G was not affected by the presence of MUS:OT NPs, mainly localized into the cells, and the resultant number of transduced cells was comparable to the control without NPs, at all the time points tested (Figure 16a). To further understand at which stage of the LV-VSV-G infectious cycle the NPs were able to produce their inhibitory effect, TOA experiment was performed adding increasing concentrations of MUS:OT NPs during or after (0h or 2h post) LV-VSV-G transduction. The ability of MUS:OT NPs to inhibit LV-VSV-G during or after the first two hours of transduction was tested on HeLa as well as on HT-1080 cells therefore excluding any possible effect dependent upon the cell line used (Figure 16b, c).

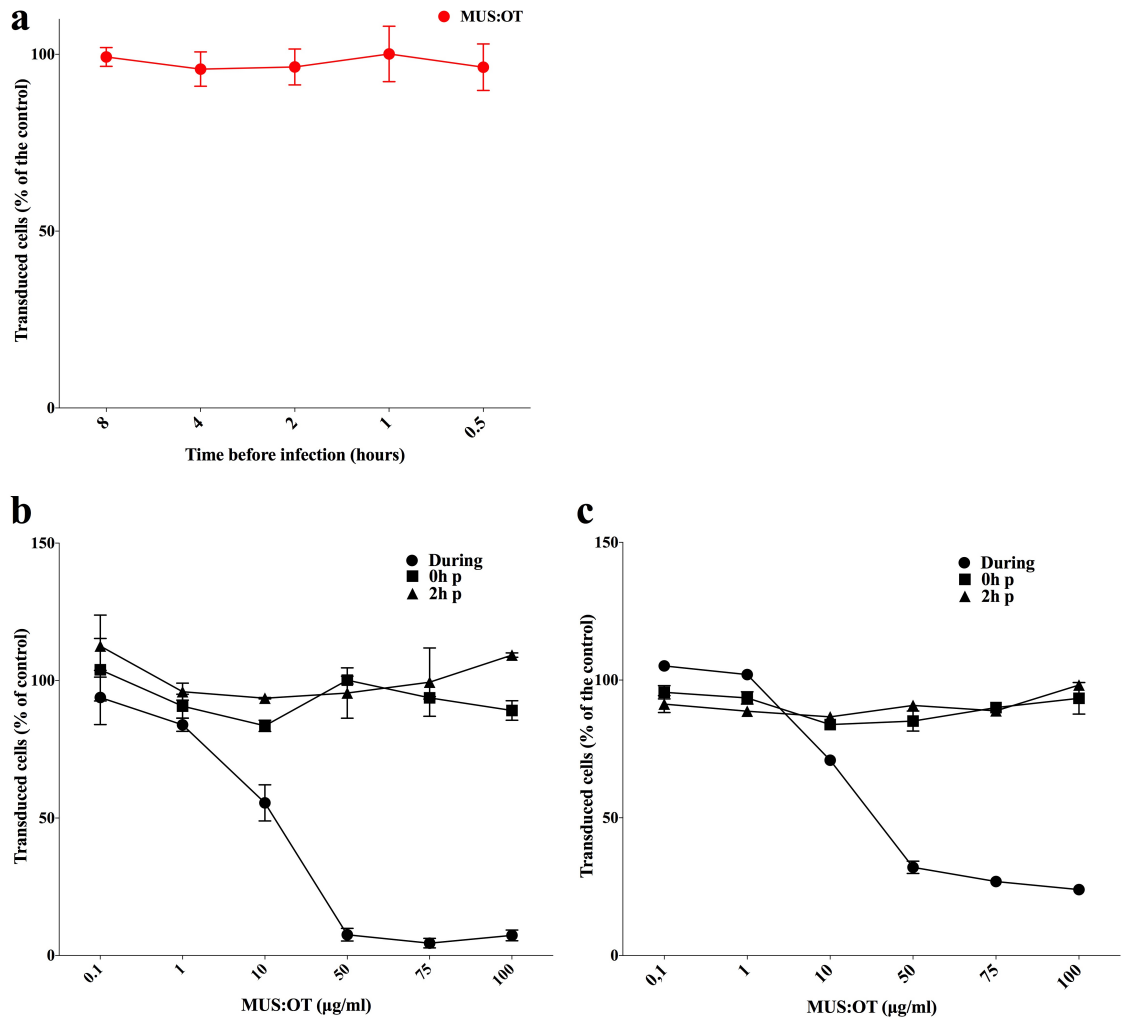


**Figure 16. TOA experiments with MUS:OT.**

(a) LV-VSV-G transduction efficiency was calculated in HeLa cells treated with MUS:OT NPs at 100 µg/ml (100 nM) at different times before the virus was delivered to the cells. NPs did not determine any reduction in the number of transduce cells when incubated with cells before the virus.

(b, c) Increasing amounts of MUS:OT NPs (µg/ml) were incubated during (circles), or after, 0h post (squares) and 2h post (triangles) LV-VSV-G transduction in HeLa (b) and HT-1080 (c) cells. LV-VSV-G transduction was inhibited when co-added with MUS:OT NPs independently from the cell line used. Percentage of transduction was normalized in respect to untreated LV-VSV-G, used as a control



Thus, this TOA approach could precisely determine how long the addition of a compound, in this case MUS:OT NPs, could be postponed before becoming ineffective. Both experiments confirmed that MUS:OT NPs were effective only when co-added with the virus, and thus during the first extracellular steps of the infectious cycle, reaching the 50% of inhibited cells at a concentration of approximately 10  $\mu\text{g/ml}$  (10 nM). No inhibitory effects were observed at 0 or 2h post entry, even at 100  $\mu\text{g/ml}$  (100 nM), the highest tested concentration of MUS:OT NPs. We included in the TOA experiments also an anti-HIV drug (AZT) with a well-characterized intracellular mechanism of inhibition (Figure 17a). This experiment allowed to assess when and where MUS:OT NPs exerted their antiviral action. Consequently, MUS:OT NPs or AZT were incubated before, during and after infection with LV-VSV-G (Figure 17b). Our results confirmed that AZT inhibits HIV-1, and consequently pseudo-HIV-1 particles like LV-VSV-G, intracellularly by blocking the retrotranscription of the viral RNA, that occurs within the first three hours after the virus entry. As it is shown in Figure 17b, AZT was able to inhibit LV-VSV-G infection in both phases, before and after transduction. When cells were pre-treated with the antiviral drug before virus transduction, the percentage of inhibition was proportional to the time of drug exposure of the cells: the longer the cells were exposed to AZT, the stronger was the inhibitory effect (Figure 17b). Before transduction, long-term incubation of AZT to cells (4h b) was more efficient than short-term incubation (10min b) or co-addition during the transduction. On the other hand, when cells were treated after transduction, it was obvious that the sooner AZT was added to the cells the stronger was the inhibitory effect. In contrast, MUS:OT NPs were found to be active only at one time point which was when NPs were co-added along with the virus indicating that they interfere only at the initial phases of lentiviral transduction, attachment or entry (Figure 17b).

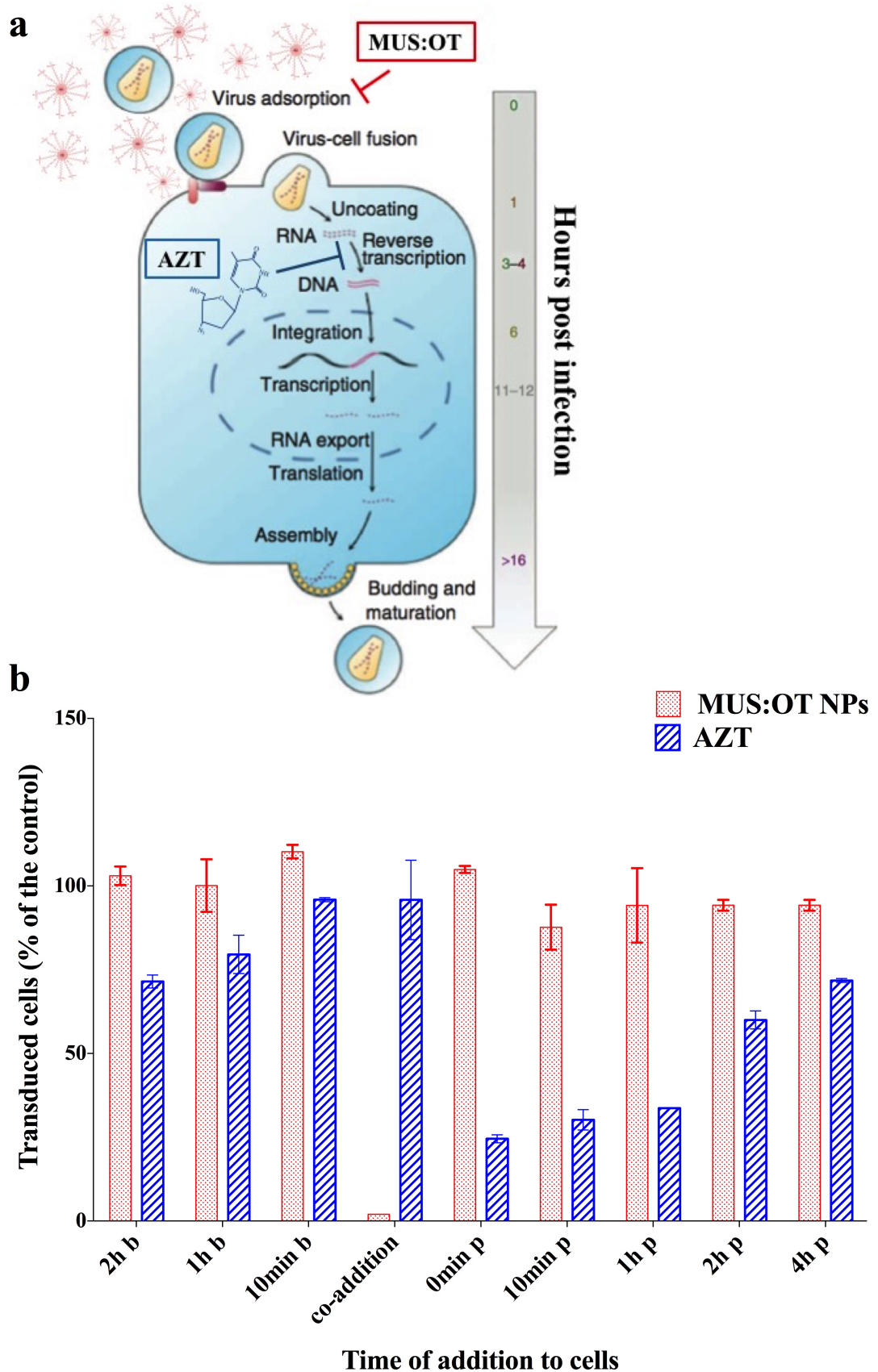


**Figure 17. Comparison of MUS:OT and AZT antiviral mechanism of action.**

(a) The hypothesized extracellular inhibition by MUS:OT NPs, was compared to that of the anti-retroviral drug AZT that acts intracellularly in the TOA experiments. Sulfonated NPs exert their

antiviral action interfering with the early steps of the infection (attachment, entry), thus within one hour after the virus was delivered to the cells. In contrast, AZT inhibits HIV-1 infection when the compound was inside the cell blocking the retrotranscriptase enzyme that converts viral RNA into proviral DNA, within the first three/four hours of infection. Image was modified from (Daelemans et al. 2011) © *Nature Prot.* (2011) Nature Publishing Group

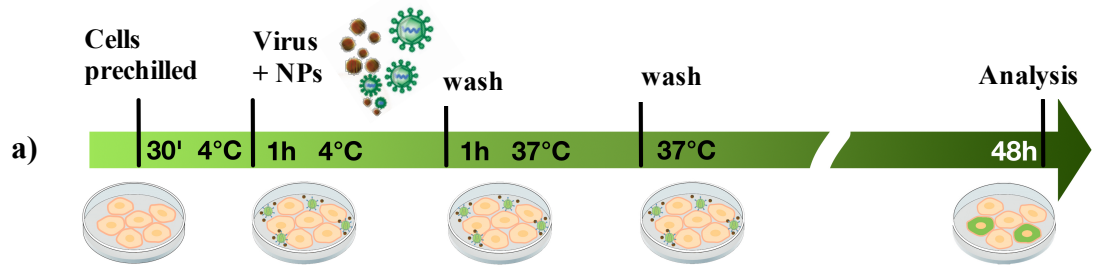
(b) The percentage of GFP transduced HeLa cells by LV-VSV-G was calculated before (b), during (co-addition) or after (p) the addition of MUS:OT NPs (red bars) or AZT compound (blue bars). MUS:OT NPs used at 100 µg/ml (100 nM) were ineffective when added before or after the infection at all time points.

These findings demonstrated that NPs were able to inhibit viral infection acting differently, in time and modality, from AZT. In order to determine whether the NPs could inhibit the replication of LV-VSV-G affecting the attachment and/or the entry step of the infection, NPs were assayed for the inhibition of the attachment and entry step.

#### **4.5 Entry and Attachment Assays**

Once determined that MUS:OT NPs could not block the events downstream LV-VSV-G entry, sulfonated NPs were assayed with LV-VSV-G to determine which of the two early infection steps (attachment and/or entry) were affected by the NPs (Figure 18). The entry and attachment assays were carried out in HT-1080 cells ( $10^5$  cells/ml) with increasing concentrations of MUS:OT NPs from 0.1 µg/ml to 150 µg/ml (0.1 to 150 nM -  $10^{10}$  NPs/ml to  $1.5 \times 10^{13}$  NPs/ml ) (Figure 19).

## MUS:OT during the attachment



## MUS:OT during the entry

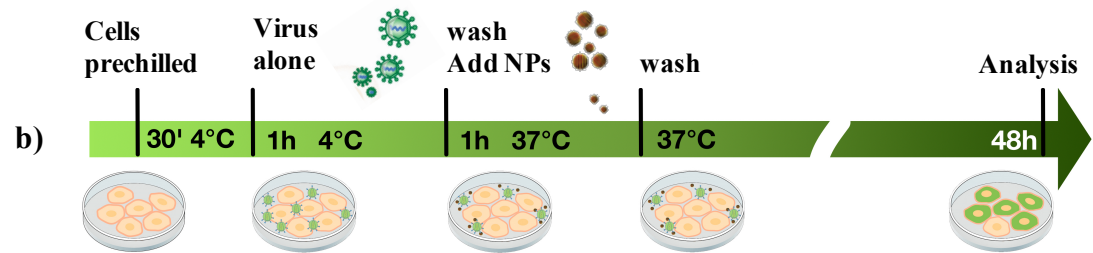


**Figure 18. Schematic representation of entry and attachment of LV-VSV-G in presence of MUS:OT NPs.**

(a) MUS:OT NPs were delivered during the attachment phase of LV-VSV-G

(b) MUS:OT NPs were incubated during the entry phase of LV-VSV-G

In the attachment assay, MUS:OT NPs and LV-VSV-G were simultaneously added to the cells for 1h at 4°C. In such condition (low temperature) endocytic processes are blocked and the virus bound to the cell membrane through its attachment receptors could not be internalized. Cells were then washed with cold PBS and the temperature increased up to 37°C for 1h, the time needed for the virus to enter into the cells. A washing step with PBS eliminated unspecifically adsorbed virus particles from the plasma membrane. Cells were subsequently analysed after 48h for the expression of the reporter gene (GFP). In the entry assay, differently from the attachment assay, MUS:OT NPs were added only after virus attachment, when the temperature was raised up to 37°C and the virus already started entering the cells. Results clearly pointed out that MUS:OT NPs were able to inhibit LV-VSV-G transduction only in the attachment phase and had no, or very limited, effect on the

entry step (Figure 19). Indeed, the percentage of transduced cells during the entry phase was almost similar to the control (untreated virus) even at the highest tested concentration of 150  $\mu\text{g/ml}$  (150 nM). In contrast, the attachment of LV-VSV-G to target cells was affected by the presence of sulfonated NPs as shown by the decreased infectivity at the increase of NPs' concentrations.

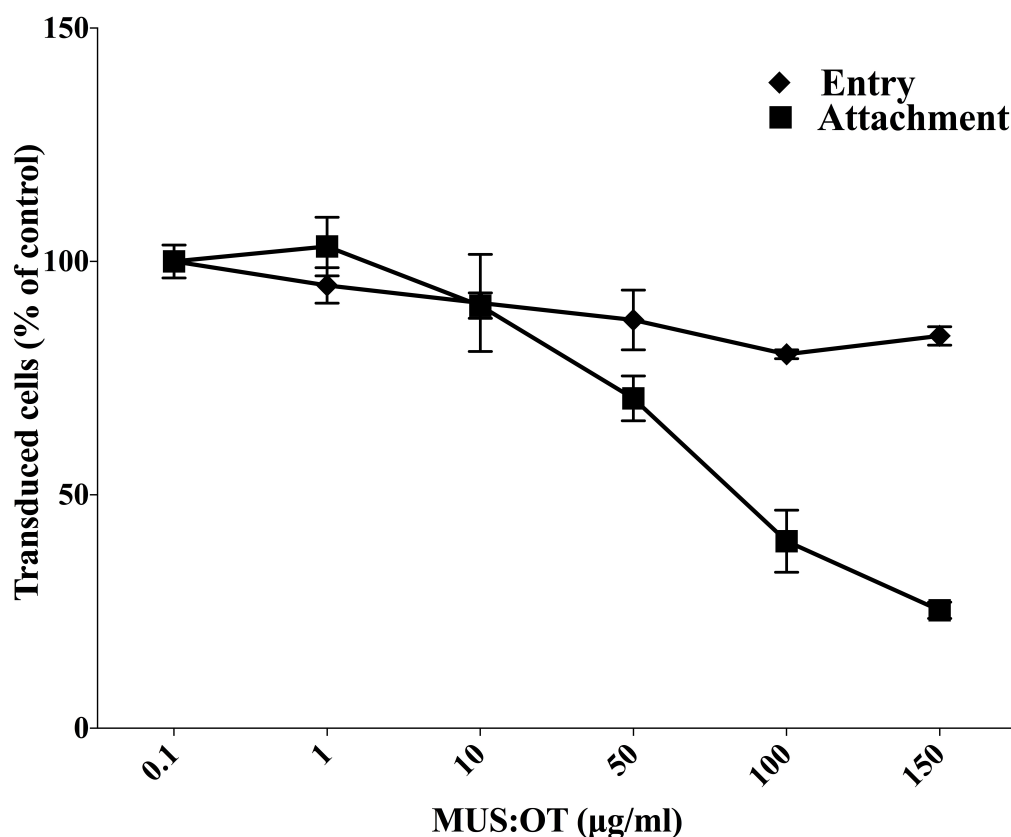


**Figure 19. Entry and attachment assays with LV-VSV-G in presence of MUS:OT.**

The percentage of HT-1080 cells transduced by LV-VSV-G was calculated at the entry (diamond) or attachment (square) steps with increasing amounts of MUS:OT NPs. Percentage of transduced cells was normalized in respect to untreated LV-VSV-G used as control.

#### 4.6 Virucidal Assay

The aim of the virucidal assay was to assess the ability of MUS:OT NPs to inactivate (make not infectious) virus particles, thereby neutralizing viruses' action, before the infection of permissive cells. Briefly, the virus was incubated 2h at 37°C with an effective inhibitory

concentration of MUS:OT NPs,  $> 100 \mu\text{g/ml}$  ( $>10^{13}$  NPs), as determined in the previous antiviral assays. Subsequently, the virus in presence of NPs was titrated by serial high fold dilutions in order to calculate the amount of virus particles that remained infective after the incubation step. The virucidal activity of MUS:OT NPs was tested both with HSPG-binding viruses (HSV-2, LV-VSV-G) as well as with non HS-dependent viruses (Ad5). The first virucidal assay, carried out with LV-VSV-G (Figure 20a), showed that only MUS:OT NPs were able to permanently inactivate virus particles after the pre-infection step (2h  $37^{\circ}\text{C}$ ) with a significant reduction ( $> 6$  log) in the number of viruses particles/ml (transducing units/ml - TU/ml). The same assay, performed with EG<sub>2</sub>-OH NPs, revealed that non-sulfonated NPs had no effect on LV-VSV-G particles which number was similar to the control. Similarly, LV-VSV-G virucidal assay was carried out with the anti-retroviral drug (AZT). Although AZT is able to inhibit LV-VSV-G transduction, it did not determine a reduction in the number of infectious particles compared to the untreated virus (Figure 20a). These findings highlighted the difference in the mechanism of inhibition between MUS:OT and AZT. Indeed, MUS:OT NPs were exerting their antiviral action interacting with viruses' capsid making the virus unable to infect (inactive) even when the mixture NPs/virus was diluted. Consequently, the inactivation of LV-VSV-G by contact with MUS:OT was due to tight interaction between the two species. On the other hand, AZT compound, inhibiting an intracellular viral enzyme (Retrotranscriptase - RT), did not cause a reduction in the number of LV-VSV-G particles and thus when diluted it could not impede the transduction of viruses. Furthermore, in a control experiment virucidal assay was performed incubating with MUS:OT NPs with a non-HS-binding virus (Ad5) (Figure 20b).

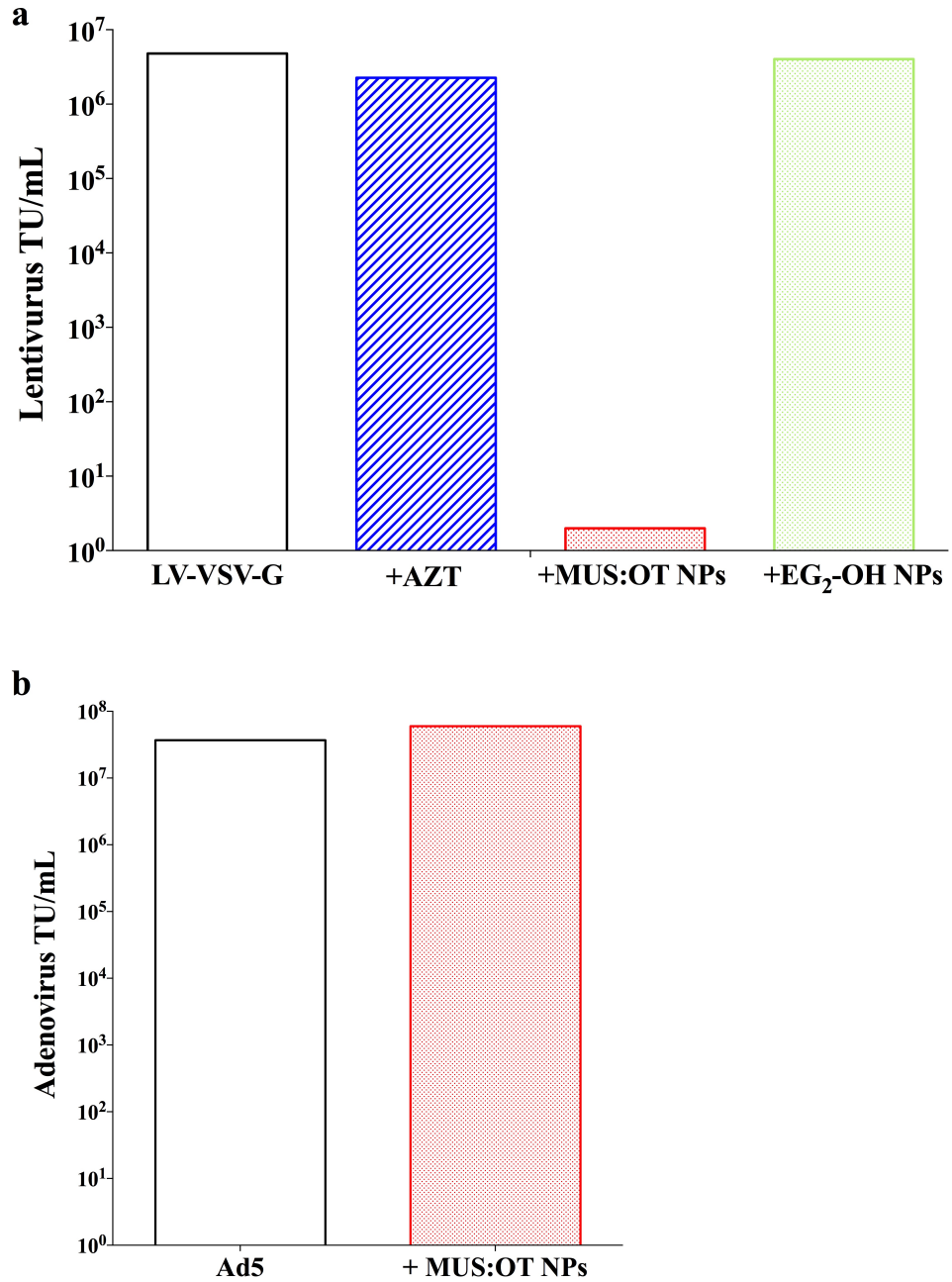


**Figure 20. Virucidal assays of LV-VSV-G and Ad5.**

(a) LV-VSV-G virucidal assay with sulfonated (MUS:OT, red bar), non-sulfonated (EG<sub>2</sub>-OH, green bar) NPs and antiviral drug (AZT, blue bar). Titration of LV-VSV-G after 2h 37°C revealed that incubation with MUS:OT (1000 µg/ml – 1 µM) significantly reduced the number of LV-VSV-G transducing units/ml. On the contrary, neither EG<sub>2</sub>-OH (1000 µg/ml – 1 µM) nor the AZT antiviral (1.8 µM) were able to diminish the number of virus particles after the incubation. (b) Ad5 virucidal assay performed after incubation for 2h 37°C with MUS:OT NPs (red bar) used at a concentration of 1000 µg/ml (1 µM).

As expected in this case MUS:OT NPs did not determine a decrease in the number of Ad5 which remained close to the virus not incubated with NPs. This result confirmed the mechanism of action of MUS:OT NPs that selectively interact and thus inactivate HSPG-binding viruses.

According to the results obtained with LV-VSV-G, we then tested the ability of MUS:OT NPs to inactivate HSV-2 wild-type virus. Following the same experimental procedure, the assay with HSV-2 showed that MUS:OT NPs could efficiently reduce the number of infectious particles (>4 log) compared to the virus not treated with NPs (Figure 21).

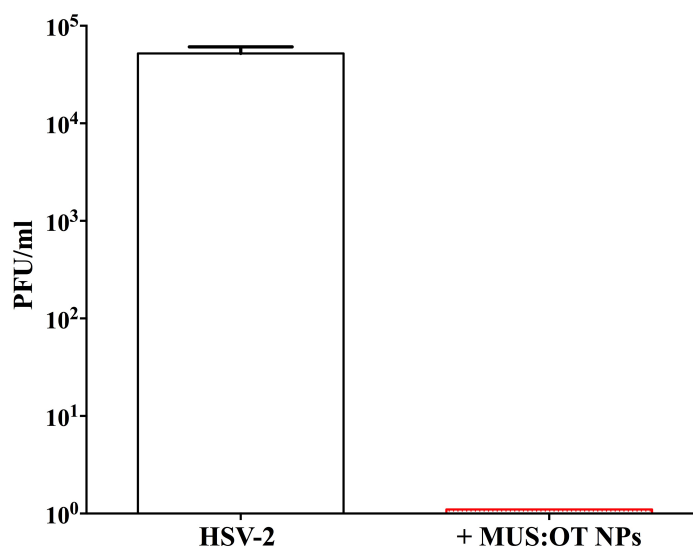


**Figure 21. Virucidal assays of HSV-2 with MUS:OT NPs.**

Virucidal assay was performed after HSV-2 incubation for 2h 37°C with MUS:OT NPs (red bar) used at a concentration of 100 µg/ml (100 nM). The number of infectious viruses (PFU/ml), calculated by serial high fold dilutions, was drastically reduced after the incubation with sulfonated NPs (MUS:OT).

Taken together, these insights indicated that MUS:OT NPs acted as virucides, thus enabling the inactivation of HSPG-binding viruses that, after interacting with NPs, were no longer able to infect. Next, we wanted to investigate the time needed to MUS:OT NPs to inactivate



viruses. Consequently, the number of LV-VSV-G particle was calculated, through titration method, after exposure with different concentrations of MUS:OT NPs at different time points. Initially, we calculated the titer of LV-VSV-G immediately after ( $t_0$ ) mixing the two components (NPs/virus). As shown in Figure 22, at  $t_0$  the number of virus particles/ml (TU/ml), was reduced of roughly one log after the exposure with the highest concentration of MUS:OT NPs (500  $\mu\text{g/ml}$ ), highlighting their rapid inactivation kinetics. Similarly, incubating LV-VSV-G for longer times (30 min, 60 min, 120 min, 360 min) and with increasing amounts of MUS:OT NPs (5, 250 and 500  $\mu\text{g/ml}$ ) was observed a reduction in the number of virus particles proportional to the concentration and the time of exposure of the NPs.

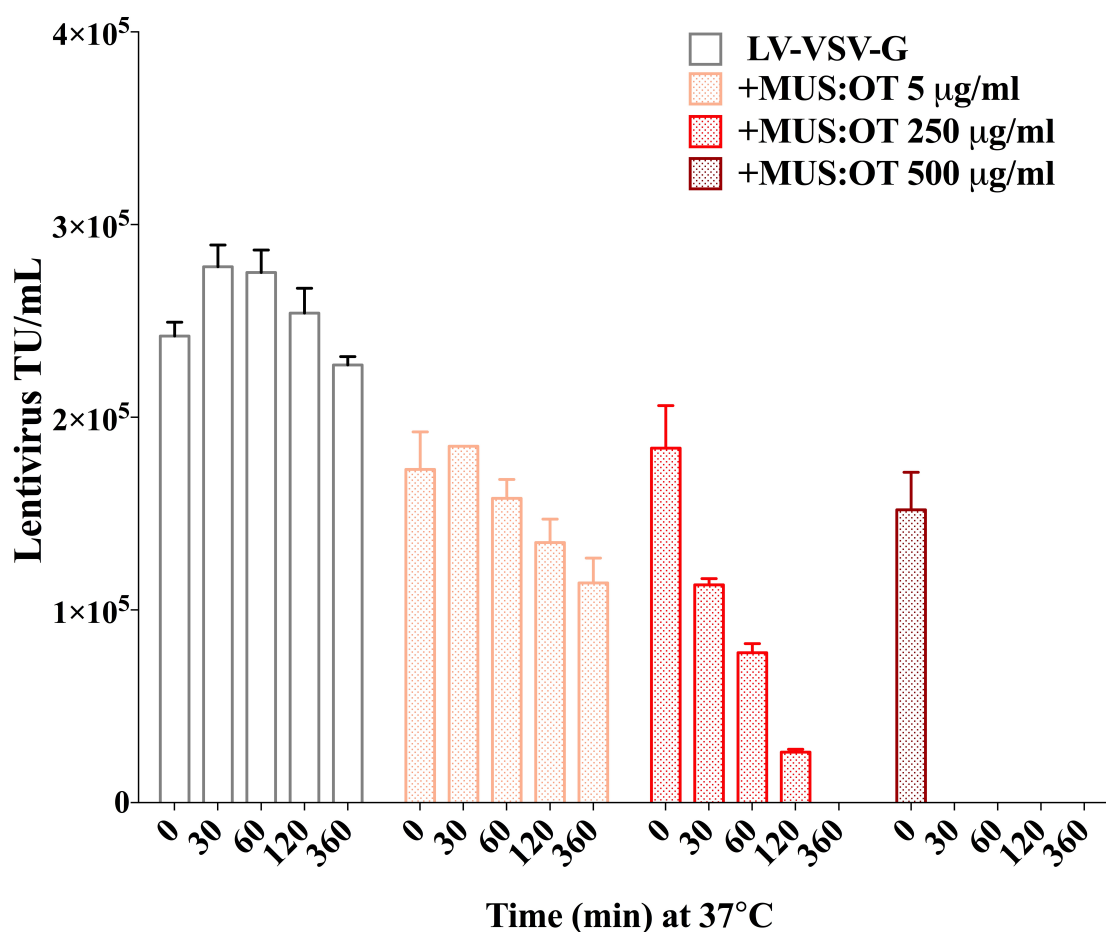


**Figure 22. Virucidal assays of LV-VSV-G with MUS:OT NPs versus time.**

LV-VSV-G was titrated (through dilution method) after exposure for different times (0, 30, 60, 120,

360 min) with increasing concentrations of MUS:OT NPs: 5 µg/ml (5 nM) (orange bars), 250 µg/ml (250 nM) (light red bars), 500 µg/ml (500 nM) (dark red bars).

However, the virucidal assay performed could not discriminate whether the viral inactivation observed was only due to irreversible coating of the viruses by NPs which prevents the recognition of target cells, thereby neutralizing the virus's infectivity, or NPs were destabilizing or dismantling virus particles acting as “molecular nanobullets” thus destroying viruses upon contact. To address this issue, we performed Cryo-TEM experiments with wild-type HSV-2 to visualize and characterize NPs/virus interactions and so to evaluate whether the NPs could permanently bind and inactivate viruses (virustatic) or could actually destroy infectious particles (virucidal).

#### **4.7 Cryo-Electron Microscopy (cryo-EM) of HSV-2 and MUS:OT**

Transmission electron microscopy (TEM), from its appearance 80 years ago, continues to play a fundamental role in the discovery, description and understanding of virus particles as well as for the identification of unknown viruses and the rapid diagnosis of viral infections from clinical specimens (Ying et al. 2013). TEM employs a fine electron beam, created by a high-voltage, electric current-heated tungsten filament, focused by magnetic lenses. The electron beam passes through an ultrathin plastic section with samples post-fixed in osmium and stained with the heavy metals uranyl and lead, which block the beam in proportion to their respective degrees of electron density (Graham & Orenstein 2007). The differential transmission of the electrons creates the image. TEM allowed to increase the level of magnification and resolution up to 0.1 nm and to visualize virus particles that could not be seen by light microscopes. In order to visualize viruses as well as biological samples, they must be stained with heavy metal salts (negative staining), such as phosphotungstic acid or uranyl acetate. Negative staining makes the virus stand out from the background and also provides morphological information about virus' external structure (Roingard 2008).

Although viruses can only be visualized by TEM, the fine detail of viral structure can be visible by the rapid freeze and vitrification of viral specimens, examined by cryo-electron microscopy (cryo-EM) (Roingard 2008). This technique is widely used in structural biology and allows to quickly create high-resolution models of molecules or enzymes (ribosomes) (Callaway 2015).

Consequently, since we wanted to investigate the intimate nature of the interactions occurring between viruses and NPs, cryo-EM experiments were performed with MUS:OT NPs and a wild-type HSPG-binding virus (HSV-2) (Figure 23). Viruses, at a concentration of  $10^7$  PFU/ml, were imaged after 1.5 h at 37°C with MUS:OT NPs at 200 µg/ml (200 nM) and untreated virus was used as a control. Although the study of NPs/virus interactions through cryo-EM is still in its initial phase, first preliminary images allowed to elucidate and narrow down the mechanism of inhibition of MUS:OT NPs toward HSPG-binding viruses. As it is shown in Figure 23, according to the hypothesized mechanism of action, MUS:OT NPs do interact with infectious virions. More specifically, HSV-2 particles incubated with MUS:OT NPs were always associated with NPs and this tight interaction might be responsible for the inhibition observed *in vitro*. Indeed, NPs can either completely cover the outer surface of the virus or bind to multiple sites onto the capsid.

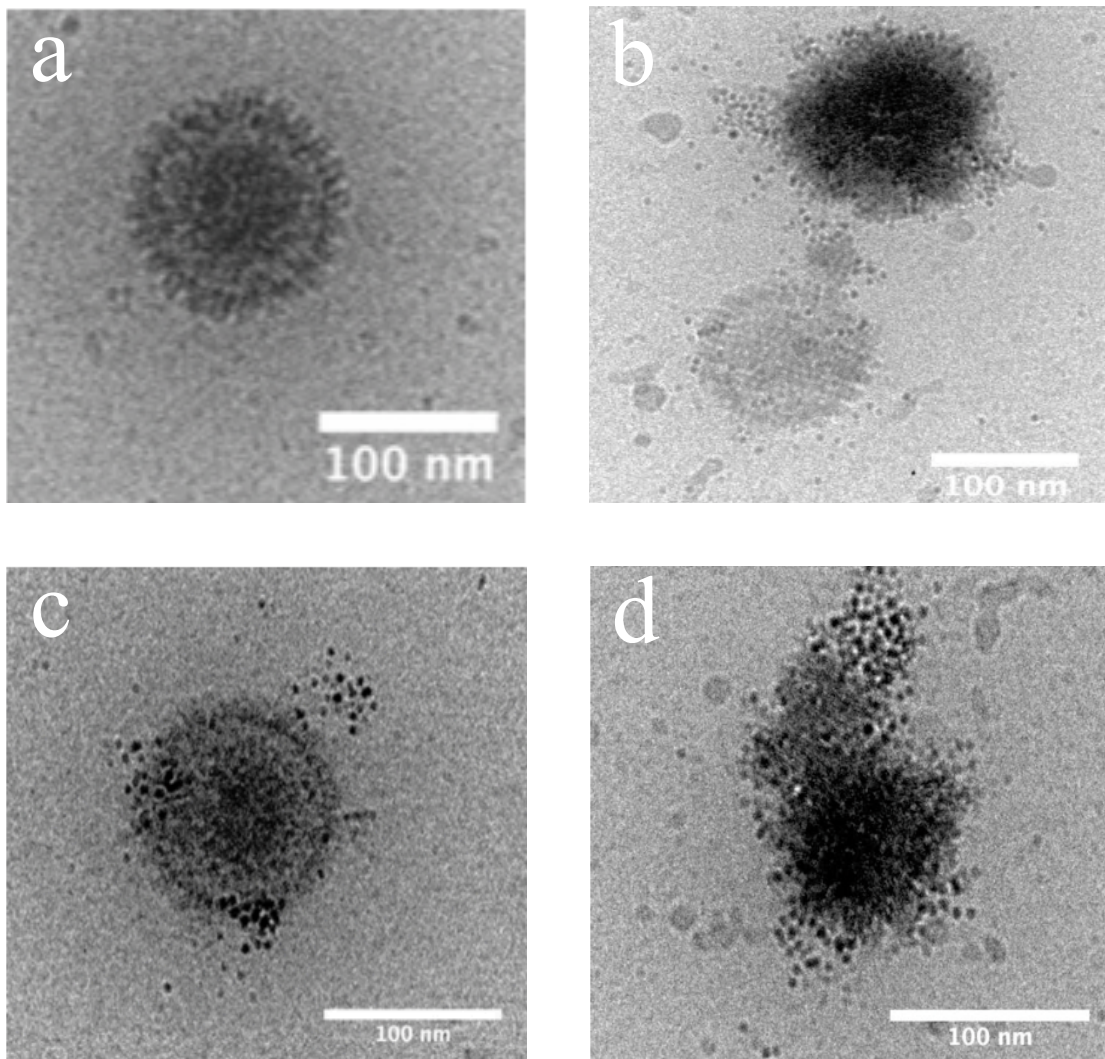


**Figure 23. Cryo-EM images of HSV-2.**

HSV2 were imaged after 1.5h at 37°C. (a) HSV-2 virions without MUS:OT NPs. (b, c, d) HSV-2 particles incubated with 200  $\mu\text{g/ml}$  of MUS:OT NPs.

## V. DISCUSSION

Viral infections represent a continuous threat to global health. The approved drugs employed for the treatment of viral diseases, act specifically by blocking viral proteins (e.g capsid proteins, viral enzymes) necessary for the infection of host cells. These virus-specific drugs, especially those against important human pathogenic viruses, have saved innumerable lives, underlining their remarkable success in clinics (Vigant et al. 2015). Despite the undoubted achievements of targeted antiviral strategies, the emergence of viral resistance and drug-related side effects, pointed out the need for the design and development of antiviral molecules with a wider activity. To address this challenge, in the present research project we investigated the potential use of Au-NPs exposing sulfonate ligands as broad-spectrum antiviral agents inhibiting early steps of infection (attachment and/or entry). We hypothesized that these NPs potentially interact with the whole subset of viruses that binds extracellular sulfates such as heparan sulfates in the glycocalyx on target cells and thereby inhibits the infection and the spread of viruses.

### **5.1 Inhibition of viruses by sulfonate-presenting NPs (MUS, MUS:OT)**

In this project we aim at assessing the ability of sulfonated NPs (MUS and MUS:OT) as potential inhibitors of a wide range of HSPG-binding viruses.

As first preliminary *in vitro* experiments, it was essential to verify that sulfonated coated Au-NPs were not inducing cytotoxicity *per se*. Cell viability was evaluated by PI staining and MTS assay in our cell culture models employing a wide range of working concentrations of sulfonated Au-NPs (Figure 6). In both assays, no significant reduction in cell viability was associated with the presence of NPs. This first observation allowed to conclude that NPs were eligible for the study of virus inhibition with cells. Indeed, it was possible to associate the decrease in the percentage of infected cells as a result of the antiviral activity of NPs and not as an increase in cell mortality due to their cytotoxic effect (Baram-Pinto et al. 2010).

Initially, the inhibitory effect of MUS:OT and MUS sulfonated NPs was evaluated for lentiviral vectors by *in vitro* experiments in HeLa cells. Lentivirus, derived from HIV-1, was pseudotyped with the G protein of VSV (LV-VSV-G) and used as viral model both for of its ability to infect a wide range of cells and for its relatively low biosafety profile (Durand & Cimarelli 2011). In particular, LV-VSV-G was chosen because its broad tropism was essential to further support that the inhibitory effect of NPs was not dependent on specific target cells. Another important feature offered by the LV-VSV-G model system was that it exploited HSPGs to infect cells (Copreni et al. 2006; Copreni et al. 2005). This last feature was fundamental to assess the hypothesized antiviral mechanism of action: the inhibition of virus infection by sulfonated NPs was based on competition with cellular HSPGs for the binding to infectious virions. Furthermore, it allowed to investigate specifically the physicochemical interactions between sulfonated NPs and viral particles and thus evaluate their ability to block the first crucial steps of the infectious process (attachment and entry phases). The first *in vitro* antiviral assays, conducted in a permissive cell line (HeLa), was carried out incubating LV-VSV-G with increasing amounts of both kinds of sulfonated NPs (MUS and MUS:OT) for 1h at 37°C prior infection (Figure 8). We observed that both sulfonated NPs were able to inhibit Lentivirus transduction of their target cells. The ability of MUS:OT to inhibit LV-VSV-G was not restricted only to one cell line (HeLa) but it was also confirmed in other HS-presenting cell models (Jurkat and HT-1080), (Fig. 9).

Next, to corroborate our findings we included in our study a set of cross-control experiments testing 1) that lentivirus was not inhibited by non-sulfonated Au-NPs (EG<sub>2</sub>-OH NPs) of the same size of MUS:OT and 2) whether MUS:OT NPs could also inhibit non-HS-binding viruses. As shown in Figure 10c, LV was not inhibited by EG<sub>2</sub>-OH NPs, even at the highest concentrations. This finding further supported our initial results showing that the exposed functional groups (SO<sub>3</sub><sup>-</sup>) on MUS:OT NPs and in particular the spatial arrangement of MUS molecules bound on the NPs' surface were essential for the observed inhibitory activity. In parallel, to assess the inhibitory ability of MUS:OT NPs on viruses that do not require

HSPGs for the attachment to host cells, we assayed MUS:OT NPs in presence of Adenovirus serotype 5 (Ad5), (Figure 10d). The replication-defective Ad5, a double-stranded DNA virus widely used for gene therapy in human diseases (Tatsis & Ertl 2004), was the ideal candidate to test our hypothesis because of its inability to bind HSPGs. Indeed, Ad5 infects target cells through the binding of a primary receptor used also by Coxsackie B virus, termed the Coxsackie and Adenovirus receptor (CAR) (Bergelson 1997). As reported by many studies, Ad5 is not able to bind CAR-defective cells as the Chinese hamster ovary (CHO) cells (Roelvink et al. 1998; Davison et al. 1999). As expected, the inhibition assay revealed that MUS:OT NPs did not induce any reduction in the number the of transduced cells by Ad5 (Figure 10d). These results proved that the antiviral activity of sulfonate exposing NPs was limited to lentivirus, which required HSPG to infect cells, while no effects were observed in the case of the Adenovirus vector.

It can be summarized that MUS:OT NPs, showed a superior antiviral effect on LV-VSV-G compared to MUS NPs. Inhibition assays conducted with MUS:OT in all *in vitro* models pointed out: 1) a high specificity of NPs toward lentiviral particles, leading to  $IC_{50}$  values in the range of nanomolar concentrations and 2) the versatility of MUS:OT NPs as antiviral system, since their effectiveness was comparable in all the cell lines tested. The peculiar surface composition of the amphiphilic Au-NPs, that contained MUS and OT ligands, compared to homoligand shell NPs (MUS NPs) (Jackson et al. 2004) could explain the enhanced ability of MUS:OT NPs to inhibit lentiviruses. Specifically, the repetitive pattern of hydrophobic and hydrophilic molecules on MUS:OT NPs seems to fit better the sulfate binding site on the virus capsid than the completely sulfonate ones (MUS NPs) and hence induce a stronger binding.

Another important issue, that required further investigation, was the role of MUS ligand alone in the inhibition of Lentivirus. Therefore, in order to assess whether the antiviral efficacy of NPs functionalized with multivalent MUS molecules was due to their arrangement on the surface or not, we compared the effect of the soluble MUS ligand in

presence of LV-VSV-G. MUS ligand was found to be completely ineffective in inhibiting the lentivirus, compared to the same amount bound to the NPs (Figure 10a). This control experiment suggested that only ligands bound to a NP and hence organized in a precise pattern and distance act as antivirals, emphasizing the importance of the spatial orientation of functional groups on the surface of NPs. Moreover, this finding underlined that multivalent interactions achieved with the use of NPs, were crucial for effectively engaging viral proteins and inhibit infection. Thus, the use of functionalized NPs, capped with molecules resembling natural viral receptor such as MUS, rather than molecules in solution, was found to be a promising tool eligible for the development of antivirals especially considering the low quantities (nM) needed to inhibit virus infection. Our results with sulfonated Au-NPs as viral inhibitor were in accordance with similar previous studies conducted by Baram-Pinto and co-workers (Baram-Pinto et al. 2010). In their study, they compared, through a plaque-reduction assay, the antiviral efficiency of Au-MES NPs respect to the ligand molecules (soluble MES) bound to the NPs. They reported a complete inhibition of wild-type HSV-1 McIntyre strain in Vero cells, obtained with Au-MES NPs, while no reduction in virus infectivity was observed when using the same amount of free MES. The outcome of their experiments allowed them to conclude that the antiviral effect was specifically due to MES functionalized NPs, whereas the two components taken on their own (unmodified Au-NPs and soluble MES ligands) did not inhibit HSV-1 infection (Baram-Pinto et al. 2010).

Having assessed the role of MUS:OT in inhibiting LV-VSV-G transduction, MUS:OT NPs were tested on several human pathogenic viruses using HSPGs as first step for virus infection, such as wild-type HSV-2, HSV-1 and HPV-16 PsV. These set of experiments were conducted in the laboratory of molecular virology in collaboration with Prof. David Lembo's group at the University of Turin, Italy. The inhibition assays run with MUS:OT NPs clearly showed that MUS:OT NPs could prevent the infection of target cells in the same range of concentrations (1-10 nM) as for initial lentivirus experiments (Figure 11). The efficacy of



MUS:OT NPs highlighted their inhibitory property also in wild-type models, further validating their potential use as broad spectrum agents against HSPG-binding viruses. Similarly, to the control experiment performed with LV-VSV-G, HSV-1, HSV-2 and HPV-16-VLP were incubated with only MUS soluble ligand, which was found to be ineffective in the inhibition the viruses (data not shown). In light of the results obtained with these important human viral pathogens, we wanted to extend our study to HIV-1, the viral pathogens responsible for the acquired immunodeficiency syndrome (AIDS), known to interact with membrane HSPGs (syndecans) for the adsorption and subsequent infection of its major target cells *in vivo*: macrophages (Saphire et al. 2001). Considering that the study of infectious replicative-competent HIV-1 viruses requires certified laboratories that can deal with class III hazard infectious substances (Prokofjeva et al. 2011), in our study we developed and used pseudo-HIV-1 lentiviral particles as safe model for the study of MUS:OT NPs against wild-type HIV (Figure 12). Such lentiviral-based HIV-1 model have been used by many researchers as safe approach for the screening of anti-HIV drugs (Prokofjeva et al. 2011; Garcia-Perez et al. 2007). The antiviral activity of MUS:OT NPs was thus tested with pseudo-HIV-1 particles which are lentiviruses expressing the envelope glycoprotein of HIV (gp160) and thus structurally, but not genetically, similar to the native virus and available for laboratory use (biosafety level 2 – BSL2). The antiviral assay confirmed that MUS:OT NPs were able to inhibit the pseudotyped-gp160 lentivirus (LV-gp160) (Figure 13). Altogether these results supported the antiviral ability of MUS:OT NPs toward sulfonate binding viruses. Finally, the initial hypothesis that MUS:OT NPs could selectively inhibit viruses binding sulfates on cell membrane by mimicking the natural viral receptor, was validated by the experiment with two serotypes of Adeno-associated virus (AAV2 and AAV5). We found inhibition of AAV2 that exploits HSPGs as attachment factor, and no effect was observed with AAV5 that binds sialic acid, which supported the proposed mechanism of interaction of the NPs (Figure 14).

The use of nanoscale materials like NPs as potential antiviral agents is an expanding field of

research. NPs represent an attractive tool to fight viral infections owing to their unique physicochemical properties, such as their size and their high surface-volume ratio, which offers more contact area for the attachment of ligands and active molecules. Several recent papers have reported that metal-based NPs, in particular Au-NPs and Ag-NPs functionalized infectious cycle, specifically the attachment and entry processes (Baram-Pinto et al. 2009; Elechiguerra et al. 2005). Indeed, NPs can be coated with molecules mimicking natural viral receptors, thus engaging multivalent interactions with virions that inhibit/prevent recognition and infection of the target cell. This strategy has been validated in many studies where metal nanoparticles have been proven to be effective antiviral agents against several types of viruses: HIV, HSV type 1, monkeypox virus (Lara et al. 2010; Lu et al. 2008; Baram-Pinto et al. 2010; Rogers et al. 2008). An example is the study conducted by Papp and co-workers (Papp et al. 2010). They observed that influenza virus infection was inhibited by using nanoparticles functionalised with sialic acid (SA)-terminated glycerol dendron that resembled the natural viral receptors on the surface of the host cell. They found that the ability of influenza virus to bind target cells was affected by the use of nanomolar concentrations of 14 nm sialic-acid Au-NPs.

## **5.2 Antiviral mechanism of action of MUS:OT NPs**

### **5.2.1 Time of addition**

The inhibition assays pointed out a selective inhibitory ability of MUS:OT NPs toward those viruses binding HSPGs as primary attachment receptor. However, the limit of the inhibition assay experiments was that they could not discriminate whether NPs were exclusively acting at the initial stage(s) of the transfection process (attachment). Another mechanism that could explain the reduced number of transduced cells was NPs' interference with intracellular replication processes that occur within the cytoplasmatic matrix, for example uncoating and replication. Indeed, as reported by Verma et al. (Verma et al. 2008), MUS:OT NPs could

passively penetrate the cell membrane, even when the endocytosis is blocked. This could indicate an intracellular inhibition especially in the light of the lower efficiency of MUS NPs, which can only penetrate cell membrane through endocytic routes. In order to understand at which stage(s) of the infection MUS:OT NPs exerted their antiviral activity, several experiments were performed, using LV-VSV-G as viral model. First, to assess whether MUS:OT were able to block the infection intracellularly, HeLa cells were preincubated with NPs for time points (8, 4, 2, 1, 0.5 hour) at 37°C before delivering lentiviral particles. It was observed that NPs already internalized into the cells did not produce any inhibitory effect (Figure 16a) resulting in the number of transduced cells comparable to the untreated control.

Next, time-of-addition (TOA) experiments were carried out to explore whether MUS:OT NPs interact with the virus during or after fusion with the cells. To address this issue, MUS:OT NPs were delivered to cells, HeLa and HT-1080, (Figure 16b, 16c) along with LV-VSV-G (co-added) or after the transduction (0h or 2h post transduction). In both cell lines, MUS:OT NPs had an antiviral effect on the transduction efficiency of LV-VSV-G only when they could interact with virions outside the cells. The addition of the NPs immediately after the transduction (0h p) or 2h after, did not affect the percentage of transduced cells compared to the untreated control (Figure 16b, 16c).

These findings indicate that MUS:OT were only exerting their antiviral action through direct interactions with virions but they could not stop any replicative process inside the cell. In order to validate these results, we carried out TOA experiment under similar experimental conditions by comparing the hypothesized antiviral mechanism of MUS:OT NPs with AZT (Figure 17), a well characterized non-nucleoside retrotranscriptase inhibitor. This inhibitor interferes with a viral enzyme intracellularly at a well-defined time point (2-3 hours after infection) in the virus replication cycle. As expected, the anti-retroviral drug AZT could only inhibit the transduction of LV-VSV-G when added within four hours post infection or long before the infection (3h), meaning that the compound could not stop the retrotranscriptase if

incubated for short times with the cells (10 min). On the other hand, NPs did not determine any effect neither before nor after the infection, in accordance to what we observed previously, while they could efficiently inhibit transduction when they were co-added with lentiviral particles. These findings allowed to conclude that although MUS:OT NPs could easily penetrate the cells, they were not able to interfere with post-fusion replicative events.

### **5.2.2 Entry vs attachment assay**

In order to understand whether the entry and/or the attachment of LV-VSV-G could be involved in the mechanism of MUS:OT inhibition we performed attachment *vs* entry assay. We found that MUS:OT NPs were able to interfere with the attachment and only partially during the entry step (Figure 19). These findings confirmed our hypothesis that sulfonated MUS:OT NPs can act as competitive antagonists for viruses binding to HSPGs on target cells.

Nevertheless, these two assays could not determine whether MUS:OT NPs:

1. bind irreversibly to the virions and hence block the recognition of HSPGs on cell surface,
2. engage weak interactions with the virions, hence upon certain conditions (dilutions) they regain infectivity,
3. were bound to viral glycoproteins as well as to viral membrane inducing some conformational changes which rendered the virus not infectious,
4. interact strongly with virions destroying them and resulting in a virucidal action.

As reported in literature, we considered other possible mechanisms such as viral inhibition by interactions between NPs and viral nucleic acids. For example, Lu et al. have reported that Ag-NPs of about 10 nm could both interact with Hepatitis B virus (HBV) as well as bind to the viral DNA, thereby impeding virus replication. Summarizing our results, we can conclude that the most likely sites for MUS:OT NPs and virus interactions were viral

envelope glycoproteins and no post-entry interaction leads to inhibition of the virus.

### **5.3 Virus inactivation by MUS:OT NPs**

In order to characterize the nature of NPs/virus interactions we performed the virucidal assay. Virucidal experiments were conducted with pseudotyped lentivirus (LV-VSV-G) as well as with HSV-2 wild type virus after incubation with MUS:OT NPs for 2h at 37°C. We observed that the amount of viruses able to infect cells, calculated by serial dilutions of the NPs/virus mixture (titration method), was drastically reduced (Figure 20a, 21). These findings confirmed that sulfonated NPs were acting through a direct binding to viruses' external structure thus rendering them no more infectious (inactive). Moreover, the experiment allowed to exclude that interactions between NPs and viruses were reversible. Indeed, although the hypothesized mechanism of interaction was based on weak electrostatic interactions, MUS:OT NPs were able to permanently inactivate viruses once they encountered HS-binding viruses even after dilution. Consequently, if interactions had been weak, NPs would have been detached from viruses' surface once diluted and thus the number of viruses able to infect the cells would have been the same as in the untreated control (Figure 24). Moreover, virucidal assay performed with MUS:OT NPs and non-HS binding virus (Adenovirus) (Figure 20b) or non-sulfonated NPs (EG<sub>2</sub>-OH NPs) and LV-VSV-G (Figure 20a) showed no decrease in the number of virus particles.

Next, we investigated the effect of MUS:OT NPs at different incubation times and with increasing concentration of MUS:OT NPs (Figure 22). Results showed that the decrease in the number of infectious viruses was directly proportional to the incubation time and concentrations tested. This finding allowed to hypothesize that MUS:OT and viruses were interacting through tight binding, which have in turn impeded the recognition of the host cell (by physically block virus receptors) or disrupted virus structure. In particular, the reduced number of virus particles, calculated within the first minutes of incubation with NPs,

highlighted the potential ability of MUS:OT NPs as virucidal agent which by definition act quickly and effectively in preventing infection of vulnerable target cells (Lara et al. 2010; Borkow et al. 1997).

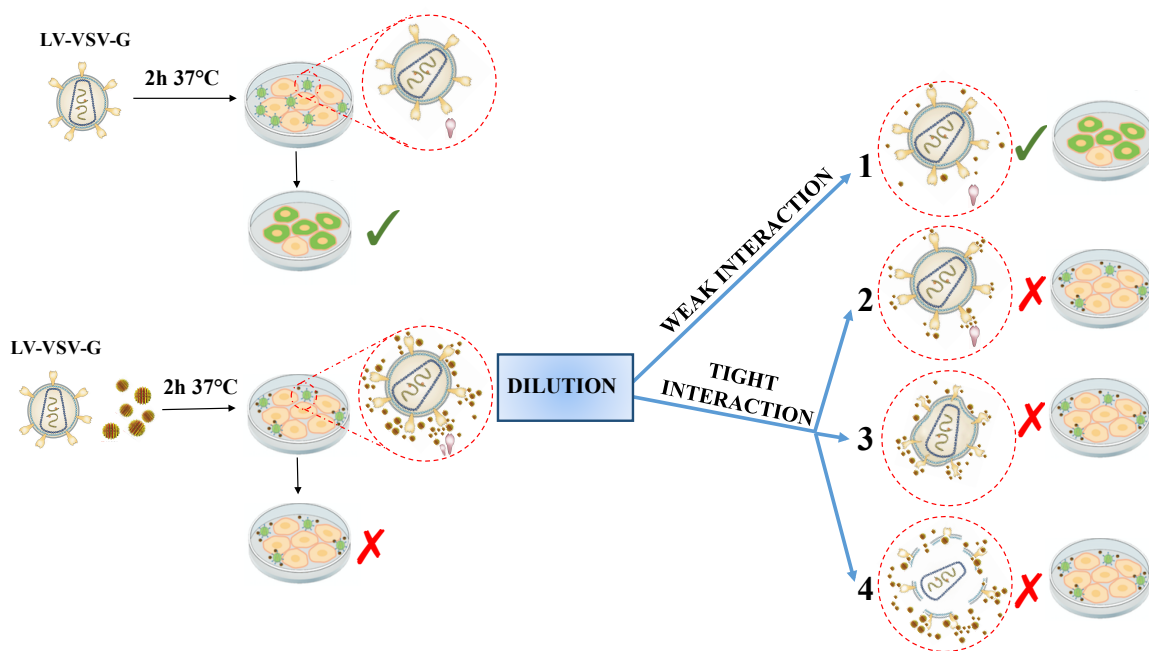


**Figure 24. Virucidal assay with MUS:OT NPs and possible mechanisms of virus inactivation.**

Once viruses are delivered to cells together with NPs they could not attach to target cells owing to the interactions between virus envelope glycoproteins and NPs.

Diluting Virus/NPs mixture, virus could:

- (1) regain its infectivity, if interactions were weak
- (2) remain non infectious (inactivated), because NPs engage tight binding to envelope glycoproteins. In this way, the virus maintains its structural conformation but can not recognize target cells (virustatic effect)
- (3) be inactivated due to changes in its structural conformation and thus can not recognize target cells and infect them (virustatic effect)
- (4) be destroyed upon contact with NPs (virucidal effect) and thus can not infect target cells

Based on the *in vitro* virucidal experiments, we could narrow down the mechanisms through which NPs could inactivate a virus. We could exclude inactivation by weak interactions that only interfere with the recognition of the cellular binding site, because by diluting NPs/virus mixture we did not observe any transduced cells. These results suggested that the inhibitory effect of MUS:OT NPs was due to tight NPs/virus interactions which could not merely impede the recognition of target cells by mimicking the natural attachment receptors. The binding of NPs to specific sites on the outer surface of HS-binding viruses, presumably on those glycoproteins responsible for the recognition of target cells, was also shown by other researchers, e.g. on Ag-NPs with anti-HIV ability (Elechiguerra et al. 2005; Lara et al. 2010). Researchers observed that NPs within a certain size range (1-10 nm) could efficiently interact with specific sites on the viral envelope and inactivate infectious HIV-1 particles. These studies (Elechiguerra et al. 2005; Lara et al. 2010) pointed out that the spatial arrangement of the Ag-NPs on HIV-1 virion, can be explained by a preferential binding on the Ag-NPs with gp160 viral envelope glycoproteins, in particular with its gp120 subunits. Following the hypothesis reported in literature, we assume that the ability of MUS:OT NPs to inactivate several types of viruses could be mainly driven by electrostatic interactions with those positively charged amino acids on viral glycoproteins that recognize HSPGs on target cells. Therefore the activity of MUS:OT NPs must be universal to all HS-binding viruses.

#### **5.4 Cryo-EM study of the NP/virus interaction**

Cryo-EM experiments were carried out to elucidate the type of interaction occurred between MUS:OT with a HS-binding virus (e.g HSV-2) (Figure 23). Our cryo-EM images showed that NPs were found to be diffusely attached to HSV-2 virions and hence indicated that a tight NPs binding leads to inactivation of infectious HSV-2. Thus cryo-EM allowed to narrow down the mechanism of action to two possible mechanisms of viral inactivation: 1) MUS:OT NPs binds to HSV-2 on its surface glycoproteins in an irreversible way that

permanently block the virus or 2) MUS:OT NPs could engage tight interactions with HSV-2 virion that lead to important conformational changes at HSV-2 structure with a resultant inability of the virus to recognise and infect target cells. Although cryo-EM indicated to one of the aforementioned mechanisms for HSV-2 inactivation, also a third mechanism is possible. We hypothesize that MUS:OT NPs interaction with viruses' capsid is so strong that it not only leads to conformational changes but also to a rupture of the virus. This possibility is still under investigation. Broglie and co-workers (Broglie et al. 2015) reported that gold/copper sulphide (Au/CuS) NPs can rapidly inactivate Norovirus virus-like particles (VLP). They suggested that NPs treatment determined capsid protein degradation and consequently the damage to VLPs explained by virus inactivation. Moreover, they found that treatment with high concentrations of Au/CuS NPs (83  $\mu$ M) could break Norovirus VLP's capsids into fragments with no evidence of structurally intact VLPs.



## VI. CONCLUSIONS AND FUTURE OUTLOOK

The use of HSPG as docking site for the attachment of a large variety of human pathogenic viruses, such as HIV, HPV, HSV, CHIKV, Ebola and Dengue (WuYang et al. 2011; Salvador et al. 2013; Gardner et al. 2014) makes surface engineered NPs, coated with sulfonates, an attractive wide-spectrum antiviral with potential virucidal properties. In particular, the efficacy of MUS:OT NPs against such broad range of viruses suggests their valuable use as novel therapeutic agent as well as a key component of new microbicidal materials. The proposed antiviral mechanism of action is given by to the characteristic arrangement of the ligands on the surface of NPs.

Differently from other studies conducted on sulfonate-capped NPs, MUS:OT NPs showed not only antiviral (blocking), but also virucidal (destructive), effect toward a wide range of HS-binding viruses at very low concentrations. Their future application can range from topical microbicide e.g. in form of a cream or gel which can prevent the infection with sexually transmissible viral diseases, to surface constituent of materials that would prevent virus transmission (e.g. air filters, protective garments). Au-NPs are an extremely versatile model that easily enables fine-tuning of surface properties; however, their non-negligible cost is a main drawback that prevents translation into a cheap and far-reaching technology. For this reason we planned to engineer NPs with the same surface characteristics as MUS:OT but with a different core such dendrimers, silica, iron oxide.



## VII. REFERENCES

- Al-jabri, A.A. et al., 2000. In vitro anti-HIV-1 virucidal activity of tyrosine-conjugated tri- and dihydroxy bile salt derivatives. *Journal of Antimicrobial Chemotherapy*, (45), pp.617–621.
- Alexis, F. et al., 2008. Factors affecting the clearance and biodistribution of polymeric nanoparticles. *Molecular Pharmaceutics*, 5(4), pp.505–515.
- Amstutz, B. et al., 2008. Subversion of CtBP1-controlled macropinocytosis by human adenovirus serotype 3. *The EMBO journal*, 27(7), pp.956–969.
- Anderson, H.A., Chen, Y. & Norkint, L.C., 1996. Bound Simian Virus 40 Translocates to Caveolin- enriched Membrane Domains , and Its Entry Is Inhibited by Drugs that Selectively Disrupt Caveolae. *Molecular Biology of the Cell*, 7(November), pp.1825–1834.
- Anon, 2006. The double life of lentiviruses. *Nature Methods*, 3(2), p.89.
- Athanasopoulos, T. et al., 2004. Recombinant adeno-associated viral (rAAV) vectors as therapeutic tools for Duchenne muscular dystrophy (DMD). *Gene Therapy*, 11 Suppl 1, pp.S109–21.
- Baram-Pinto, D. et al., 2009. Inhibition of herpes simplex virus type 1 infection by silver nanoparticles capped with mercaptoethane sulfonate. *Bioconjugate Chemistry*, 20(8), pp.1497–502.
- Baram-Pinto, D. et al., 2010. Inhibition of HSV-1 attachment, entry, and cell-to-cell spread by functionalized multivalent gold nanoparticles. *Small*, 6(9), pp.1044–1050.
- Barré-sinoussi, F., Ross, A.L. & Delfraissy, J., 2013. Past, present and future: 30 years of HIV research. *Nature Publishing Group*, 11(12), pp.877–883.
- Bartlett, A.H. & Park, P.W., 2011. Heparan Sulfate Proteoglycans in Infection. *Glycans in Diseases and Therapeutics*. pp. 31–62.
- Baseman, J.G. & Koutsky, L.A., 2005. The epidemiology of human papillomavirus infections. *Journal of Clinical Virology*, 32, pp.16–24.
- Bastian, A.R. et al., 2011. Cell-Free HIV-1 virucidal action by modified peptide triazole inhibitors of Env gp120. *ChemMedChem*, 6, pp.1335–1339.
- Bender, A.R. et al., 1996. Efficiency of nanoparticles as a carrier system for antiviral agents in human immunodeficiency virus-infected human monocytes / macrophages in vitro. *Antimicrobial Agents and Chemotherapy*, 40(6), pp.1467–1471.
- Bergelson, J.M., 1997. Isolation of a common receptor for Coxsackie B Viruses and Adenoviruses 2 and 5. *Science*, 275(5304), pp.1320–1323.
- Bernard, H.-U. et al., 2010. Classification of papillomaviruses (PVs) based on 189 PV types and proposal of taxonomic amendments. *Virology*, 401(1), pp.70–79.
- Bernfield, M. et al., 1999. Functions of cell surface heparan sulfate proteoglycans. *Annual Review of Biochemistry*, 68, pp.729–777.
- Bishop, J.R., Schuksz, M. & Esko, J.D., 2007. Heparan sulphate proteoglycans fine-tune mammalian physiology. *Nature*, 446(April), pp.1030–1037.
- Borkow, G. et al., 1997. Chemical barriers to human immunodeficiency virus type 1 (HIV-

- 1) infection: retrovirucidal activity of UC781, a thiocarboxanilide nonnucleoside inhibitor of HIV-1 reverse transcriptase. *Journal of virology*, 71(4), pp.3023–3030.
- Bosch, F.X. et al., 2008. Epidemiology and natural history of human papillomavirus infections and type-specific implications in cervical neoplasia. *Vaccine*, 26 Suppl 1, pp.K1–16.
- Bosch, F.X. et al., 2002. The causal relation between human papillomavirus and cervical cancer. *Journal of clinical pathology*, 55, pp.244–265.
- Brogie, J.J. et al., 2015. Antiviral activity of gold/copper sulfide core/shell nanoparticles against human norovirus virus-like particles. *PloS one*, 10, pp.1–14.
- Buck, C.B. et al., 2006. Carrageenan is a potent inhibitor of papillomavirus infection. *PLoS Pathogens*, 2(7), pp.671–680.
- Buck, C.B. et al., 2005. Generation of HPV pseudovirions using transfection and their use in neutralization assays. *Methods in molecular medicine*, 119, pp.445–462.
- Büning, H. et al., 2003. Receptor targeting of adeno-associated virus vectors. *Gene therapy*, 10(14), pp.1142–51.
- Burd, E., 2003. Human papillomavirus and cervical cancer. *Clin Microbiol Rev*, 16(1), pp.1–17.
- Callaway, E., 2015. The revolution will not be crystallized. *Nature*, 525, pp.172–174.
- Cavalli, R. et al., 2012. Enhanced antiviral activity of acyclovir loaded into  $\beta$ -cyclodextrin-poly(4-acryloylmorpholine) conjugate nanoparticles. *Journal of Controlled Release*, 137, pp.116-122
- Chakrabarty, A.N., Mookerjee, M. & Dastidar, S.G., 2000. Screening for anti-HIV drugs that can combine virucidal and virustatic activities synergistically. *International Journal of Antimicrobial Agents*, 14, pp.215–220.
- Cheshenko, N. et al., 2007. Multiple receptor interactions trigger release of membrane and intracellular calcium stores critical for herpes simplex virus entry. *Molecular Biology of the Cell*, 18, pp.3119–3130.
- Choudhary, S. et al., 2011. Herpes simplex virus type-1 (HSV-1) entry into human mesenchymal stem cells is heavily dependent on heparan sulfate. *Journal of Biomedicine & Biotechnology*, 2011, pp.1–11.
- Christianson, H.C. & Belting, M., 2014. Heparan sulfate proteoglycan as a cell-surface endocytosis receptor. *Matrix Biology*, 35, pp.51–55.
- De Clercq, E., 2015. AMD3100 / CXCR4 inhibitor. *Frontiers in Immunology*, 6(June), pp.9–11.
- De Clercq, E., 2004. Antivirals and antiviral strategies. *Nature Reviews Microbiology*, 2(September), pp.704-720.
- De Clercq, E., 2002. Strategies in the design of antiviral drugs. *Nature Reviews Drug Discovery*, 1(January), pp.13–25.
- Connell, B.J. & Lortat-Jacob, H., 2013. Human immunodeficiency virus and heparan sulfate: From attachment to entry inhibition. *Frontiers in Immunology*, 4(November), pp.1–12.
- Copreni, E. et al., 2005. Gene transfer to the airway epithelium mediated by a third generation HIV-1 based vector: efficiency and role of heparan sulfate. *Molecular*

*Therapy*, 11(May), p.S140

- Copreni, E. et al., 2006. Involvement of glycosaminoglycans in VSV-G pseudotyped lentiviral vector mediated gene transfer into airway epithelial cells. *Molecular Therapy*, 13(May), pp.S268–S269.
- Coyne, C.B. et al., 2007. Coxsackievirus entry across epithelial tight junctions requires occludin and the small GTPases Rab34 and Rab5. *Cell Host Microbe*, (September), pp.181–192.
- Daelemans, D. et al., 2011. A time-of-drug addition approach to target identification of antiviral compounds. *Nature Protocols*, 6(6), pp.925–933.
- Davidson, B.L. & Breakefield, X.O., 2003. Viral vectors for gene delivery to the nervous system. *Nature Reviews Neurosciences*, 4(May), pp.353–364.
- Davison, E., Kirby, I. & Elliott, T., 1999. The Human HLA-A \* 0201 Allele , Expressed in Hamster Cells , Is Not a High-Affinity Receptor for Adenovirus Type 5 Fiber. *Journal of Virology*, 73(5), pp.4513–4517.
- Daya, S. & Berns, K.I., 2008. Gene therapy using adeno-associated virus vectors. *Clinical Microbiology Reviews*, 21(4), pp.583–93.
- Dhaliwal, S. et al., 2008. Mucoadhesive microspheres for gastroretentive delivery of acyclovir: in vitro and in vivo evaluation. *The AAPS journal*, 10(2), pp.322–330.
- Dragic, T. et al., 2000. A binding pocket for a small molecule inhibitor of HIV-1 entry within the transmembrane helices of CCR5. *PNAS*, 97(10), pp.5639–5644.
- Durand, S. & Cimarelli, A., 2011. The inside out of lentiviral vectors. *Viruses*, 3, pp.132–159.
- Elechiguerra, J.L. et al., 2005a. Interaction of silver nanoparticles with HIV-1. *Journal of Nanobiotechnology*, 3, pp.1-10
- Filipovic, J., Martinac, A. & Jals, I., 2005. Development and in vitro evaluation of a liposomal vaginal delivery system for acyclovir. *Journal of controlled release*, 106, pp.34–43.
- Galabrov, A.S., 2007. Virucidal agents in the eve of manorapid synergy ®. *GMS Krankenhaushygiene Interdisziplinar*, 2(1), pp.1–8.
- Garcia-Perez, J. et al., 2007. A New Strategy Based on Recombinant Viruses as a Tool for Assessing Drug Susceptibility of Human Immunodeficiency Virus Type 1. *Journal of medical virology*, 79, pp.127–137.
- Gardner, C.L. et al., 2014. Deliberate attenuation of chikungunya virus by adaptation to heparan sulfate-dependent infectivity: a model for rational arboviral vaccine design. *PLoS neglected tropical diseases*, 8(2), pp.1–16.
- Ghosh, T. et al., 2008. Focus on antivirally active sulfated polysaccharides: From structure-activity analysis to clinical evaluation. *Glycobiology*, 19(1), pp.2–15.
- Graham, L. & Orenstein, J.M., 2007. Processing tissue and cells for transmission electron microscopy in diagnostic pathology and research. *Nature Protocols*, 2(10), pp.2439–2450.
- Guibinga, G.H. et al., 2002. Cell surface heparan sulfate is a receptor for attachment of envelope protein-free retrovirus-like particles and VSV-G pseudotyped MLV-derived retrovirus vectors to target cells. *Molecular Therapy*, 5(5), pp.538–546.

- Hädicke, A. & Blume, A., 2013. Interactions of pluronic block copolymers with lipid monolayers studied by epi-fluorescence microscopy and by adsorption experiments. *Journal of Colloid and Interface Science*, 407, pp.327–338.
- Hadigal, S. & Shukla, D., 2013. Exploiting herpes simplex virus entry for novel therapeutics. *Viruses*, 5(6), pp.1447–1465.
- Harisinghani, M.G. et al., 2007. Noninvasive Detection of Clinically Occult Lymph-Node Metastases in Prostate Cancer. *New England Journal of Medicine*, 348(25), pp.2491–2499.
- Hilgard, P. & Stockert, R., 2000. Heparan sulfate proteoglycans initiate dengue virus infection of hepatocytes. *Hepatology*, 32(5), pp.1069–77.
- Hobbs, S.K. et al., 1998. Regulation of transport pathways in tumor vessels: role of tumor type and microenvironment. *PNAS*, 95(8), pp.4607–4612.
- Huang, C. et al., 2008. A Novel Cellular Protein , VPEF , Facilitates Vaccinia Virus Penetration into HeLa Cells through Fluid Phase Endocytosis. *Journal of Virology*, 82(16), pp.7988–7999.
- Jackson, A.M., Myerson, J.W. & Stellacci, F., 2004. Spontaneous assembly of subnanometre- ordered domains in the ligand shell of monolayer-protected nanoparticles. *Nature Materials*, 3(May), pp.330–336.
- de Jalón, E.G. et al., 2001. Topical application of acyclovir-loaded microparticles: quantification of the drug in porcine skin layers. *Journal of Controlled Release*, 75(1-2), pp.191–7.
- Jolly, C.L. & Sattentau, Q.J., 2013. Attachment factors. *Advances in Experimental Medicine and Biology*, 790, pp.1–23.
- De Jong, W.H. & Borm, P.J. a, 2008. Drug delivery and nanoparticles: applications and hazards. *International Journal of Nanomedicine*, 3(2), pp.133–149.
- Kaludov, N. et al., 2001. Adeno-Associated Virus Serotype 4 ( AAV4 ) and AAV5 both require sialic acid binding for hemagglutination and efficient transduction but differ in sialic acid linkage specificity. *Journal of Virology*, 4, pp.6884-6893
- Kanekiyo, M. et al., 2013. Self-assembling influenza nanoparticle vaccines elicit broadly neutralizing H1N1 antibodies. *Nature*, 499, pp.102–106.
- Karasneh, G. a & Shukla, D., 2011. Herpes simplex virus infects most cell types in vitro: clues to its success. *Virology Journal*, 8(1), p.481.
- Kerr, M.C. & Teasdale, R.D., 2009. Defining macropinocytosis. *Traffic*, (10), pp.364–371.
- Kim, B.Y.S., Rutka, J.T. & Chan, W.C.W., 2010. Nanomedicine. *New England Journal of Medicine*, 363(25), pp.2434–43.
- Kwong, P.D. et al., 1998. Structure of an HIV gp120 envelope glycoprotein in complex with the CD4 receptor and a neutralizing human antibody. *Nature*, 393(June), pp.648-659
- Lara, H.H. et al., 2010. Mode of antiviral action of silver nanoparticles against HIV-1. *Journal of Nanobiotechnology*, 8, pp.1-10
- Lembo, D. et al., 2008. Sulfated K5 escherichia coli polysaccharide derivatives as wide-range inhibitors of genital types of human papillomavirus. *Antimicrobial Agents and Chemotherapy*.52, pp.1374-1381

- Lembo, D. & Cavalli, R., 2010. Nanoparticulate delivery systems for antiviral drugs. *Antiviral Chemistry & Chemotherapy*, 21, pp.53–70.
- Liberali, P., Renkema, G.H. & Hyypia, T., 2008. A raft-derived, Pak1-regulated entry participates in  $\alpha_2\beta_1$  integrin-dependent sorting to caveosomes. *Molecular Biology of the Cell*, 19(July), pp.2857–2869.
- Littler, E. & Oberg, B., 2005. Achievements and challenges in antiviral drug. *Antiviral Chemistry & Chemotherapy*, 16, pp.155–168.
- Liu, J. & Thorp, S.C., 2002. Cell surface heparan sulfate and its roles in assisting viral infections. *Medicinal Research Review*, 22(1), pp.1–25.
- Lozano, R. et al., 2012. Global and regional mortality from 235 causes of death for 20 age groups in 1990 and 2010: a systematic analysis for the Global Burden of Disease Study 2010. *Lancet*, 380, pp.2095–2128.
- Lu, L. et al., 2008. Silver nanoparticles inhibit hepatitis B virus replication. *Antiviral Therapy*, 10(5).
- Lüscher-Mattli, M., 2000. Polyanions--a lost chance in the fight against HIV and other virus diseases? *Antiviral chemistry & chemotherapy*, 11(4), pp.249–259.
- Mallipeddi, R. & Rohan, L.C., 2010. Progress in antiretroviral drug delivery using nanotechnology. *International Journal of Nanomedicine*, 5, pp.533–547.
- Malmsten, M., 2011. Antimicrobial and antiviral hydrogels. *Soft Matter*, pp.8725–8736.
- Marsh, M. & Helenius, A., 2006. Virus entry: open sesame. *Cell*, 124(4), pp.729–40.
- McGeoch, D.J., Rixon, F.J. & Davison, A.J., 2006. Topics in herpesvirus genomics and evolution. *Virus research*, 117(1), pp.90–104.
- McMahon, H.T.H.T. & Boucrot, E., 2011. Molecular mechanism and physiological functions of clathrin-mediated endocytosis. *Nature Reviews Molecular Cell Biology*, 12(8), pp.517–33.
- Meier, O. et al., 2002. Adenovirus triggers macropinocytosis and endosomal leakage together with its clathrin-mediated uptake. *The Journal of Cell Biology*, 158(6), pp.1119–1131.
- Meier, O. & Greber, U.F., 2004. Adenovirus endocytosis. *The Journal of Gene Medicine*, 6, pp.S152–63.
- Mercer, J. & Helenius, A., 2008. Vaccinia virus uses macropinocytosis and apoptotic mimicry to enter host cells. *Science*, 320, pp.531–536.
- Mercer, J. & Helenius, A., 2009. Virus entry by macropinocytosis. *Nature cell biology*, 11(5), pp.510–20.
- Mistry, N., Wibom, C. & Evander, M., 2008. Cutaneous and mucosal human papillomaviruses differ in net surface charge, potential impact on tropism. *Virology Journal*, 5(1), p.118.
- Naldini, L. et al., 1996. *In vivo* gene delivery and stable transduction of nondividing cells by a lentiviral vector. *Science*, 9(13), pp.263–267.
- Nam, J.-M., Thaxton, C.S. & Mirkin, C. a, 2003. Nanoparticle-based bio-bar codes for the ultrasensitive detection of proteins. *Science*, 301(5641), pp.1884–1886.
- Nicoll, M.P., Proença, J.T. & Efsthathiou, S., 2012. The molecular basis of herpes simplex virus latency. *FEMS microbiology reviews*, 36(3), pp.684–705.

- Ohtake, S., Arakawa, T. & Koyama, A.H., 2010. Arginine as a synergistic virucidal agent. *Molecules*, pp.1408–1424.
- Papp, I. et al., 2010a. Inhibition of influenza virus infection by multivalent sialic-acid-functionalized gold nanoparticles. *Small*, 6(24), pp.2900–2906.
- Paul, A.M. et al., 2014. Delivery of antiviral small interfering RNA with gold nanoparticles inhibits dengue virus infection in vitro. *Journal of General Virology*, 95, pp.1712–1722.
- Pelkmans, L., Kartenbeck, J. & Helenius, A., 2001. Caveolar endocytosis of simian virus 40 reveals a new two-step vesicular- transport pathway to the ER. *Nature Cell Biology*, 3(May), pp.473–484.
- Peltier, J. & Schaffer, D. V., 2010. Chapter 7 - Viral packaging and transduction of adult hippocampal neural progenitors. *Protocols for Adult Stem Cells*. pp. 103–116.
- Pérez-Berná, A.J. et al., 2012. The role of capsid maturation on Adenovirus priming for sequential uncoating. *The Journal of Biological Chemistry*, 287(37), pp.31582–31595.
- Pietäinen, V.M. et al., 2005. Viral entry, lipid rafts and caveosomes. *Annals of Medicine*, 37(6), pp.394–403.
- Pirrone, V., Wigdahl, B. & Krebs, F.C., 2011. The rise and fall of polyanionic inhibitors of the human immunodeficiency virus type 1. *Antiviral research*, 90(3), pp.168–82.
- Plotkin, S. a, 2005. Vaccines: past, present and future. *Nature medicine*, 11(4), pp.S5–S11.
- Plotkin, S. a, 2009. Vaccines: the fourth century. *Clinical and vaccine immunology*, 16(12), pp.1709–19.
- Plotkin, S.A. & Plotkin, S.L., 2011. The development of vaccines: how the past led to the future. *Nature*, 9(12), pp.889–893.
- Poon, K. & Gari, J., 2007. Cell-surface proteoglycans as molecular portals for cationic peptide and polymer entry into cells. *Biochemical Society Transactions*, 35, pp.35–37.
- Posthuma-Trumpie, G.A., Korf, J. & van Amerongen, A., 2009. Lateral flow (immuno)assay: its strengths, weaknesses, opportunities and threats. A literature survey. *Analytical and Bioanalytical Chemistry*, 393(2), pp.569–82.
- Prencipe, G. et al., 2009. PEG branched polymer for functionalization of nanomaterials with ultralong blood circulation. *Journal of the American Chemical Society*, 131(13), pp.4783–7.
- Prokofjeva, M.M. et al., 2011. Screening of potential HIV-1 inhibitors / replication blockers using secure lentiviral *in vitro* system. *Acta naturae*, 3(11), pp.55–65.
- Robinson, M.S., 2004. Adaptable adaptors for coated vesicles. *TRENDS in Cell Biology*, 14(4), pp.167-174.
- Roelvink, P.W. et al., 1998. The Coxsackievirus-Adenovirus receptor protein can function as a cellular attachment protein for adenovirus serotypes from subgroups A, C, D, E, and F. *Journal of Virology*, 72(10), pp.7909–7915
- Rogers, J. V et al., 2008. A preliminary assessment of silver nanoparticle inhibition of Monkeypox virus plaque formation. *Nanoscale Research Letters*, 3(4), pp.129–133.
- Roingard, P., 2008. Viral detection by electron microscopy: past , present and future. *Biology of the Cell*, 100, pp.491–501.
- Roldão, A. et al., 2015. Virus-like particles in vaccine development. *Expert Reviews*



*Vaccines*, 9(10), pp.1149-1176

- Rossmann, M.G., He, Y. & Kuhn, R.J., 2002. Picornavirus – receptor interactions. *TRENDS in Microbiology*, 10(7), pp.324–331.
- Rupp, R., Rosenthal, S.L. & Stanberry, L.R., 2007. VivaGel™ (SPL7013 Gel): A candidate dendrimer - microbicide for the prevention of HIV and HSV infection. *International Journal of Nanomedicine*, 2(4), pp.561–566.
- Saeed, M.F. et al., 2010. Cellular entry of ebola virus involves uptake by a macropinocytosis-like mechanism and subsequent trafficking through early and late endosomes. *PLOS Pathogens*, 6(9), pp.1-15.
- Salamon, G.M., 2003. Acyclovir terminated thiophosphate dendrimers. *Tetrahedron Letters*, 44, pp.7449–7453.
- Salvador, B. et al., 2013. Filoviruses utilize glycosaminoglycans for their attachment to target cells. *Journal of virology*, 87(6), pp.3295–304.
- de Sanjosé, S. et al., 2007. Worldwide prevalence and genotype distribution of cervical human papillomavirus DNA in women with normal cytology: a meta-analysis. *Lancet Infectious Diseases*, 7(7), pp.453–459.
- Saphire, A.C.S. et al., 2001. Syndecans serve as attachment receptors for human immunodeficiency virus type 1 on macrophages. *Journal of virology*, 75(19), pp.9187-9200
- Sapp, M. et al., 1995. Organization of the major and minor capsid proteins in human papillomavirus type 33 virus-like particles. *The Journal of general virology*, 76 ( Pt 9)(1995), pp.2407–2412.
- Sasisekharan, R. et al., 2002. Roles of heparan-sulphate glycosaminoglycans in cancer. *Nature Reviews Cancer*, 2(July), pp.521–528.
- Shafti-keramat, S. et al., 2003. Different heparan sulfate proteoglycans serve as cellular receptors for human papillomaviruses. *Journal of virology*, 77(24), pp.13125–13135.
- Sirena, D. et al., 2004. The human membrane cofactor CD46 is a receptor for species B adenovirus serotype 3. *Journal of virology*, 78(9), pp.4454–4462.
- Skehel, J.J. & Wiley, D.C., 2000. Receptor binding and membrane fusion in virus entry: the influenza hemagglutinin. *Annual Review Biochemistry*, 69, pp.531-569
- Smith, A.E. & Helenius, A., 2004. How Viruses Enter Animal Cells. *Science*, 304(April), pp.237–243.
- Smith, A.E., Lilie, H. & Helenius, A., 2003. Ganglioside-dependent cell attachment and endocytosis of murine polyomavirus-like particles. *FEBS Letters*, 555, pp.199–203.
- Spillmann, D., 2001. Heparan sulfate: anchor for viral intruders ?. *Biochimie*, 83, pp.811-817.
- Stehle, T. et al., 1996. The structure of simian virus 40 refined at 3.1 Å resolution. *Structure*, 4(2), pp.165–182.
- Steven, A.C. et al., 2005. Virus maturation : dynamics and mechanism of a stabilizing structural transition that leads to infectivity. *Current Opinion in Structural Biology*, 15, pp.227–236.
- Subramanian, R.P. & Geraghty, R.J., 2007. Herpes simplex virus type 1 mediates fusion through a hemifusion intermediate by sequential activity of glycoproteins D, H, L,

- and B. *PNAS*, 104(8), pp.2903–2908.
- Sun, L. et al., 2008. Silver Nanoparticles inhibit replication of Respiratory Syncytial Virus. *Journal of Biomedical Nanotechnology*, 4, pp.149–158.
- Szunerits, S. et al., 2015. Nanostructures for the inhibition of viral infections. *Molecules*, 20, pp.14051–14081.
- Tatsis, N. & Ertl, H.C.J., 2004. Adenoviruses as vaccine vectors. *Molecular Therapy*, 10(4), pp.616–629.
- Tiscornia, G., Singer, O. & Verma, I.M., 2006. Production and purification of lentiviral vectors. *Nature protocols*, 1(1), pp.241–245.
- Tripathi, S. et al., 2007. Anti HIV-1 virucidal activity of polyamide nucleic acid-membrane transducing peptide conjugates targeted to primer binding site of HIV-1 genome. *Virology*, 363, pp.91–103.
- Tsai, B. et al., 2003. Gangliosides are receptors for murine polyoma virus and SV40. *EMBO Journal*, 22(17).
- Uzun, O. et al., 2008. Water-soluble amphiphilic gold nanoparticles with structured ligand shells. *Chemical communications*, pp.196–198.
- Vandermeulen, G. et al., 2012. Highly potent delivery method of gp160 envelope vaccine combining lentivirus-like particles and DNA electrotransfer. *Journal of Controlled Release*, 159(3), pp.376–383.
- Verma, A. et al., 2008. Surface-structure-regulated cell-membrane penetration by monolayer-protected nanoparticles. *Nature materials*, 7(July), pp.588–595.
- Vigant, F., Santos, N.C. & Lee, B., 2015. Broad-spectrum antivirals against viral fusion. *Nature Publishing Group*, 13(7), pp.426–437.
- de Villiers, E.-M. et al., 2004. Classification of papillomaviruses. *Virology*, 324(1), pp.17–27.
- Wagner, V. et al., 2006. The emerging nanomedicine landscape. *Nature Biotechnology*, 24(10), pp.1211–1217.
- Wolkowicz, R. & Schaechter, M., 2008. What makes a virus a virus ?. *Nature Reviews Microbiology*, 319.
- Wu, Z., Asokan, A. & Samulski, R.J., 2006. Adeno-associated virus serotypes : vector toolkit for human gene therapy. *Molecular Therapy*, 14(3), pp.316–327.
- Wutzler, P. & Sauerbrei, A., 2004. Virucidal activity of the new disinfectant monopercitric acid. *Letters in Applied Microbiology*, 39, pp.194–198.
- WuYang, Z., JiangJiao, L. & GuoDong, L., 2011. How does cellular heparan sulfate function in viral pathogenicity?\*. *Biomedical and Environmental sciences*, 24(1), pp.81–88.
- Ying, Z. et al., 2013. Electron microscopy : essentials for viral structure, morphogenesis and rapid diagnosis. *Science China Life Sciences*, 56(5), pp.421–430.
- Zakaria, S.M. et al., 2013. Nanophase hydroxyapatite as a biomaterial in advanced hard tissue engineering : a review. *Tissue Engineering*, 19(5).
- Zheng, N. & Stucky, G.D., 2006. Adenovirus receptors. *Journal of Virology*, 79(19), pp.12125–12131.